

Dry Storage and Transportation of High Burnup Spent Nuclear Fuel

Draft Report for Comment

AVAILABILITY OF REFERENCE MATERIALS IN NRC PUBLICATIONS

NRC Reference Material

As of November 1999, you may electronically access NUREG-series publications and other NRC records at the NRC's Public Electronic Reading Room at <http://www.nrc.gov/reading-rm.html>. Publicly released records include, to name a few, NUREG-series publications; *Federal Register* notices; applicant, licensee, and vendor documents and correspondence; NRC correspondence and internal memoranda; bulletins and information notices; inspection and investigative reports; licensee event reports; and Commission papers and their attachments.

NRC publications in the NUREG series, NRC regulations, and Title 10, "Energy," in the *Code of Federal Regulations* may also be purchased from one of these two sources.

1. The Superintendent of Documents

U.S. Government Publishing Office
Washington, DC 20402-0001
Internet: <http://bookstore.gpo.gov>
Telephone: 1-866-512-1800
Fax: (202) 512-2104

2. The National Technical Information Service

5301 Shawnee Road
Alexandria, VA 22161-0002
<http://www.ntis.gov>
1-800-553-6847 or, locally, (703) 605-6000

A single copy of each NRC draft report for comment is available free, to the extent of supply, upon written request as follows:

U.S. Nuclear Regulatory Commission

Office of Administration
Multimedia, Graphics and Storage & Distribution Branch
Washington, DC 20555-0001
E-mail: distribution.resource@nrc.gov
Facsimile: (301) 415-2289

Some publications in the NUREG series that are posted at the NRC's Web site address <http://www.nrc.gov/reading-rm/doc-collections/nuregs> are updated periodically and may differ from the last printed version. Although references to material found on a Web site bear the date the material was accessed, the material available on the date cited may subsequently be removed from the site.

Non-NRC Reference Material

Documents available from public and special technical libraries include all open literature items, such as books, journal articles, transactions, *Federal Register* notices, Federal and State legislation, and congressional reports. Such documents as theses, dissertations, foreign reports and translations, and non-NRC conference proceedings may be purchased from their sponsoring organization.

Copies of industry codes and standards used in a substantive manner in the NRC regulatory process are maintained at—

The NRC Technical Library

Two White Flint North
11545 Rockville Pike
Rockville, MD 20852-2738

These standards are available in the library for reference use by the public. Codes and standards are usually copyrighted and may be purchased from the originating organization or, if they are American National Standards, from—

American National Standards Institute

11 West 42nd Street
New York, NY 10036-8002
<http://www.ansi.org>
(212) 642-4900

Legally binding regulatory requirements are stated only in laws; NRC regulations; licenses, including technical specifications; or orders, not in NUREG-series publications. The views expressed in contractor-prepared publications in this series are not necessarily those of the NRC.

The NUREG series comprises (1) technical and administrative reports and books prepared by the staff (NUREG-XXXX) or agency contractors (NUREG/CR-XXXX), (2) proceedings of conferences (NUREG/CP-XXXX), (3) reports resulting from international agreements (NUREG/IA-XXXX), (4) brochures (NUREG/BR-XXXX), and (5) compilations of legal decisions and orders of the Commission and Atomic and Safety Licensing Boards and of Directors' decisions under Section 2.206 of NRC's regulations (NUREG-0750).

DISCLAIMER: This report was prepared as an account of work sponsored by an agency of the U.S. Government. Neither the U.S. Government nor any agency thereof, nor any employee, makes any warranty, expressed or implied, or assumes any legal liability or responsibility for any third party's use, or the results of such use, of any information, apparatus, product, or process disclosed in this publication, or represents that its use by such third party would not infringe privately owned rights.

Dry Storage and Transportation of High Burnup Spent Nuclear Fuel

Draft Report for Comment

Manuscript Completed: April 2018

Date Published: July 2018

Prepared by:

T. Ahn

H. Akhavannik

G. Bjorkman

F.C. Chang

W. Reed

A. Rigato

D. Tang

R.D. Torres

B.H. White

V. Wilson

Office of Nuclear Material Safety and Safeguards

COMMENTS ON DRAFT REPORT

Any interested party may submit comments on this report for consideration by the staff of the U.S. Nuclear Regulatory Commission (NRC). Comments may be accompanied by additional relevant information or supporting data. Please specify the report number **NUREG-2224** in your comments, and send them by the end of the comment period specified in the Federal Register notice announcing the availability of this report.

Addresses: You may submit comments by any one of the following methods. Please include Docket ID **NRC-2018-0066** in the subject line of your comments. Comments submitted in writing or in electronic form will be posted on the NRC Web site and on the Federal rulemaking Web site (<http://www.regulations.gov>).

Federal Rulemaking Web site: Go to <http://www.regulations.gov> and search for documents filed under Docket ID **NRC-2018-0066**. Address questions about NRC dockets to Jennifer Borges; telephone: 301-287-9127; e-mail: Jennifer.Borges@nrc.gov.

Mail comments to: May Ma, Director, Program Management, Announcements and Editing Branch (PMAE), Office of Administration, Mail Stop: TWFN-7-A-60M, U.S. Nuclear Regulatory Commission, Washington, DC 20555-0001.

For any questions about the material in this report, please contact: Wendy Reed, 301-415-7213 or, e-mail at Wendy.Reed@nrc.gov.

Please be aware that any comments that you submit to the NRC will be considered a public record and entered into the Agencywide Documents Access and Management System. Do not provide information you would not want to be publicly available.

ABSTRACT

1

2 Time-dependent changes on the cladding performance of high burnup (HBU) spent nuclear fuel
3 (SNF) are all primarily driven by the fuel's temperature, rod internal pressure (and
4 corresponding pressure-induced cladding hoop stresses), and the environment during dry
5 storage or transport operations. Historically, the potential for these changes to compromise the
6 analyzed fuel configuration in dry storage systems and transportation packages has been
7 addressed through safety review guidance. This guidance defines adequate fuel conditions,
8 including peak cladding temperatures during short-term loading operations to prevent or
9 mitigate degradation of the cladding. The purpose of this report is to expand the technical basis
10 in support of that guidance, as it pertains to the mechanism of hydride reorientation in HBU SNF
11 cladding.

12 Hydride reorientation is a process in which the orientation of hydrides precipitated in HBU SNF
13 cladding during reactor operation changes from the circumferential-axial to the radial-axial
14 direction. Research results over the last decade have shown that hydride reorientation can still
15 occur at temperatures and stresses lower than those assumed in the current staff review
16 guidance. Therefore, the U.S. Nuclear Regulatory Commission (NRC) has since sponsored
17 additional research to better understand whether hydride reorientation could affect the
18 mechanical behavior of HBU SNF cladding and compromise the fuel configuration analyzed in
19 dry storage systems and transportation packages.

20 This report provides an engineering assessment of the results of research on the mechanical
21 performance of HBU SNF following hydride reorientation. Based on the conclusions of that
22 assessment, the report then presents example approaches for licensing and certification of HBU
23 SNF for dry storage (under Title 10 of the *Code of Federal Regulations* (10 CFR) Part 72,
24 "Licensing Requirements for the Independent Storage of Spent Nuclear Fuel and High-Level
25 Radioactive Waste, and Reactor-Related Greater Than Class C Waste") and transportation
26 (under 10 CFR Part 71, "Packaging and Transportation of Radioactive Material").

27 The information in this report is not intended for use in applications for wet storage facilities or
28 monitored retrievable storage installations licensed under 10 CFR Part 72.

29 Nothing contained in this report is to be construed as having the force or effect of regulations.
30 Comments regarding errors or omissions, as well as suggestions for improvement of this
31 NUREG should be sent to the Director, Division of Spent Fuel Management, U.S. Nuclear
32 Regulatory Commission, Washington, D.C., 20555-0001.

Paperwork Reduction Act

33
34
35 This NUREG provides guidance for implementing the mandatory information collections in 10
36 CFR Parts 71 and 72 that are subject to the Paperwork Reduction Act of 1995 (44 U.S.C. 3501
37 et. seq.). These information collections were approved by the Office of Management and Budget
38 (OMB) under control numbers 3150-0008 and 3150-0132. Send comments regarding this
39 information collection to the Information Services Branch, U.S. Nuclear Regulatory Commission,
40 Washington, DC 20555-0001, or by e-mail to Infocollects.Resource@nrc.gov, and to the Desk
41 Officer, Office of Information and Regulatory Affairs, NEOB-10202, (3150-0008, 3150 -0132)
42 Office of Management and Budget, Washington, DC 20503.
43

1 **Public Protection Notification**

2 The NRC may not conduct or sponsor, and a person is not required to respond to, a collection
3 of information unless the document requesting or requiring the collection displays a currently
4 valid OMB control number.

CONTENTS

1			
2	ABSTRACT		iii
3	CONTENTS		v
4	LIST OF FIGURES		vii
5	LIST OF TABLES		ix
6	ACKNOWLEDGMENTS		xi
7	ABBREVIATIONS AND ACRONYMS		xiii
8	1 INTRODUCTION		1-1
9	1.1 Background.....		1-1
10	1.2 Fuel Cladding Performance and Staff's Review Guidance		1-2
11	1.3 Cladding Creep.....		1-4
12	1.4 Effects of Hydrogen on Cladding Mechanical Performance.....		1-5
13	1.5 Hydride Reorientation		1-7
14	1.5.1 Hydride Dissolution and Precipitation		1-8
15	1.5.2 Fuel Cladding Fabrication Process.....		1-10
16	1.5.3 End-Of-Life Rod Internal Pressures and Cladding Hoop		
17	Stresses		1-11
18	1.5.3.1 End-Of-Life Rod Internal Pressures for Pressurized-		
19	Water Reactor Fuel Rods		1-11
20	1.5.3.2 Gas Temperatures for Fuel Rods During Drying-		
21	Transfer, Storage and Transportation		1-14
22	1.5.3.3 Peak Cladding Hoop Stresses for Pressurized-Water		
23	Reactor Fuel Rods During Drying-Transfer and		
24	Storage/Transport Operations		1-15
25	1.5.4 Ring Compression Testing		1-18
26	1.5.5 Staff's Assessment of Ring Compression Testing Results.....		1-24
27	2 ASSESSMENT OF STATIC BENDING AND FATIGUE STRENGTH		
28	RESULTS ON HIGH BURNUP SPENT NUCLEAR FUEL		2-1
29	2.1 Introduction		2-1
30	2.2 Cyclic Integrated Reversible Fatigue Tester.....		2-1
31	2.3 Application Of The Static Test Results		2-4
32	2.3.1 Spent Fuel Rod Behavior in Bending.....		2-5
33	2.3.2 Composite Behavior of a Spent Fuel Rod.....		2-6
34	2.3.3 Calculation of Cladding Strain Using Factored Cladding-Only		
35	Properties.....		2-10
36	2.3.3.1 Two Alternatives for Calculating Cladding Stress and		
37	Strain During Drop Accidents.....		2-13
38	2.3.4 Applicability to Dry Storage and Transportation.....		2-14
39	2.3.4.1 Use of Static Test Results to Evaluate Safety Margins		
40	in an HAC Side Drop Event		2-17
41	2.3.4.2 Dynamic Response of a Fuel Rod		2-19
42	2.3.4.3 Seismic Response of a Fuel Rod.....		2-19
43	2.4 Application of Fatigue Test Results.....		2-20

1	2.4.1	Lower Bound Fatigue S-N Curves	2-20
2	2.4.2	Fatigue Cumulative Damage Model.....	2-22
3	2.4.3	Applicability to Storage and Transportation	2-23
4	3	DRY STORAGE OF HIGH BURNUP SPENT NUCLEAR FUEL	3-1
5	3.1	Introduction	3-1
6	3.2	Uncanned Fuel (Intact and Undamaged Fuel).....	3-4
7	3.2.1	Leaktight Confinement.....	3-6
8	3.2.2	Non-Leaktight Confinement.....	3-7
9	3.2.3	Dry Storage Up To 20 Years	3-10
10	3.2.4	Dry Storage Beyond 20 Years	3-11
11	3.2.4.1	Supplemental Results from Confirmatory	
12		Demonstration	3-11
13	3.2.4.1.1	Initial Licensing or Certification	3-12
14	3.2.4.1.2	Renewal Applications	3-12
15	3.2.4.2	Supplemental Safety Analyses	3-12
16	3.2.4.2.1	Materials and Structural.....	3-13
17	3.2.4.2.2	Confinement.....	3-13
18	3.2.4.2.3	Thermal	3-14
19	3.2.4.2.4	Criticality.....	3-15
20	3.2.4.2.5	Shielding.....	3-17
21	3.3	Canned Fuel (Damaged Fuel).....	3-19
22	4	TRANSPORTATION OF HIGH BURNUP SPENT NUCLEAR FUEL	4-1
23	4.1	Introduction	4-1
24	4.2	Uncanned Fuel (Intact and Undamaged Fuel).....	4-4
25	4.2.1	Leaktight Containment.....	4-7
26	4.2.2	Non-Leaktight Containment.....	4-7
27	4.2.3	Direct Shipment from the Spent Fuel Pool and Shipment of	
28		Previously Dry-Stored Fuel (Up To 20 Years since Fuel was	
29		Initially Loaded)	4-11
30	4.2.4	Shipment of Previously Dry-Stored Fuel (Beyond 20 Years	
31		since Fuel was Initially Loaded).....	4-12
32	4.2.4.1	Supplemental Data from Confirmatory Demonstration.....	4-12
33	4.2.4.2	Supplemental Safety Analyses	4-12
34	4.2.4.2.1	Materials and structural	4-13
35	4.2.4.2.2	Containment.....	4-13
36	4.2.4.2.3	Thermal	4-14
37	4.2.4.2.4	Criticality.....	4-15
38	4.2.4.2.5	Shielding.....	4-18
39	4.3	Canned Fuel	4-20
40	5	CONCLUSIONS	5-1
41	6	REFERENCES	6-1
42	7	GLOSSARY	7-1

LIST OF FIGURES

1			
2	Figure 1-1	Hydride Content [H] and Distribution (Average, Inner 2/3 Diameter Of	
3		Cladding) in HBU SNF Cladding (From Billone et al., 2013)	1-6
4	Figure 1-2	Dissolution (C_d) and Precipitation (C_p) Concentration Curves Based on the	
5		Data of Kammenzind et al. (1996) for Non-Irradiated Zircaloy-4 (Zry-4)	1-9
6	Figure 1-3	Publicly-Available Data Collected by EPRI For PWR End-Of-Life Rod	
7		Internal Pressures at 25°C.....	1-12
8	Figure 1-4	Calculated Rod Internal Pressures for the First 10 Cycles of the Watts	
9		Bar Nuclear Plant Unit 1 Reactor Under Vacuum Drying Conditions	1-13
10	Figure 1-5	Aggregated Measured and Calculated Values for End-Of-Life Rod Internal	
11		Pressures for PWR Fuel Rods. Pressures are Presented at 25 °C (77 °F)	1-14
12	Figure 1-6	Calculated Rod Internal Pressure as a Function of the Spatially Averaged	
13		Gas Temperature for PWR Fuel Rods (i.e. Standard Rods), ZIRLO-Clad	
14		IFBA Rods With Hollow (Annular) Blanket Pellets, and ZIRLO-Clad IFBA	
15		Rods with Solid Blanket Pellets	1-15
16	Figure 1-7	Fuel Cladding Tube with Stress Element	1-16
17	Figure 1-8	Calculated Values of Cladding Hoop Stress Vs.the Spatially-Averaged	
18		Internal Gas Temperature for Standard 17×17 PWR Fuel Rods with	
19		Corrosion Layers of 10 μm, 40 μm, and 80 μm.....	1-17
20	Figure 1-9	PWR Hoop Stress as a Function of Internal Gas Temperature for 17 × 17	
21		IFBA Fuel Rods (for Both Hollow Blanket and Solid Blanket Pellets) with a	
22		40-μm Corrosion Layer	1-18
23	Figure 1-10	RCT of a Sectioned Cladding Ring Specimen in ANL’s Instron’s	
24		8511 Test Setup.....	1-19
25	Figure 1-11	Ductility Vs. RCT for Two PWR Cladding Alloys Following Slow Cooling	
26		from 400°C at Peak Target Hoop Stresses of 110 Mpa and 140 Mpa	1-20
27	Figure 1-12	Ductility Data, as Measured by RCT, for As-Irradiated Zircaloy-4 and	
28		Zircaloy-4 Following Cooling from 400 °C Under Decreasing Internal	
29		Pressure and Hoop Stress Conditions	1-21
30	Figure 1-13	Ductility Data, as Measured by RCT, for As-Irradiated ZIRLO and ZIRLO	
31		Following Cooling from 400 °C Under Decreasing Internal Pressure and	
32		Hoop Stress Conditions	1-22
33	Figure 1-14	Ductility Data, as Measured By RCT, for As-Irradiated M5 and M5	
34		Following Cooling from 400 °C Under Decreasing Internal Pressure and	
35		Hoop Stress Conditions	1-23
36	Figure 1-15	Geometric Models for Spent Fuel Assemblies in Transportation Packages	1-25
37	Figure 2-1	Horizontal Layout of ORNL U-Frame Setup, Rod Specimen and Three	
38		Lvdts for Curvature Measurement, and Front View of CIRFT Installed in	
39		ORNL Hot Cell	2-2
40	Figure 2-2	Schematic Diagram of End and Side Drop Accident Scenarios	2-5
41	Figure 2-3	Typical Composite Construction of a Bridge	2-6

1	Figure 2-4	Influence of cg Position on Composite Beam Stiffness	2-7
2	Figure 2-5	Images of Cladding-Pellet Structure in HBU SNF Rod	2-8
3	Figure 2-6	Approximate Extreme Fiber Tensile Stresses Between Pellet-Pellet Crack	2-9
4	Figure 2-7	Comparison of CIRFT Static Bending Results with Calculated PNNL	
5		Moment Curvature (Flexural Rigidity) Derived from Cladding-Only	
6		Stress-Strain Curve.....	2-10
7	Figure 2-8	Characteristic Points on Moment-Curvature Curve	2-11
8	Figure 2-9	High Magnification Micrograph Showing Radial Hydrides of a HBR HBU	
9		SNF Hydride-Reoriented Specimen Tested Under Phase II (Specimen	
10		HR1 Results Shown; Hydrogen Content \approx 360–400 Wppm).....	2-15
11	Figure 2-10	Representative Conditions Used for Radial Hydride Treatment for	
12		Preparation of HBR HBU SNF Hydride-Reoriented Specimens Tested	
13		Under Phase II	2-16
14	Figure 2-11	Plots of Half of the Cladding Strain Range ($\Delta\varepsilon/2$) and the Maximum Strain	
15		(ε_{max}) as a Function of Number of Cycles to Failure.....	2-21
16	Figure 2-12	CIRFT Dynamic (Fatigue) Test Results for As-Irradiated and	
17		Hydride-Reoriented H.B. Robinson Zircaloy-4 HBU Fuel Rods.....	2-22
18	Figure 3-1	Example Licensing and Certification Approaches for Dry Storage of High	
19		Burnup Spent Nuclear Fuel	3-3
20	Figure 3-2	First Approach for Evaluating Design-Bases Drop Accidents During	
21		Dry Storage	3-5
22	Figure 3-3	Second Approach for Evaluation of Design-Bases Drop Accidents During	
23		Dry Storage	3-6
24	Figure 4-1	Example Approaches for Approval of Transportation Packages with High	
25		Burnup Spent Nuclear Fuel	4-3
26	Figure 4-2	First Approach for Evaluation of Drop Accidents During Transport.....	4-5
27	Figure 4-3	Second Approach for Evaluation of Drop Accidents During Transport	4-6
28	Figure 4-4	Evaluation of Vibration Normally Incident to Transport.....	4-7

LIST OF TABLES

1			
2	Table 2-1	Comparison of Average Flexural Rigidity Results between CIRFT Static	
3		Testing and PNNL Cladding-Only Data.....	2-12
4	Table 2-2	Characteristic Points and Quantities Based on Moment-Curvature Curves.....	2-12
5	Table 2-3	Properties of PWR 15 × 15 SNF Rod.....	2-17
6	Table 2-4	Summary of CIRFT Dynamic Test Results for As-Irradiated and Hydride-	
7		Reoriented HBR HBU SNF	2-20
8	Table 2-5	Coordinates for Lower-Bound Enveloping S-N Curve for the HBR HBU	
9		SNF Rods.....	2-21
10	Table 3-1	Fractions of Radioactive Materials Available for Release from HBU SNF	
11		Under Conditions of Dry Storage.....	3-8
12	Table 4-1	Fractions of Radioactive Materials Available for Release from HBU SNF	
13		Under Conditions Of Transport.....	4-9

1

ACKNOWLEDGMENTS

2 The working group is very grateful to M. Billone (Argonne National Laboratory) for providing
3 valuable input for the writing of the report. R. Einziger (Nuclear Waste Technical Review Board),
4 J. Wang (Oak Ridge National Laboratory), and M. Flanagan-Bales (U.S. Nuclear Regulatory
5 Commission) also provided valuable insights, observations, and recommendations.

ABBREVIATIONS AND ACRONYMS

ADAMS	Agencywide Documents Access and Management System
AMP	aging management program
ANL	Argonne National Laboratory
ANS	American Nuclear Society
ANSI	American National Standards Institute
b	width
BWR	boiling-water reactor
C_d	concentration at dissolution
C_p	concentration at precipitation
CFR	<i>Code of Federal Regulations</i>
cg	center of gravity
CoC	Certificate of Compliance
CIRFT	cyclic integrated reversible-bending fatigue tester
CRUD	Chalk River unknown deposit
CWSRA	cold worked stress relieved annealed
δ_p/D_{mo}	offset strain
ΔT_{dp}	temperature hysteresis (dissolution-precipitation)
D_{mi}	inner (metal) cladding diameter
D_{mo}	outer (metal) cladding diameter
DLF	dynamic load factor
DTT	ductility transition temperature
DOE	U.S. Department of Energy
DSS	dry storage system
ε	average tensile strain
ε -N	strain per number of cycles
E	elastic modulus
E_c	elastic modulus of the cladding
E_p	elastic modulus of the fuel pellet
EOL	end-of-life
EPRI	Electric Power Research Institute
GBC	general burnup credit
GTCC	greater-than-Class-C waste
h	height
h_m	cladding (metal) thickness
HAC	hypothetical accident conditions (transportation)
HBR	H. B. Robinson
HBU	high burnup
HRT	hydride reorientation treatment
Hz	hertz
I	moment of inertia
I_c	moment of inertia of the cladding

I_p	moment of inertia of the fuel pellet
IAEA	International Atomic Energy Agency
IFBA	integral fuel burnable absorber
ISFSI	independent spent fuel storage installation
ISG	Interim Staff Guidance
κ	curvature
κ -N	curvature per number of cycles
k_{eff}	k-effective
l	rod length between spacers
LBU	low burnup
LVDT	linear variable differential transformer
M	bending moment
n_i	number of strain cycles at strain level ϵ_i
N_i	number of strain cycles to produce failure at ϵ_i
NCT	normal conditions of transport
NRC	U.S. Nuclear Regulatory Commission
ORNL	Oak Ridge National Laboratory
P_i	rod internal pressure
P_o	rod external pressure
PNNL	Pacific Northwest National Laboratory
PWR	pressurized-water reactor
r	outer radius
RCT	ring compression testing
RHCF	radial hydride continuity factor
RIP	rod internal pressure
RXA	recrystallized annealed
σ	average tensile stress
σ_θ	cladding hoop stress
σ_z	cladding longitudinal stress
SNF	spent nuclear fuel
SRP	standard review plan
SSC	structure, system, and component
T_d	dissolution temperature
T_p	precipitation temperature
w	uniform applied load
y_{max}	distance to the neutral axis

Units of Measure

C	Celsius
F	Fahrenheit
ft	foot
g	9.806 m/s ²
GWd/MTU	gigawatt-days per metric ton of uranium
h	hour
in.	inch
lb	pound
m	meter
μm	micrometer, 1×10^{-6} meter
mm	millimeter, 0.001 meter
MPa	megapascal, 1×10^6 pascals
N	newton
N·m	newton meter
Pa	pascal
psi	pounds per square inch
s	second
Torr	Torr (unit of pressure)
wppm	parts per million by weight

1 INTRODUCTION

1.1 Background

As required by Title 10 of the *Code of Federal Regulations* (10 CFR) 72.44(c), a specific license for dry storage of spent nuclear fuel (SNF) is to include technical specifications that, among other things, define limits on the fuel and allowable geometric arrangements. Further, as required by 10 CFR 72.236(a), a Certificate of Compliance (CoC) for a dry storage system (DSS) design must include specifications for the type of spent fuel (i.e., boiling water reactor (BWR), pressurized water reactor (PWR), or both), maximum allowable enrichment of the fuel prior to any irradiation, burn-up (i.e., megawatt-days/MTU), minimum acceptable cooling time of the spent fuel before storage in the spent fuel storage cask, maximum heat designed to be dissipated, maximum spent fuel loading limit, condition of the spent fuel (i.e., intact assembly or consolidated fuel rods), and inerting atmosphere requirements. These specifications ensure that the loaded SNF assemblies remain within the bounds of the safety analyses in the approved design basis.

The regulations in 10 CFR Part 72, “Licensing Requirements for the Independent Storage of Spent Nuclear Fuel, High-Level Radioactive Waste, and Reactor-Related Greater Than Class C Waste,” include a number of fuel-specific and DSS-specific requirements that may be dependent of the design-basis condition of the fuel cladding. As required by 10 CFR 72.122(h)(1), the SNF cladding is to be protected against degradation that leads to gross ruptures or the fuel must be otherwise confined such that degradation of the fuel during storage will not pose operational safety problems with respect to its removal from storage. In addition, 10 CFR 72.122(l) states that the DSS must be designed to allow ready retrieval of the SNF. According to Interim Staff Guidance (ISG)-2, Revision 2, “Fuel Retrievability in Spent Fuel Storage Applications,” issued in April 2016 (NRC, 2016a).¹ This may be demonstrated on an assembly basis per the approved design basis. The condition of the fuel cladding may also impact the safety analyses used to demonstrate compliance with DSS-specific requirements in 10 CFR 72.124(a), 10 CFR 72.128, and 10 CFR 72.236(m).

Similarly for transportation, the regulations in 10 CFR Part 71, “Packaging and Transportation of Radioactive Material,” also include a number of fuel-specific and package-specific requirements. The regulations in 10 CFR 71.31, “Contents of Application” and 10 CFR 71.33, “Package description,” requires an application for a transportation package to describe the proposed package in sufficient detail to identify the package accurately and provide a sufficient basis for evaluation of the package, which includes a description of the chemical and physical form of the allowable contents. The regulations in 10 CFR Part 71 also require that (1) the geometric form of the package contents not be substantially altered under the tests for normal conditions of transport (NCT) (10 CFR 71.55(d)(2)) and (2) a package used for the shipment of fissile material is to be designed and constructed and its contents so limited that under the tests for hypothetical accident conditions (HAC) specified in 10 CFR 71.73, “Hypothetical Accident Conditions,” the package remains subcritical (10 CFR 71.55(e)). The requirement assumes that

¹ The current revisions of all ISG documents will be rolled into revised standard review plans (SRPs) for dry storage and transportation of SNF, as appropriate, and will then be removed from the public domain. The revised SRPs will be issued for public comment prior to being finalized.

1 the fissile material is in the most reactive credible configuration consistent with the
2 damaged condition of the package and the chemical and physical form of the contents
3 (10 CFR 71.55(e)(1)).

4 To comply with the requirements mentioned above, the fuel cladding generally serves a design
5 function in both DSSs and transportation packages for ensuring that the configuration of
6 undamaged and intact fuel remains within the bounds of the reviewed safety analyses.²
7 Therefore, an application should address potential degradation mechanisms that could result in
8 gross cladding ruptures during operations. To assist the safety review of potential degradation
9 mechanisms, the U.S. Nuclear Regulatory Commission (NRC) staff (the staff) has historically
10 issued guidance on acceptable storage and transport conditions that limit SNF degradation
11 during operations and ensure that the reviewed safety analyses remain valid.

12 **1.2 Fuel Cladding Performance and Staff's Review Guidance**

13 Time-dependent (i.e., age-related, not event-related) mechanisms resulting in changes to the
14 fuel cladding performance are all primarily driven by the fuel's temperature, rod internal
15 pressure (and corresponding pressure-induced cladding hoop stresses), and the environment
16 during dry storage or transport operations. Contrary to the hoop stresses experienced by the
17 fuel cladding during reactor operation, which are generally compressive because of the high
18 reactor coolant pressure, the hoop stresses during drying-transfer, dry storage, and transport
19 operations are tensile because of the low pressure external to the cladding. For instance, the
20 pressure of the environment surrounding the fuel in the reactor can be 16 MPa (1.2×10^5 Torr)
21 while the environment surrounding the fuel in the DSS confinement cavity may be as low as
22 400 Pa (3 Torr) at the end of vacuum drying and 0.5 MPa (3.75×10^3 Torr) during dry storage.
23 The magnitude of the cladding hoop stresses will depend on the differential pressure across the
24 cladding wall and thus the rod internal pressure at a given time. Various factors determine the
25 rod internal pressure, including the fuel's fabrication and irradiation conditions (i.e., fabrication
26 gas fill pressure, cladding thickness, presence of burnable absorbers, burnup) and the average
27 gas temperature within the fuel rods. The average gas temperature within the fuel rods has a
28 first-order effect on the hoop stress in the cladding and thus cladding performance, and
29 therefore it is critical to controlling the peak cladding temperature of the fuel rods during vacuum
30 drying and storage/transport operations to temperatures demonstrated to preserve cladding
31 integrity.

32 To assist in the safety review of DSS and transportation packages, the staff has developed
33 guidance with a supporting technical basis for setting adequate fuel conditions, including
34 acceptable peak cladding temperatures during short-term loading operations so that the
35 cladding meets the pertinent regulations. Historically, guidance has been issued as ISG-11,
36 "Cladding Considerations for the Transportation and Storage of Spent Fuel," which has been
37 revised multiple times to incorporate new data and lessons learned from the staff's review
38 experience. Initial standard review plans (SRPs) prior to ISG-11 stated that DSSs and
39 transportation packages needed to be dried to a level where galvanic corrosion could be ruled
40 out as a fuel degradation mechanism. The guidance specified moisture levels only for low
41 burnup (LBU) fuel (i.e., burnup below 45 GWd/MTU) because of the lack of degradation data at
42 higher burnup values. In 1999, the staff first issued ISG-11 to supplement the SRPs by

² If the fuel is classified as damaged, a separate canister (e.g., a can for damaged fuel) that confines the assembly contents to a known volume may be used to provide this assurance.

1 addressing potential degradation of high burnup (HBU) fuel (i.e., burnup exceeding
2 45 GWd/MTU).

3 A year later, the staff issued ISG-11, Revision 1 to incorporate new data, but also to give the
4 applicant the responsibility for demonstrating that the cladding was adequately protected. ISG-
5 11, Revision 1 stated that cladding oxidation should not be credited as load-bearing in the fuel
6 cladding structural evaluation and also defined a 1-percent creep strain limit on the cladding. It
7 also discussed the use of damaged fuel cans for confining fuel with gross ruptures. ISG-11,
8 Revision 1, accounted only for Zircaloy-clad fuel rods and not for other advanced cladding alloys
9 (e.g., ZIRLO and M5).

10 In 2002, the staff issued ISG-11, Revision 2, to change the definition of damaged fuel, remove
11 the 1-percent creep strain limit, and discuss criteria to limit hydride reorientation in the cladding.
12 It also made the guidance applicable to all zirconium-based claddings and all burnup levels.
13 The revision described onerous calculations, dependent on the characteristics of the fuel to be
14 stored, to determine the maximum cladding temperature for the design-basis fuel per a justified
15 creep strain limit. Gruss et al. (2004) discuss in more detail the data used for supporting ISG-
16 11, Revision 2. Historically, ISG-11 has not discussed the use of an inert atmosphere to
17 mitigate fuel degradation. Peehs (1998) indicated that air could be used as an atmosphere
18 below 200 °C (392 °F) but later research indicated a lower temperature was necessary.
19 Therefore, ISG-22, "Potential Rod Splitting Due to Exposure to an Oxidizing Atmosphere during
20 Short-Term Cask Loading Operations in LWR or Other Uranium Oxide Based Fuel," issued
21 May 2006 (NRC, 2006), addressed the use of an inert atmosphere for loading operations.

22 In November 2003, the staff issued ISG-11, Revision 3, "Cladding Considerations for the
23 Transportation and Storage of Spent Fuel" (NRC, 2003a). The guidance was eventually
24 incorporated into NUREG-1536, Revision 1, "Standard Review Plan for Spent Fuel Dry Storage
25 Systems at a General License Facility," issued in July 2010 (NRC, 2010), although not yet
26 incorporated into a revision of NUREG-1567, "Standard Review Plan for Spent Fuel Storage
27 Facilities," issued in March 2000 (NRC, 2000a) (i.e. the standard review plan for specific
28 licenses under 10 CFR Part 72). ISG-11, Revision 3 replaced the calculation of the maximum
29 cladding temperature per a justified creep strain limit with a generic 400 °C (752 °F) peak
30 cladding temperature limit applicable to normal conditions of storage and transportation, as well
31 as short-term loading operations (e.g., drying, backfilling with inert gas, and transfer of the DSS
32 cask or canister to the storage pad). ISG-11, Revision 3 also defined a higher short-term
33 temperature limit applicable to LBU fuel if the applicant demonstrated by calculation that the
34 cladding hoop stress would not exceed 90 MPa (1.3×10^4 psi) for the proposed temperature
35 limit. The guidance also defined a generic maximum cladding temperature limit of 570 °C
36 (1,058 °F) for off-normal and accident conditions applicable to all burnups.

37 In addition to creep, ISG-11, Revision 3 (NRC, 2003a), also considered minimizing hydride
38 reorientation. At the time of its issuance, the technical basis discussed in ISG-11, Revision 3
39 supported the staff's conclusion that hydride reorientation would be minimized by maintaining
40 cladding temperatures below 400 °C (752 °F) and restricting the change in cladding
41 temperatures during drying-transfer operations to less than 65 °C (117 °F). This temperature
42 change limit was based on the temperature drop required to obtain the degree of
43 supersaturation required for the precipitation of radial hydrides in a short thermal cycle
44 (see Section 1.5.1). Therefore, ISG-11, Revision 3, states that the cladding should not
45 experience more than 10 thermal cycles, each not exceeding 65 °C (117 °F), which provided
46 assurance that hydride reorientation would be limited.

1 Research results obtained since the ISG-11, Revision 3, have shown that hydride reorientation
2 can still occur below the generic 400 °C (752 °F) peak cladding temperature limit (Aomi et al,
3 2008; Billone et al., 2013; Billone et al., 2014; Billone et al., 2015). To better understand
4 hydride reorientation, both the NRC and the U.S. Department of Energy (DOE) have obtained
5 additional data on the performance of HBU SNF cladding with reoriented hydrides to determine
6 if the guidance in ISG-11, Revision 3, ought to be revised.

7 **1.3 Cladding Creep**

8 Creep is the time-dependent deformation of a material under stress. The main driving force for
9 cladding creep at a given temperature is the hoop stress caused by internal rod pressure, which
10 results from the fission and decay gases released to the gap between the fuel and cladding (Ito,
11 at al., 2004). Fuel pellet swelling may also result in localized stresses on the cladding due to
12 the mechanical interaction between the cladding and the fuel. Pellet swelling may occur due to:
13 (1) the incorporation of soluble and insoluble solid fission products in the fuel matrix, (2) the
14 formation of intra- and intergranular fission gas bubbles, particularly in the hot interior region of
15 a fuel pellet, and (3) the formation of a large number of small gas bubbles in the fine-grained
16 ceramic structure that builds inward from the outer pellet surface for HBU fuel. If excessive
17 creep of the cladding were to occur during dry storage, it could lead to thinning, hairline cracks,
18 or gross ruptures (Hanson et al, 2012) and potentially compromise the ability to safely retrieve
19 by normal means the HBU fuel on a single-assembly basis (if required by the design basis).

20 The appendix to ISG-11, Revision 3 (NRC, 2003a) reviewed the data used by the staff to obtain
21 reasonable assurance that creep will not result in gross ruptures for peak cladding temperatures
22 below 400 °C (752 °F). The fabrication of fuel rods is such that the creep of the cladding is self-
23 limiting. As the cladding creeps, the internal volume of the rod increases and stress decreases.
24 However, as the gas volume within the fuel column increases, the average gas temperature
25 also increases. The net effect is a slow decrease in pressure and hoop stress with increasing
26 creep strain. The stress also decreases with increasing storage or transport time due to the
27 decrease in internal pressure with decreasing temperature. ISG-11, Revision 3, concluded the
28 following:

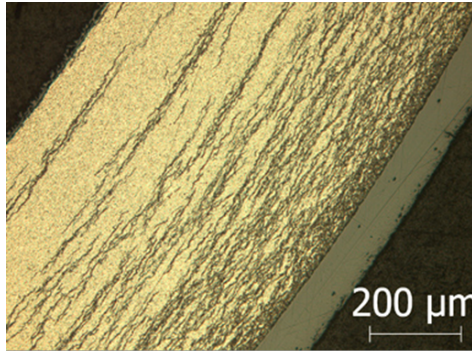
- 29 1. *deformation caused by creep will proceed slowly over time and will decrease the rod*
30 *pressure,*
- 31 2. *the decreasing cladding temperature also decreases the hoop stress, and this too will*
32 *slow the creep rate so that during later stages of dry storage, further creep deformation*
33 *will become exceedingly small, and*
- 34 3. *in the unlikely event that a breach of the cladding due to creep occurs, it is believed that*
35 *this will not result in gross rupture.*

36 These conclusions are considered applicable to fuel at all burnups because the relatively small
37 differences in creep rate as a function of materials and burnup are not expected to have a
38 significant impact on the maximum creep strains in the rod. The technical basis in ISG-11,
39 Revision 3 (NRC, 2003a) has provided reasonable assurance to the staff that creep strains
40 during dry storage and transportation will not result in fuel failures nor compromise the assumed
41 fuel configuration in the safety analyses. However, the staff recognizes the uncertainties
42 associated with extrapolating short-term accelerated test data to extended periods of dry storage.
43 The staff further recognizes the separate-effects nature of the accelerated creep testing
44 conducted to date, which would not account for potential combined effects with other
45 phenomena occurring during dry storage (e.g., annealing of irradiation hardening, hydride
46 reorientation). Therefore, the staff considers it prudent that long-term observation of HBU SNF

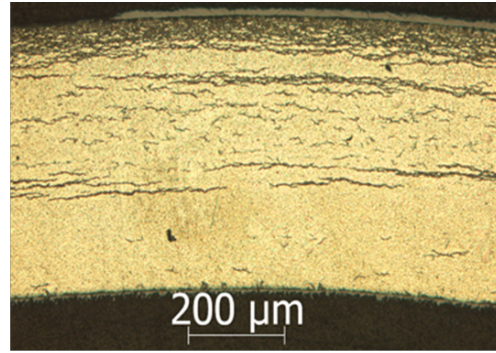
1 stored in a deployed DSS be used to confirm the conclusions of the accelerated short-term
2 testing. To aid users in demonstrating adequate creep performance during storage periods
3 beyond 20 years, in June 2016, the staff issued guidance in NUREG-1927, Revision 1,
4 “Standard Review Plan for Renewal of Specific Licenses and Certificates of Compliance for Dry
5 Storage of Spent Nuclear Fuel” (NRC, 2016b), which discusses the use of an Aging
6 Management Program using a surrogate surveillance and monitoring program to provide this
7 confirmatory long term data.

8 **1.4 Effects of Hydrogen on Cladding Mechanical Performance**

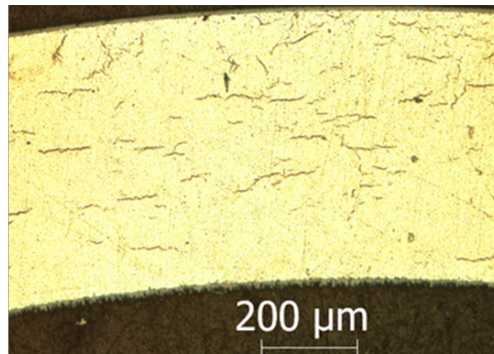
9 During irradiation, hydrogen is generated due to water-coolant corrosion (i.e., oxidation) of the
10 cladding, which diffuses into the zirconium-based material. As the solubility limit of hydrogen in
11 the cladding is exceeded, circumferential hydrides precipitate (Figure 1-1). The preferential
12 circumferential precipitation of the hydrides during reactor operation results from the texture of
13 cladding, which is determined by the manufacturing process. The number density of these
14 circumferential hydrides varies across the cladding wall due to the temperature drop from the
15 fuel side (hotter) to the coolant side (cooler) of the cladding. When the cladding absorbs
16 significant hydrogen, migration and precipitation of dissolved hydrogen into the coolant side of
17 the cladding can result in the formation of a rather dense hydride rim just below the outer
18 cladding oxide layer. The hydride number density and thickness of this hydride rim depend on
19 cladding design and reactor operating conditions for a given fuel type. For example, fuel rods
20 operated at high linear heat rating to high burnup generally have a very dense hydride rim that
21 is less than 10 percent of the cladding wall thickness. Conversely, fuel rods operated at low
22 linear heat ratings to high burnup have a more diffuse hydride distribution that could extend as
23 far as 50 percent across the cladding wall.



Zircaloy-4
67 GWd/MTU
[H]_{average}: 640 ± 140 wppm
[H]_{inner 2/3}: 640 ± 140 wppm



ZIRLO™
68 GWd/MTU
[H]_{average}: 530±70 wppm
[H]_{inner 2/3}: 136 ± 7 wppm



M5®
72 GWd/MTU
[H]_{average}: 76±5 wppm
[H]_{inner 2/3}: ~ 76 wppm

1 **Figure 1-1 Hydride Content [H] and Distribution (Average, Inner 2/3 Diameter of**
 2 **Cladding) in HBU SNF Cladding (from Billone et al., 2013)**

3 The staff concluded in ISG-11, Revision 3 (NRC, 2003a), that the hydride rim, along with any
 4 cladding metal oxidized during reactor operation, should not be considered as load bearing
 5 when determining the effective cladding thickness for the structural evaluation of the assembly
 6 in the DSS or transportation package. However, the staff recognizes that there is no reliable
 7 predictive tool available to calculate this rim thickness, which varies along the fuel-rod length,
 8 around the circumference at any particular axial location, from fuel rod to fuel rod within an
 9 assembly, and from assembly to assembly. Moreover, recent data generated by Argonne
 10 National Laboratory (ANL) have shown that for the full range of gas pressures anticipated during
 11 drying and storage, the hydride rim remains intact following slow cooling under conditions of
 12 decreasing pressure. The results suggest that hydride rims have some load bearing capacity
 13 (Billone et al., 2013; Billone et al., 2014; Billone et al., 2015). These results indicate that it may
 14 be appropriate to include the hydride rim in the effective cladding thickness calculation.
 15 Therefore, the staff considers acceptable the inclusion of the hydride rim thickness in the
 16 calculation of the effective cladding thickness when mechanical test data referenced in the
 17 structural evaluation have adequately accounted for its presence. Historically, this has been the
 18 case during the review of DSS and transportation packages, as applicants have provided

1 mechanical property data generated from tests with irradiated cladding samples with an intact
2 hydride rim. These data includes test results derived from uniaxial tensile tests or pressurized
3 tube tests of samples that do not have a machined gauge section.

4 Applicants have generally relied on a public database of materials properties for Zircaloy-4,
5 Zircaloy-2 and ZIRLO to analyze the behavior of as-irradiated cladding (Geelhood et al, 2008;
6 Geelhood et al, 2013) during dry storage and transportation. Additional data for engineering
7 properties (e.g., yield stress, ultimate tensile stress, and uniform elongation) can be found in the
8 open literature for ZIRLO (Cazalis et al., 2005; Pan et al., 2013), Optimized ZIRLO (Pan et al.,
9 2013), and M5 (Cazalis et al., 2005; Fourgeaud et al., 2009; Bouffieux et al., 2013). The
10 applicant should adequately justify the use of any of these properties for the fuel designs cited
11 for use in the DSS or transportation package application. Any use of mechanical properties
12 from uniaxial-tension and ring-expansion tests on cladding specimens with machined gauge
13 sections, where some of the hydride rim would have been inadvertently removed during outer-
14 surface oxide removal, should be adequately justified. The mechanical property data from
15 these specimens are still valuable, but characterization of their remaining rim thickness, post-
16 test determination of their hydrogen concentration, or both may be needed.

17 **1.5 Hydride Reorientation**

18 As discussed in Section 1.4, hydrogen infiltrates the cladding during reactor operation. The
19 excess hydrogen (i.e., hydrogen exceeding the solubility limit in the cladding) precipitates
20 primarily in the circumferential-axial direction. However, under temperature and stress
21 conditions experienced during vacuum drying and storage/transport operations, some of these
22 hydrides may redissolve and subsequently reprecipitate as new hydrides. During this process,
23 the orientation of these precipitated hydrides may change from the circumferential-axial to the
24 radial-axial direction.

25 The technical basis discussed in ISG-11, Revision 3 (NRC, 2003a) has supported the staff's
26 conclusion that if peak cladding temperatures are maintained below 400 °C (752 °F) and the
27 pressure-induced hoop stresses in the cladding were maintained below 90 MPa (1.3×10^4 psi),
28 then hydride reorientation would be minimized. The database used for this determination (see
29 Figure 3 in Chung, 2004) had a mixture of results from irradiated and non-irradiated material,
30 high and low hydrogen concentrations, different cladding types, different cooling rates, and
31 other variables. In addition, the methods to determine if there were radial hydrides varied
32 considerably from researcher to researcher. Since the issuance of ISG-11, Revision 3,
33 research results generated at ANL (Billone et al., 2013; Billone et al., 2014; Billone et al., 2015)
34 and in Japan (Aomi et al., 2008) have shown that hydride reorientation can still occur at lower
35 temperatures and stresses than those assumed in ISG-11, Revision 3. Because of the number
36 of variables involved, the staff agreed that it would not be practical to precisely determine the
37 temperature and stress conditions to prevent reorientation. Rather, the critical question was
38 what effect hydride reorientation would have on the mechanical behavior of the cladding,
39 particularly since the design-basis structural evaluation of the SNF assembly generally assumes
40 as-irradiated cladding mechanical properties (i.e., properties not accounting for hydride
41 reorientation). If hydride reorientation had an observable effect on the mechanical behavior of
42 the cladding (i.e., it decreased the failure strain limit of the cladding in response to stresses
43 during operations), then the failure limits as defined in the design-basis structural evaluations
44 would have to be modified.

45 Because both circumferential and radial hydrides are oriented in the planes parallel to the
46 principal normal tensile stress during bending loading, the staff has expected that HBU SNF

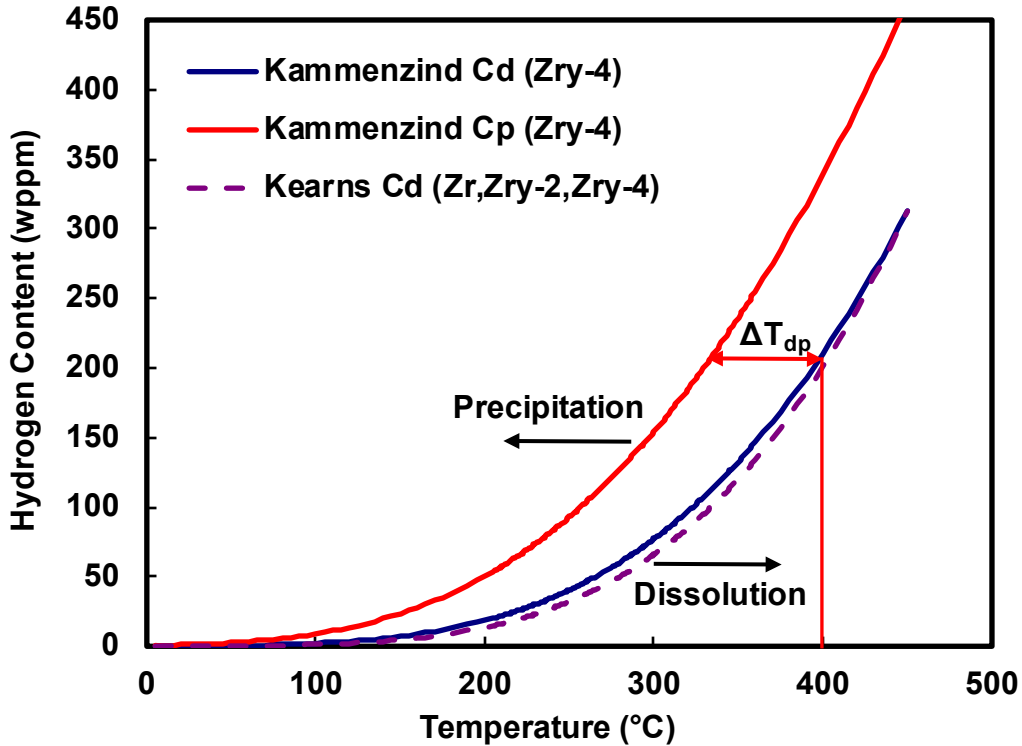
1 fatigue strength and bending stiffness would not be sensitive to the hydride orientation under
2 bending moments that produce longitudinal tensile stresses in the rod (Tang et al, 2015).³
3 Experimental confirmation of this expectation was prudent. Therefore, the NRC and DOE
4 conducted complementary research programs to investigate the cyclic fatigue and bending
5 strength performance of HBU SNF cladding in both as-irradiated and reoriented conditions
6 (Wang et al., 2016; NRC, 2017).

7 Even with the expectation that hydride orientation would not have a significant impact on the
8 fatigue strength and bending stiffness of HBU SNF under bending moments that produce
9 longitudinal tensile stresses in the rod, the staff expressed concern that hydride orientation
10 could impact the failure stresses and strains under pinch-type loads. Pinch-type loads could
11 potentially occur during postulated drop accidents in storage, normal conditions of transport
12 (NCT), or hypothetical accident conditions (HAC) during transportation. The staff was
13 particularly concerned with reduced cladding ductility during the HAC 9-m (30-ft) side drop or a
14 tip-over handling accident, where pinch loads could occur due to rod-to-grid spacer contact, rod-
15 to-rod contact, or rod-to-basket contact. If the fuel temperature were to be sufficiently low at the
16 time of the accident, these pinch loads could compromise the analyzed fuel configuration.
17 Thus, research was conducted in the United States and Japan to study the ductility of cladding
18 with reoriented hydrides under diametrically-opposed pinch loads. Ring compression testing
19 (RCT) was used to assess residual ductility of de-fueled HBU SNF cladding specimens
20 subjected to hydride reorientation (see Section 1.5.4). This testing led to the establishment of a
21 ductility transition temperature (DTT) (i.e., a temperature at which the tested cladding segments
22 were determined to lose ductility relative to as-irradiated cladding). The following section
23 discuss important parameters affecting the DTT and provides the staff's conclusion on its
24 relevance for future licensing and certification actions involving HBU SNF.

25 **1.5.1 Hydride Dissolution and Precipitation**

26 During drying-transfer operations, the cladding temperature increases, which causes some of
27 the circumferential hydrides to dissolve as hydrogen. The amount of hydrogen dissolved
28 depends on the temperature (T_d) and increases according to the solubility curve (C_d) for
29 zirconium-based alloys (Kammenzind et al., 1996; Kearns, 1967; McMinn, et al., 2000).
30 Zirconium-based alloys are materials that can have hydrogen in a supersaturated solution
31 because of the extra energy (strain, thermal) required to precipitate zirconium hydrides in the
32 cladding matrix. This results in a hysteresis in the solubility-precipitation curves as shown in
33 Figure 1-2.

³ Hydrides are essentially two-dimensional features since their thickness is relatively small compared to the other two dimensions. Radial hydrides span in the longitudinal and radial directions, and circumferential hydrides span in the longitudinal and circumferential directions. The bending tensile stresses are in the longitudinal direction. Therefore, the bending tensile stresses are parallel to the plane of both the radial and circumferential hydrides.



1 **Figure 1-2** Dissolution (C_d) and Precipitation (C_p) Concentration Curves Based on the
 2 Data of Kammenzind et al. (1996) for Non-Irradiated Zircaloy-4 (Zry-4)
 3 (Revised Figure 1 from Billone, et al., 2014). Also Shown Is the Best Fit to
 4 the Dissolution Curve (C_d) for Zirconium (Zr), Zircaloy-2 (Zry-2), and
 5 Zircaloy-4, Which Includes the Zircaloy-2 and Zircaloy-4 Data Generated by
 6 Kearns (1967). $\Delta t_{dp} = T_d - T_p$ Refers to the Temperature Drop Required for
 7 Precipitation, where T_d and T_p are the Corresponding Temperatures in the
 8 Solubility and Precipitation Curves for the Same Hydrogen Content

9 The solubility curves (C_d) plotted in Figure 1-2 indicate that the amount of hydrogen that
 10 dissolves increases with increasing temperature, but it is relatively independent of alloy
 11 composition and fabricated microstructure (recrystallized annealed (RXA) and cold worked
 12 stress relieved annealed (CWSRA)) (Kearns, 1967). Both Kammenzind et al (1996) and Kearns
 13 (1967) used diffusion couples, with one sample containing excess hydrogen and the other
 14 sample containing essentially no hydrogen, exposed to long annealing times (e.g., 2 days at
 15 525 °C (977 °F) and 10 days at 260 °C (500 °F)). As shown in Figure 1-2, Kearns' dissolution
 16 correlation for Zircaloy-2 and Zircaloy-4 is in excellent agreement with the correlation of
 17 Kammenzind et al. (e.g., 207 wppm versus 210 wppm at 400 °C (752 °F), and 127 wppm versus
 18 133 wppm at 350 °C (662 °F)) and is well within experimental error. In terms of precipitation,
 19 the temperature drop ($\Delta T_{dp} = T_d - T_p$, where T_d and T_p are the corresponding temperatures in
 20 the solubility and precipitation curves at the same hydrogen content) required for precipitation is
 21 approximately 65 °C (117 °F). That is, for irradiated cladding that contains no radial hydrides
 22 prior to heating, the 65 °C (117 °F) temperature decrease is necessary to initiate precipitation of

1 radial hydrides.⁴ However, if circumferential hydrides are present at the peak cladding
2 temperature, some hydrogen will precipitate by growth of the existing circumferential hydrides
3 during this 65 °C (117 °F) temperature drop because of the lower energy required to grow rather
4 than to initiate precipitation of new hydrides (Colas et al., 2014). The strain field remaining from
5 the regions of the hydrides that dissolved during heating also facilitates the growth of existing
6 hydrides.

7 McMinn et al. (2000) used a different method (differential scanning calorimetry) to generate an
8 independent data set for dissolution-precipitation curves per non-irradiated and lightly-irradiated
9 Zircaloy-2 and Zircaloy-4 samples with low hydrogen content (≤ 77 wppm with most data at ≤ 60
10 wppm) exposed to temperatures less than 320°C (608 °F). The data show the effects of
11 irradiation (increase in solubility), as well as pre-annealing time and temperature (decrease in
12 solubility). The increase in hydrogen solubility for irradiated materials is likely the result of
13 hydrogen trapped in irradiation-induced defects. However, it is not clear yet whether the
14 trapped hydrogen is available for precipitation unless the temperature is high enough to anneal
15 out some of these defects. Extrapolation of the dissolution correlation of McMinn et al. (2000)
16 for non-irradiated cladding alloys gives only 172 wppm of dissolved hydrogen at 400 °C (752 °F)
17 and 102 wppm at 350 °C (662 °F), while the data for irradiated cladding agree quite well with
18 the correlations of Kammenzind et al (1996) and Kearns (1967). The staff considers these two
19 sources to be reasonably representative of dry storage and transportation because the long
20 annealing times used to achieve equilibrium for dissolution are more applicable to drying-
21 storage than the much shorter times used for measurements taken by differential scanning
22 calorimetry. Further, the staff considers these data to provide an upper bound for non-irradiated
23 cladding and close to a best fit for irradiated cladding.

24 The amount of hydrogen dissolved will depend on the peak cladding temperature during drying-
25 transfer, dry storage, and transport operations. This temperature is typically achieved during
26 vacuum drying, which generally takes about 8 to 40 hours depending on the DSS or transport
27 package design and loading parameters. Figure 1-2, along with an assessment of the axial
28 hydrogen content of the fuel rods and the peak cladding temperature, can be used to estimate
29 the amount of dissolved hydrogen for a given allowable fuel in a DSS or transportation package.
30 The degree of reorientation will depend on the fuel cladding fabrication process, as well as the
31 cladding hoop stresses and temporal thermal profile of the fuel during operations. The following
32 discussions provide additional details on these parameters.

33 **1.5.2 Fuel Cladding Fabrication Process**

34 The cladding alloy and corresponding fabrication process are important factors for determining
35 the extent of hydride reorientation. Two predominant cladding microstructures are produced
36 during fabrication of zirconium-based cladding: CWSRA and RXA. Zircaloy-4 and ZIRLO are
37 generally CWSRA, whereas Zircaloy-2 and M5 are RXA. Because hydrides tend to precipitate
38 in the grain boundaries, RXA claddings are more susceptible to hydride reorientation, since
39 these cladding types have a larger fraction of grain boundaries in the radial direction (equiaxed
40 grains) relative to CWSRA claddings (which have more elongated grains).

⁴ This hysteresis is the basis for the guidance in ISG-11, Revision 3 (NRC, 2003a), to limit repeated thermal cycling (repeated heatup/cool-down cycles) during loading operations to less than 10 cycles, with cladding temperature variations that are less than 65 °C (117 °F) each.

1 1.5.3 End-Of-Life Rod Internal Pressures and Cladding Hoop Stresses

2 Most rods are initially backfilled with a pressurized inert helium atmosphere to improve thermal
3 conductivity during irradiation and to decrease the rate of cladding creep-down onto the fuel.
4 During the course of irradiation, fission gases are generated in the fuel pellets. Some of the
5 fission gas will be released to the void volume within the fuel column and plenum. The fission
6 gas released is about 1 to 3 percent for PWR fuel rods irradiated under low-to-moderate
7 conditions up to a burnup of about 45 GWd/MTU, at which point the rate of release increases
8 gradually to about 5 to 7 percent for a burnup of 65 GWd/MTU. For BWR fuel rods, the fission
9 gas release can be in the range of 10 to 15 percent at burnups exceeding 45 GWd/MTU. PWR
10 fuel rods with internal burnable poisons (e.g., boron-10 in zirconium-diboride coating on fuel
11 pellets) can also release decay gases (e.g., helium) within the fuel rod. The pressure of these
12 gases in PWR fuel rods increases with burnup due to the increase in fission gas release, the
13 decay gases released from the burnable poisons, and the decrease in void volume resulting
14 from cladding creep down and fuel swelling.

15 The internal pressure of the rod exerts hoop and axial stresses in the cladding, which increase
16 with burnup because of the increase in internal pressure and the decrease in cladding thickness
17 due to waterside corrosion (i.e., oxidation). For BWR fuels, increased cladding oxidation and
18 hydrogen pickup are observed at burnups exceeding 50 GWd/MTU. In PWRs, hydrogen pickup
19 is usually correlated to the oxide thickness, which varies depending on the alloy. The condition
20 of the fuel as it is removed from the reactor is described more fully in the International Atomic
21 Energy Agency (IAEA) Nuclear Energy Series NF-T-3.8 (IAEA, 2011).

22 Post-irradiation examination of cladding specimens subjected to representative drying-transfer
23 and dry storage operations has shown that the degree of radial hydride precipitation is very
24 sensitive to the peak cladding hoop stresses. The range of relevant hoop stresses depends on
25 the range of end-of-life (EOL) rod internal pressures (RIPs), the range of average gas
26 temperatures within fuel rods during drying and storage, and geometric factors used to convert
27 the pressure differences across the cladding to cladding hoop stresses. The following sections
28 discuss these topics.

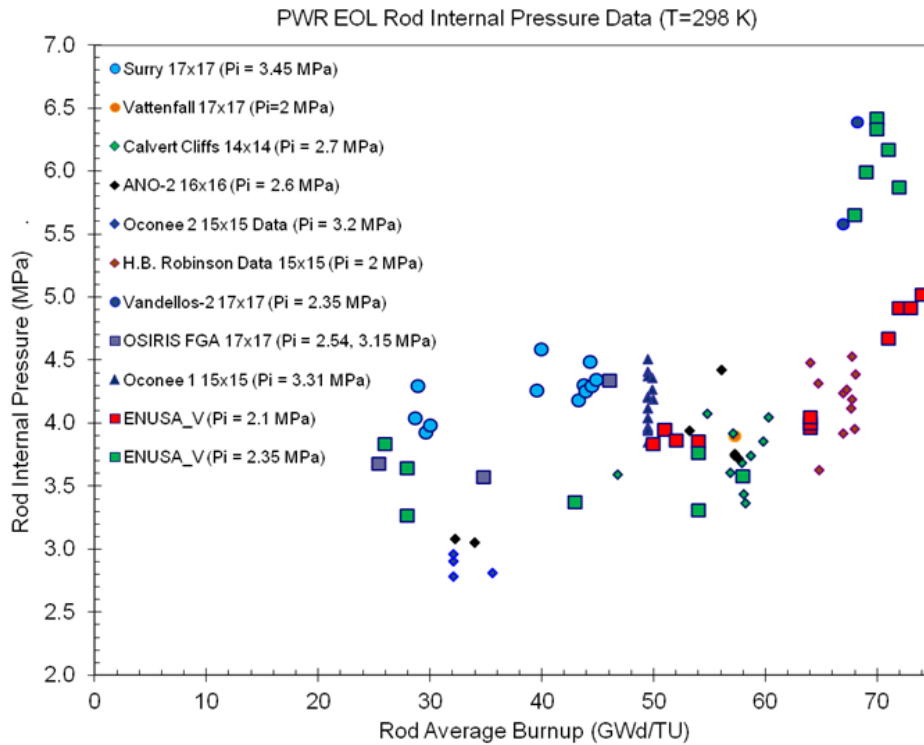
29 1.5.3.1 End-Of-Life Rod Internal Pressures for Pressurized-Water Reactor Fuel Rods

30 The publicly-available database for EOL RIPs for PWR fuel rods is sparse relative to the
31 number of rods that have been irradiated. In addition, the RIP data in this database are for
32 standard fuel rods, mostly those clad in zirconium-tin alloy (Zircaloy-4) with older (1975-1985)
33 fuel designs and reactor operating conditions. Thus, the database is heavily populated with
34 data from what are generally called “legacy” fuel rods. Figure 1-3 shows the publicly-available
35 data for standard fuel rods, as collected by the Electric Power Research Institute (EPRI)
36 (Machiels, 2013). Data points are for EOL RIPs extrapolated to 25 °C (77 °F), and are identified
37 by the reactor, the assembly design, and the as-fabricated helium fill pressure at 25°C (77 °F).
38 Data points labeled as “ENUSA” are for fuel rods irradiated in the Vandellós Unit 2 reactor in
39 Spain.

40 The database consists of 92 data points:

- 41 • 27 at ≤ 45 GWd/MTU (24 Zircaloy-4 and 3 ZIRLO)
- 42 • 35 in the range of >45 GWd/MTU to 60 GWd/MTU (25 Zircaloy-4 and 10 ZIRLO)
- 43 • 30 in the range of >60 GWd/MTU to 74 GWd/MTU (15 each of Zircaloy-4 and ZIRLO)

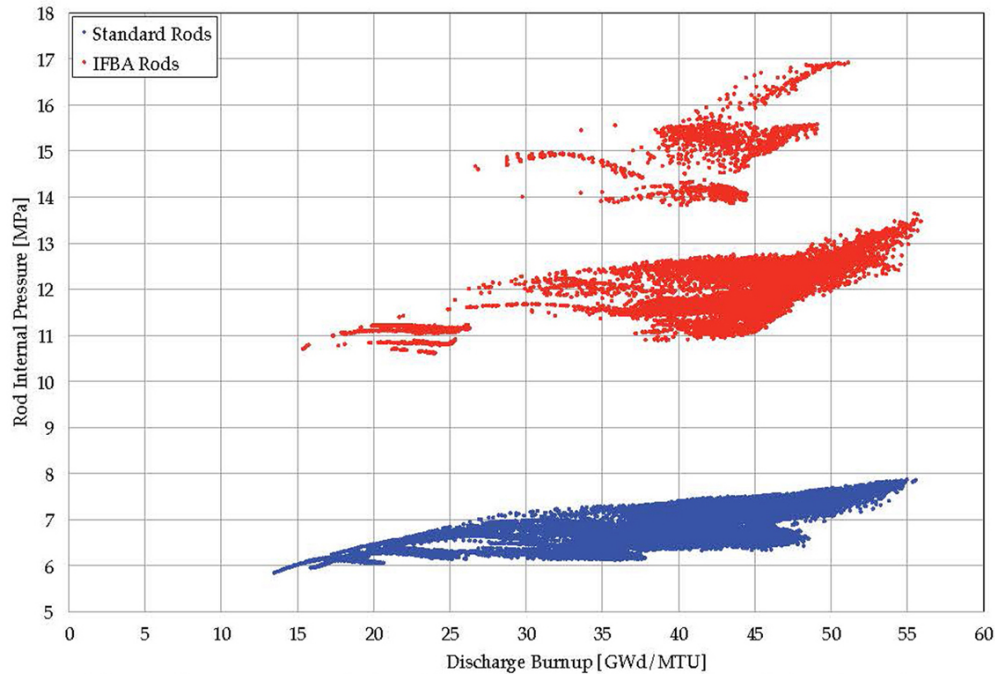
1 Publicly available EOL RIP data are not available for M5-clad SNF rods. Helium fill pressures at
 2 fabrication range from 2.00 MPa (290 psi) – 3.45 MPa (500 psi). The EOL RIP data appear to
 3 be relatively flat between about 40 GWd/MTU and 65 GWd/MTU.



4 **Figure 1-3 Publicly-Available Data Collected by EPRI for PWR End-Of-Life**
 5 **Rod Internal Pressures at 25°C (77 °F) (Reproduction of Figure 2-1 from**
 6 **Machiels (2013))**

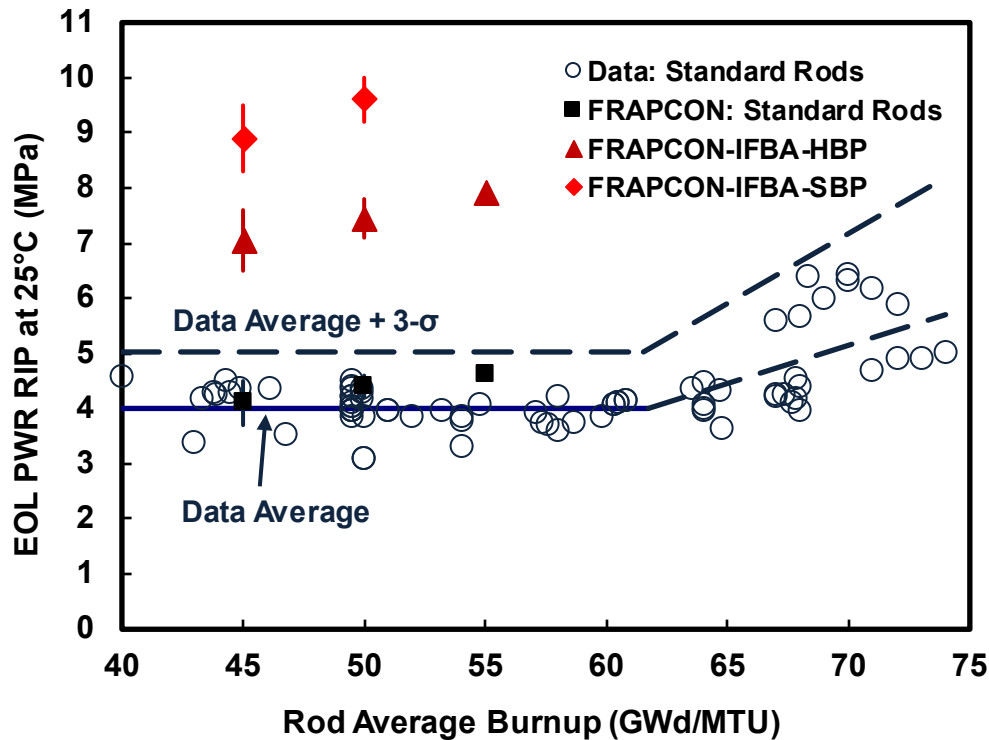
7 Publicly available data are also not available for ZIRLO-clad integral fuel burnable absorber
 8 (IFBA) rods (zirconium diboride-based), which would have the highest EOL RIP values. Given
 9 the sparsity of the database and the absence of publicly available data for standard M5-clad
 10 rods and ZIRLO-clad IFBA rods, predictions are needed for a wide range of advanced cladding
 11 alloys, advanced fuel designs, and more current operating conditions.

12 Two more recent public reports provided EOL RIP values for ZIRLO-clad IFBA rods from
 13 calculations performed with FRAPCON, an NRC-sponsored fuel performance code. Oak
 14 Ridge National Laboratory (ORNL) published a set of calculations for over 68,000 Zircaloy-4
 15 and ZIRLO fuel rods irradiated during the first 10 cycles of the Watts Bar Nuclear Plant Unit 1
 16 reactor (Bratton et al, 2015). FRAPCON was used to predict RIPs for standard rods and IFBA
 17 rods irradiated for one cycle, two cycles, and three cycles, with each cycle consisting of
 18 18 months. ORNL modified the FRAPCON code to account for the helium release from the
 19 IFBA rods. Figure 1-4 shows the results extrapolated to 400 °C (752 °F), which show the end-
 20 of-cycle RIP values for the IFBA rods were calculated to be higher than the values for
 21 standard rods.



1 **Figure 1-4** Calculated Rod Internal Pressures for the First 10 Cycles of the Watts Bar
 2 Nuclear Plant Unit 1 Reactor Under Vacuum Drying Conditions ($P_o = 133$ Pa
 3 (1 Torr); $T_{\text{cladding}(\text{Max})} = 400^\circ\text{C}$ (752 °F) (Reproduction of Figure 4.24 from
 4 Bratton et al. (2015)). The Data Points Shaded in Blue are for Standard Fuel
 5 Rods (Approximately 21,000 Rods). The Data Points Shaded in Red are for
 6 IFBA Fuel Rods (Approximately 47,000 Rods), with the Lower Values for
 7 IFBA Fuel with Annular Blanket Pellets and the Higher Values for Solid
 8 Blanket Pellets

9 ORNL's calculated end-of-cycle RIPs from Figure 1-4 were extrapolated to 25 °C (i.e. the
 10 temperature for EPR's EOL RIP data) to allow comparison with the results in Figure 1-4.
 11 Figure 1-5 shows the aggregated RIP data at 25 °C (77 °F) within the burnup range of 40 to
 12 74 GWd/MTU, along with best-fit and 3- σ correlations. Within the relevant burnup range of 40
 13 to 62 GWd/MTU, the average $\pm 3\text{-}\sigma$ values are 4.0 ± 1.0 MPa ($(5.8 \pm 1.4) \times 10^2$ psi) for standard
 14 fuel rods with Zircaloy-4 and ZIRLO cladding alloys. The 3- σ value of 5.0 MPa (7.3×10^2 psi) is
 15 a reasonable upper bound of data and calculated values for standard fuel rods. Furthermore,
 16 reasonable upper bounds for data on IFBA rods are 7.9 MPa (1.1×10^3 psi) at 25 °C (77 °F) for
 17 fuel designs with hollow (annular) pellets and 10.0 MPa (1.5×10^3 psi) for fuel designs with solid
 18 pellets.



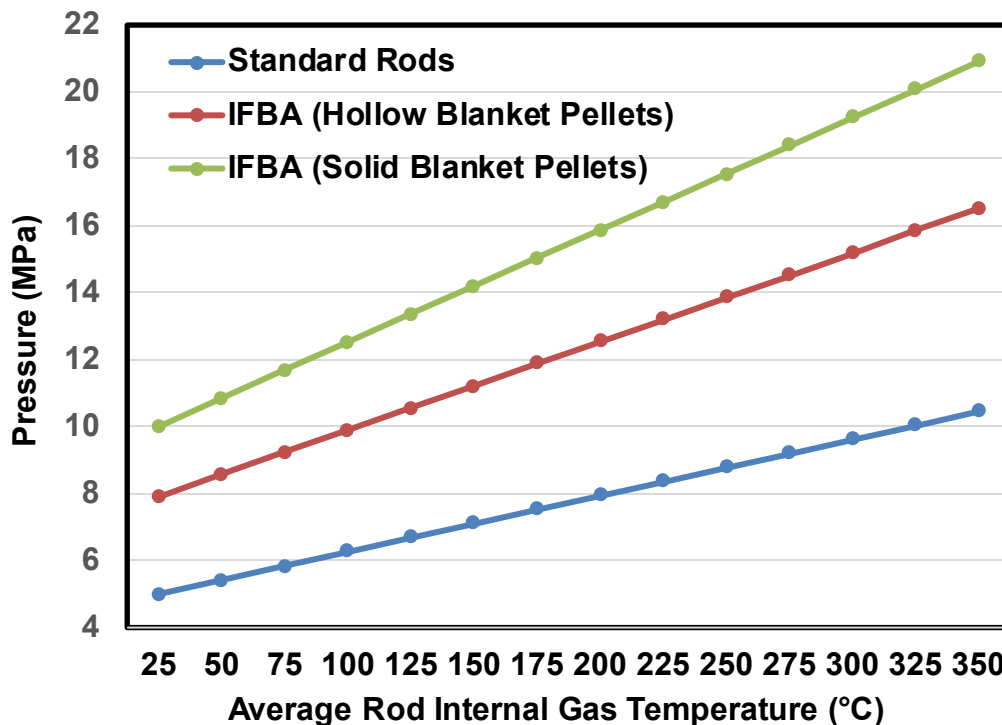
1 **Figure 1-5 Aggregated Measured and Calculated Values for End-Of-Life Rod Internal**
 2 **Pressures for PWR Fuel Rods. Pressures are Presented at 25 °C (77 °F)**

3 More recently, Richmond and Geelhood (2017) used FRAPCON to calculate EOL RIP for three
 4 modern fuel designs with three representative dry storage thermal transients, each involving
 5 drying operations with a peak cladding temperature of 400 °C (752 °F). The analyses
 6 characterized the effects of fuel design to determine reasonably bounding cladding hoop
 7 stresses. The report provides results for maximum EOL RIP for IFBA rods to be limited to
 8 10.6 MPa (1.5×10^3 psi). These results suggest that, even at a peak cladding temperature of
 9 400 °C (752 °F), the maximum cladding hoop stresses remain below 90 MPa (1.3×10^4 psi) for
 10 the bounding ZIRLO-clad IFBA rods. At these pressures, the extent of hydride reorientation will
 11 be very limited, if observed at all, which would indicate that the mechanical properties from the
 12 as-irradiated condition will remain unchanged. The staff recognizes the discrepancies in the
 13 results between Bratton et al. (2015) and Richmond and Geelhood (2017) and is evaluating the
 14 merits of both approaches used for the FRAPCON analyses. Until that evaluation is complete,
 15 since the data of Bratton et al (2015) results in the highest EOL RIP and corresponding hoop
 16 stresses, the staff will assume those values to be conservative and bounding when evaluating
 17 the potential of hydride reorientation.

18 **1.5.3.2 Gas Temperatures for Fuel Rods During Drying-Transfer, Storage And**
 19 **Transportation**

20 Peak temperatures for the gas inside fuel rods are highly dependent on the DSS or
 21 transportation package design, fuel system design, fuel burnup, operating history, package
 22 loading density, and the length of time the fuel was cooling in the spent fuel pool. Figure 1-6

1 shows the extrapolation of the upper-bound pressures shown in Figure 1-5 to rod internal gas
 2 temperatures that may be experienced during drying-transfer, dry storage and transportation.
 3 The data are presented for the relevant burnup range of 45 to 62 GWd/MTU.



4 **Figure 1-6** Calculated Rod Internal Pressure (Average + 3σ ; 45 To 62 Gwd/MTU) as a
 5 **Function of the Spatially Averaged Gas Temperature for PWR Fuel Rods**
 6 **(i.e., Standard Rods), ZIRLO-Clad IFBA Rods with Hollow (Annular) Blanket**
 7 **Pellets, and ZIRLO-Clad IFBA Rods with Solid Blanket Pellets**

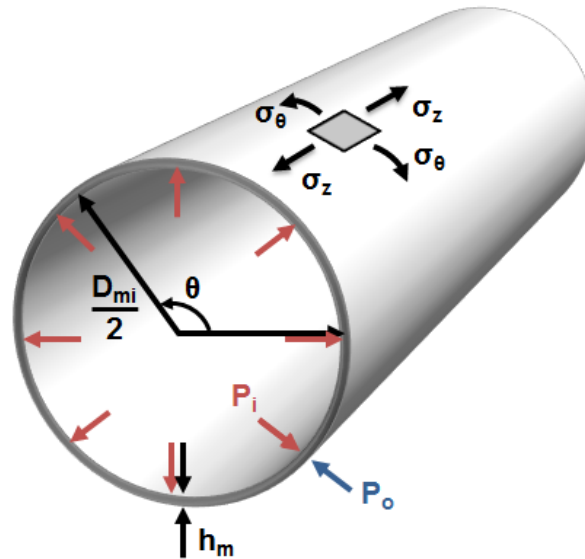
8 **1.5.3.3** *Peak Cladding Hoop Stresses for Pressurized-Water Reactor Fuel Rods During*
 9 *Drying-Transfer and Storage/Transport Operations*

10 The cladding hoop stress (σ_{θ}) is a function of the gas pressure difference across the cladding
 11 wall ($P_i - P_o$), where P_i is the internal rod pressure and P_o is the external pressure, the cladding
 12 inner diameter (D_{mi}), and the cladding metal wall thickness (h_m), as shown in Eqn. 1-1 for the
 13 average hoop stress across the cladding wall (Figure 1-7). Gap closure is not considered.

14
$$\sigma_{\theta} = [D_{mi} / (2 \cdot h_m)] (P_i - P_o) \quad \text{(Eqn. 1-1)}$$

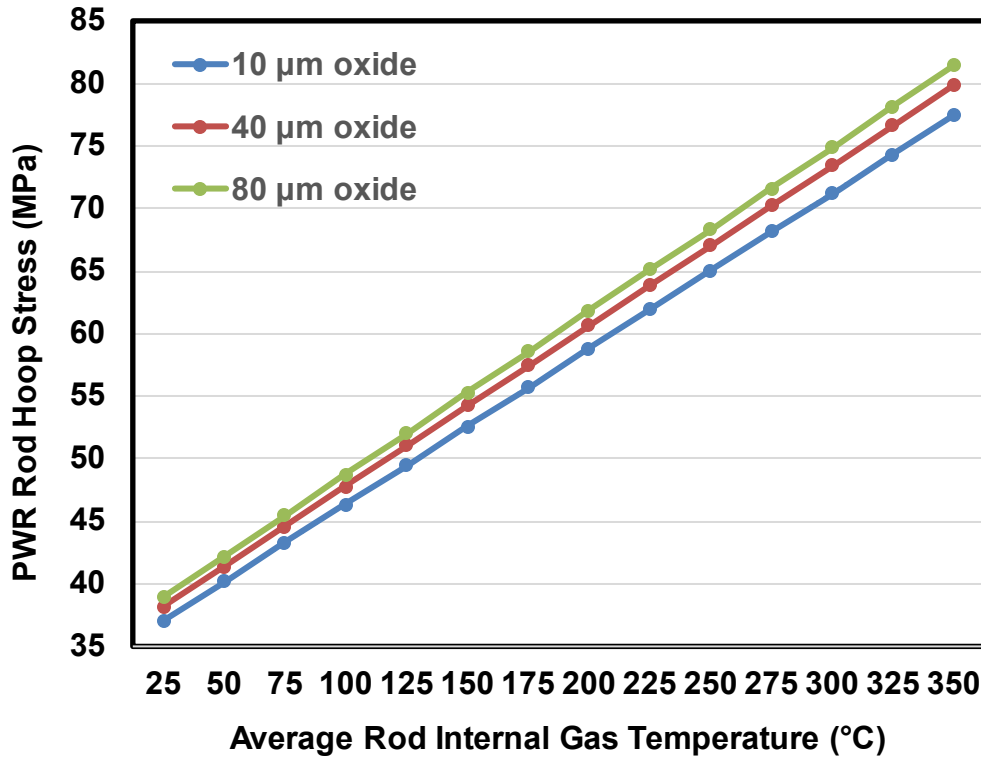
15 The geometrical parameter $D_{mi}/(2 \cdot h_m)$ will tend to increase with burnup due to waterside
 16 corrosion of the cladding outer surface, which reduces h_m . Nominal as-fabricated values of D_{mi}
 17 and h_m for standard 17 × 17 PWR fuel rods are 8.36 mm and 0.57 mm, respectively, which
 18 gives a geometrical factor of 7.33. However, fuel rod cladding is manufactured to specifications
 19 with tolerances (i.e., ± values) for the outer diameter and inner diameter and a minimum wall
 20 thickness (e.g., > 0.56 mm). Thus, even for fresh fuel rods, the geometrical parameter will vary
 21 somewhat along the length of one fuel rod and from fuel rod to fuel rod. For LBU SNF, the
 22 decrease in h_m is small and is partially counteracted by the decrease in D_{mi} due to creep down.

- 1 For HBU SNF with creep out resulting from fuel-cladding mechanical interaction, D_{mi}
 2 approaches its as-fabricated value and h_m continues to decrease with burnup.



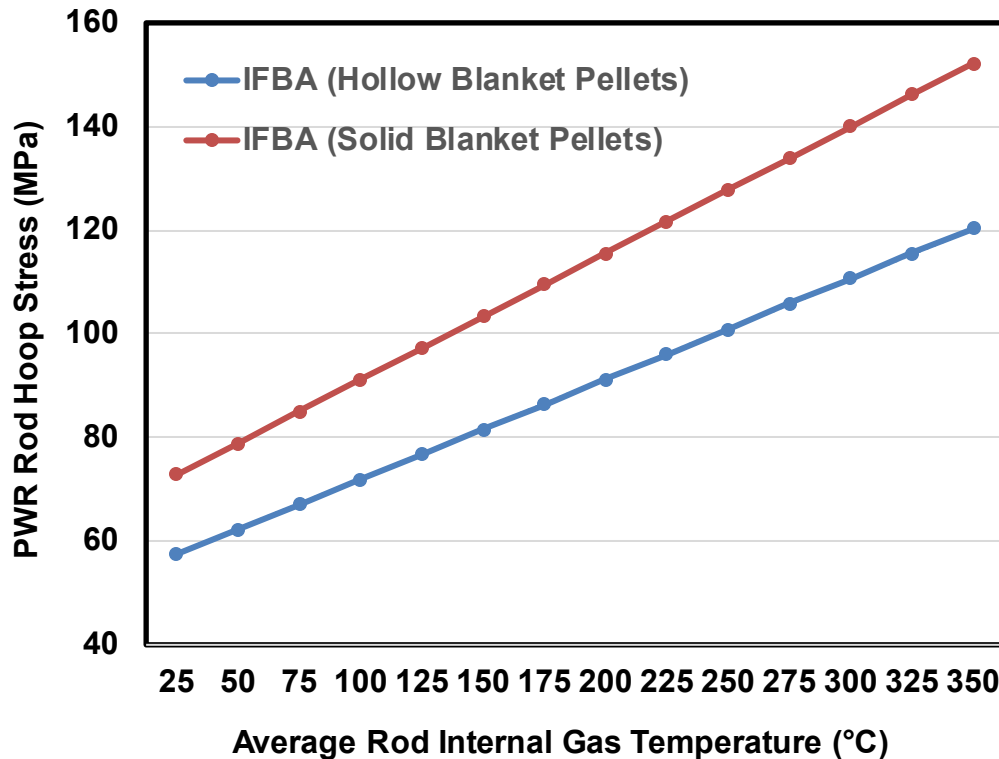
3 **Figure 1-7 Fuel Cladding Tube with Stress Element Displaying Hoop Stress (Σ_{θ}),**
 4 **Longitudinal Stress (Σ_z), Internal Pressure (P_i), Cladding Thickness (H_m),**
 5 **External Pressure (P_o), Circumferential Coordinate (Θ), and Inner Cladding**
 6 **Diameter (D_{mi})**

7 Example calculations may be performed assuming that the EOL inner cladding diameter (D_{mi}) is
 8 8.36 mm (i.e., the as-fabricated value) with oxide layer thicknesses of 10 μm (e.g., M5), 40 μm
 9 (e.g., ZIRLO), and 80 μm (e.g., Zircaloy-2, Zircaloy-4). The corresponding values of the
 10 geometrical factor for these corrosion layers are: 7.41, 7.64, and 7.79. These factors are used
 11 in Eqn. 1-1 to generate the cladding hoop stress versus average gas temperature for several
 12 values of corrosion layer thickness. The value of P_o (varies from approximately 4×10^{-4} MPa
 13 (3 Torr) for vacuum drying to less than 0.5 MPa (3.8×10^3 Torr) for storage) is assumed to be
 14 zero for these calculations. Figure 1-8 shows that the hoop stress is a strong function of the
 15 average gas temperature and a weaker function of the corrosion-layer thickness. Calculated
 16 cladding hoop stress values varied from 57 MPa (8.3×10^3 psi) at 180 $^{\circ}\text{C}$ (356 $^{\circ}\text{F}$) for the 10- μm
 17 oxide case to 83 MPa (1.2×10^4 psi) at 340 $^{\circ}\text{C}$ (644 $^{\circ}\text{F}$) for the 80- μm oxide case.



1 **Figure 1-8** Calculated Values of Cladding Hoop Stress (Average + 3σ ; 45 To 62
 2 **Gwd/MTU) Vs. the Spatially-Averaged Internal Gas Temperature for**
 3 **Standard 17×17 PWR Fuel Rods With Corrosion Layers of 10 μm, 40 μm,**
 4 **and 80 μm**

5 For ZIRLO-clad IFBA rods, some 17 × 17 designs use smaller diameter cladding
 6 (9.14 mm (0.360 in.)) and comparable cladding wall thickness (0.572 mm (0.023 in.)). This
 7 design is called the “optimized fuel assembly.” The geometrical factor for converting pressure to
 8 hoop stress is 7.00 for as-fabricated cladding and 7.28 for cladding with a 40-μm corrosion
 9 layer, which assumes the cladding inner diameter (8.00 mm (0.315 in.)) remains the same as the
 10 as-fabricated inner diameter for HBU SNF. Figure 1-9 shows that the cladding hoop stress for
 11 the 40-μm corrosion-layer case increases with gas temperature from about 90 MPa
 12 (1.3×10^4 psi) to 120 MPa (1.7×10^4 psi) for IFBA fuel with hollow blanket pellets and from
 13 about 110 MPa (1.6×10^4 psi) to 150 MPa (2.2×10^4 psi) for IFBA fuel with solid blanket pellets.



1 **Figure 1-9 PWR Hoop Stress as a Function of Internal Gas Temperature for 17 × 17**
 2 **IFBA Fuel Rods (for Both Hollow Blanket and Solid Blanket Pellets) with a**
 3 **40-μm Corrosion Layer**

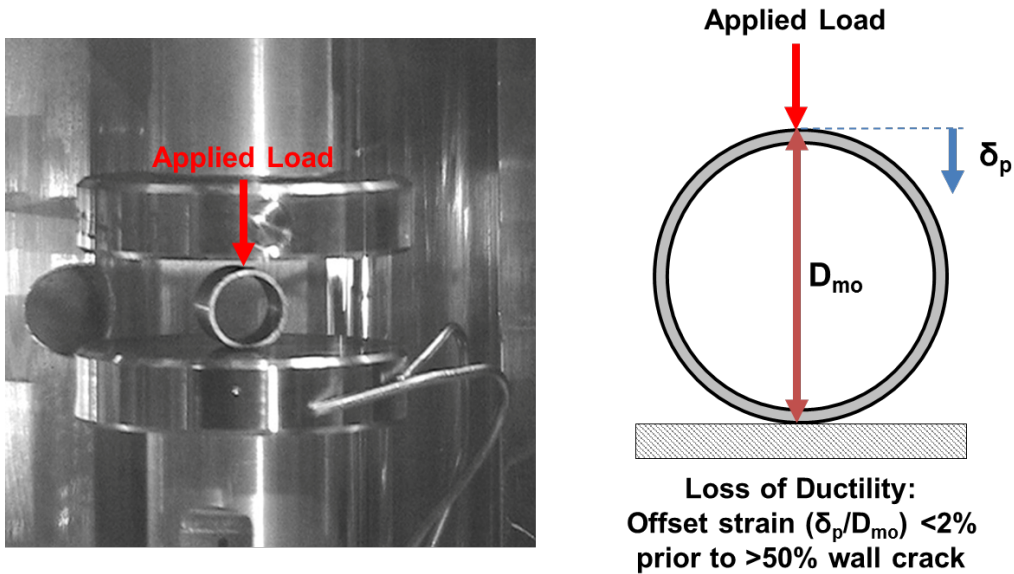
4 The above discussion provides a technical basis for the staff to define conservative bounding
 5 cladding hoop stress conditions for the testing of HBU SNF mechanical performance, as the
 6 assessment in Chapter 2 will discuss.

7 **1.5.4 Ring Compression Testing**

8 Ring compression testing (RCT) has been conducted in the United States and Japan to assess
 9 residual ductility of cladding with reoriented hydrides following pinch loads (Aomi et al., 2008;
 10 Billone et al., 2013; Billone et al., 2014; Billone et al., 2015). RCT of zirconium-based cladding
 11 alloys has shown reduced ductility when subjected to pinch loads at a sufficiently low
 12 temperature; this temperature has been generally referred to as a ductile-to-brittle transition
 13 temperature or ductility transition temperature (DTT).

14 In previous NRC-sponsored research, Argonne National Laboratory (ANL) sectioned rings from
 15 pressurized-and-sealed rodlets fabricated with cladding from ZIRLO-clad and Zircaloy-4-clad
 16 fuel rods irradiated to high burnup (beyond the NRC’s peak rod licensing limit in
 17 commercial PWRs) (Billone et al., 2013) (Figure 1-10). These rodlets had been heated to a
 18 peak temperature of 400 °C (752 °F) (consistent with the guidance limit in ISG-11, Revision 3
 19 (NRC, 2003a) and held at this temperature for 1 to 24 hours with variable target hoop stresses
 20 (110 MPa (1.6 × 10⁴ psi), 140 MPa (2.0 × 10⁴ psi)), and then slow-cooled at 5 °C/h (9 °F/h)
 21 under conditions of decreasing pressure and hoop stress. Metallographic examination of one
 22 cladding ring surface per rodlet was used to quantify the degree of radial hydride precipitation in
 23 terms of the average length of radial hydrides. Several other rings were used to determine the

- 1 average hydrogen content of the rodlet, along with circumferential and axial variations in
- 2 hydrogen content. Up to four rings were subjected to RCT to induce pinch loads at test
- 3 temperatures from 20 °C (68 °F) to 200 °C (392 °F).

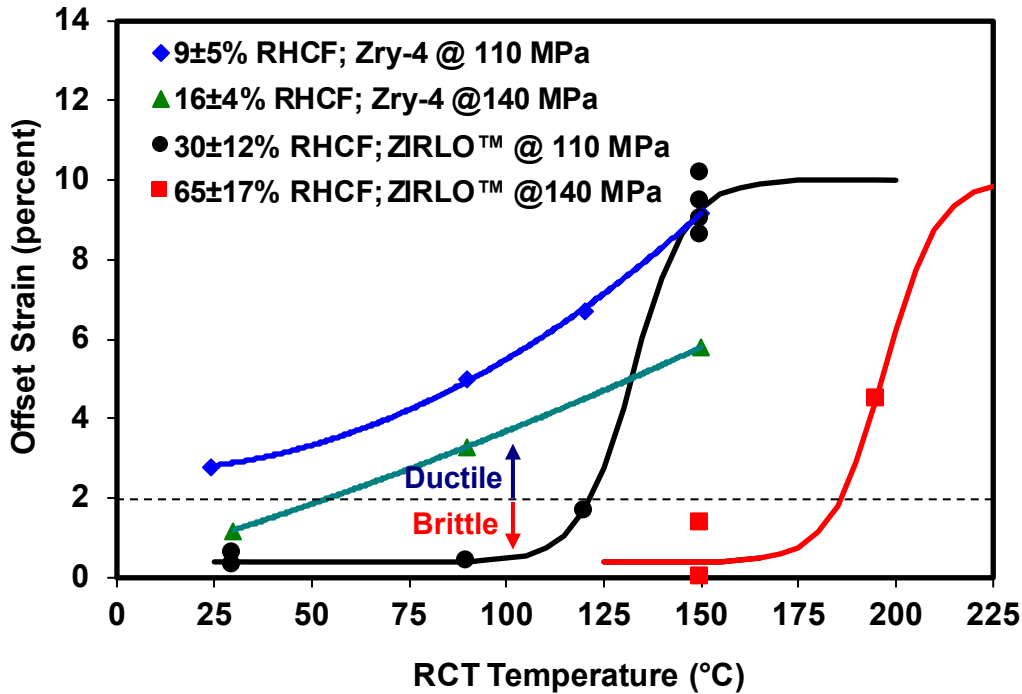


4 **Figure 1-10 RCT of a Sectioned Cladding Ring Specimen in ANL’s Instron’s 8511 Test**
 5 **Setup. Tests Were Conducted in the Displacement-Controlled Mode to a**
 6 **1.7-Mm Maximum Displacement in a Controlled Temperature Environment (**
 7 **Δ_p = RCT Offset Displacement at 12 O’clock Position Relative to Static**
 8 **Support at 6 O’clock; D_{mo} = Outer Diameter of Cladding Metal; Δ_p/D_{mo} =**
 9 **RCT Offset Strain (Percent)) (Reproduction Of Figure 6 From Billone et al.,**
 10 **2012))**

11 RCT load-displacement curves were used to determine the offset displacement (normalized to
 12 the pretest sample outer diameter to give offset strain) as a function of test temperature. The
 13 offset strain was plotted against test temperature for each rodlet to determine the DTT
 14 (see Figure 1-11). Post-RCT metallographic examinations were also performed to determine
 15 the number and extent of cracks that had formed, as well as to generate additional data for the
 16 degree of radial hydride precipitation (Billone, et al., 2013).

17 To define ductility per RCT load-displacement data, a 2-percent offset strain (δ_p/D_{mo}) before a
 18 crack extended through more than 50 percent of the cladding wall thickness was chosen as the
 19 figure of merit for the transition between ductile and brittle behavior (Billone et al., 2013). Figure
 20 1-11 shows representative deformation (i.e., offset strain) curves as a function of the alloy, peak
 21 hoop stress at a 400 °C (752 °F) peak cladding temperature, and actual RCT temperature. The
 22 figure also shows the radial hydride continuity factor (RHCF), which represents the effective
 23 radial length of continuous radial-circumferential hydrides normalized to the wall thickness. ANL
 24 used the RHCF as a figure of merit for determining the degree and severity of radial hydride
 25 precipitation. The radial hydrides in Zircaloy-4 HBU SNF ring specimens were relatively short
 26 (i.e., RHCF of 9 percent for a peak hoop stress of 110 MPa (1.6×10^4 psi), and 16 percent for a
 27 peak hoop stress of 140 MPa (2.0×10^4 psi)) and the ductility increased gradually with
 28 temperature. In ZIRLO-clad HBU SNF ring specimens, the radial hydrides were longer (i.e.,
 29 RHCF of 30 percent for a peak hoop stress of 110 MPa (1.6×10^4 psi), and 65 percent for a

1 peak hoop stress of 140 MPa (2.0×10^4 psi)) and the ductility increased sharply with the
 2 increase in RCT temperature. ANL fit the limited ZIRLO data points with S-shaped curves
 3 (hyperbolic tangent functions) typical of materials that exhibit a ductile-to-brittle transition. The
 4 data show that the DTT shifted from around room temperature in a cladding material with short
 5 radial hydrides to higher values in a cladding material with longer radial hydrides. The limited
 6 data also indicates a trend of lower DTTs for materials with lower peak cladding stresses.



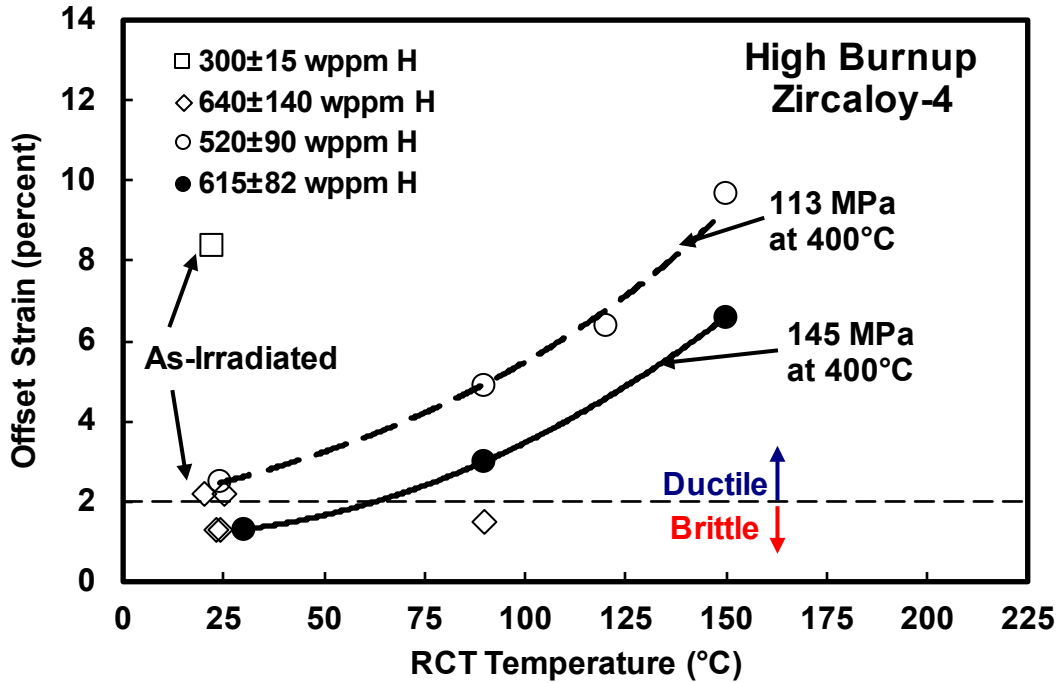
7 **Figure 1-11 Ductility vs. RCT for Two PWR Cladding Alloys Following Slow Cooling**
 8 **from 400°C (752 °F) at Peak Target Hoop Stresses of 110 Mpa (1.6×10^4 Psi)**
 9 **and 140 Mpa (2.0×10^4 Psi) (From Billone et al., 2013)**

10 ANL also conducted RCT research under DOE sponsorship. It obtained results for the following
 11 (Billone et al., 2014; Billone et al., 2015):

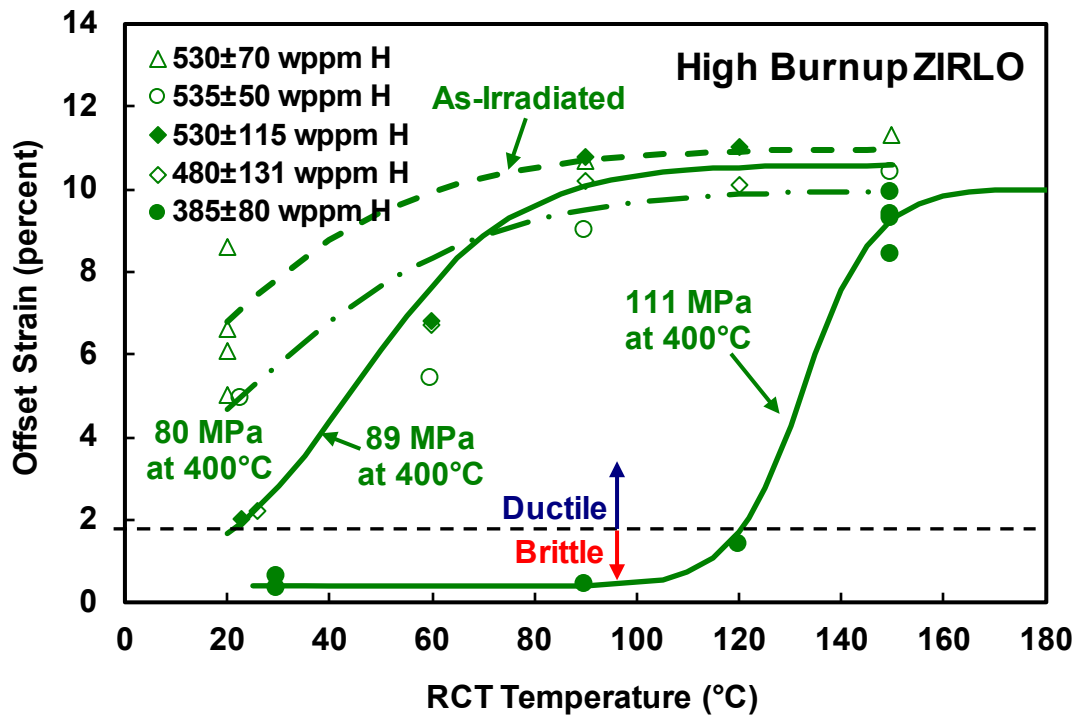
- 12 • HBU Zircaloy-4 in the as-irradiated condition with moderate-to-high hydrogen content
- 13 • HBU ZIRLO in the as-irradiated condition and following simulated drying-storage at peak
 14 temperatures of 400 °C (752 °F) and 350 °C (662 °F) with peak hoop stresses from
 15 80 MPa (1.2×10^4 psi) to 94 MPa (1.4×10^4 psi)
- 16 • HBU M5 in the as-irradiated condition and following simulated drying-storage at
 17 400 °C (752 °F) with peak hoop stresses of 90 MPa (1.3×10^4 psi), 110 MPa
 18 (1.6×10^4 psi), and 140 MPa (2.0×10^4 psi)

19 ANL conducted two additional tests with HBU ZIRLO cladding subjected to three drying cycles
 20 (e.g., from 400 °C (752 °F) to 300 °C (572 °F) and from 350 °C (662 °F) to 250 °C (482 °F)) at
 21 peak hoop stress of about 90 MPa (1.3×10^4 psi). The latter results suggest that multiple drying

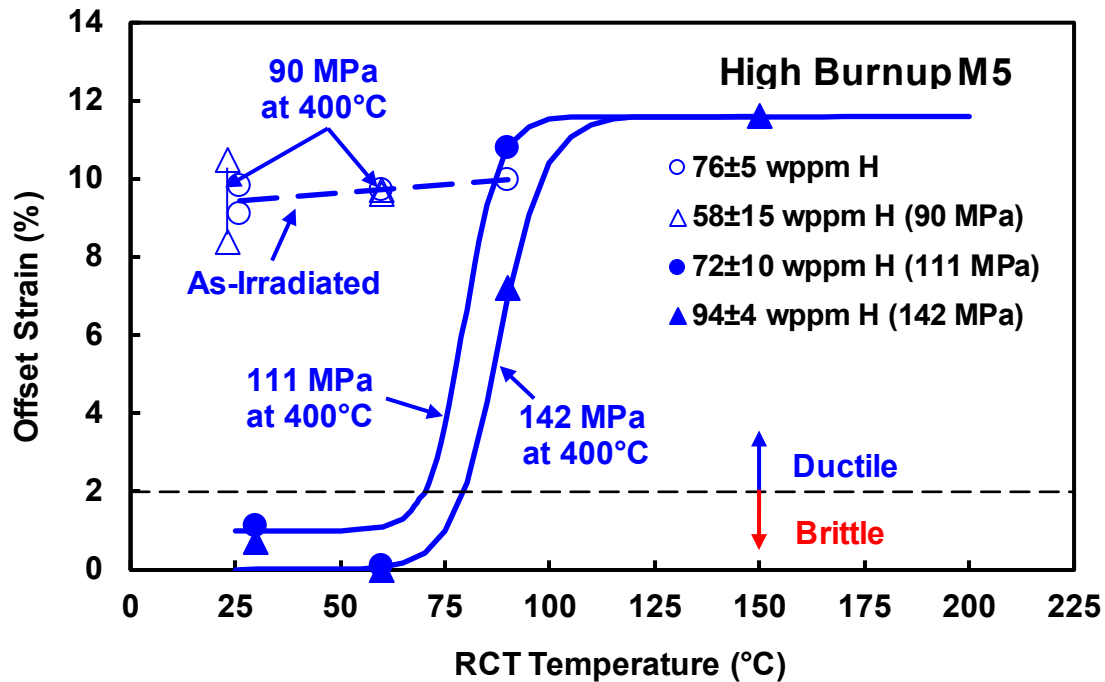
1 cycles have no effect on the length of radial hydrides or the DTT at this low stress level. Figures
 2 1-12 through 1-14 show results for Zircaloy-4, ZIRLO, and M5 in both as-irradiated and hydride-
 3 reoriented condition following cooling from 400°C (752 °F) (Billone et al., 2014; Billone et al.,
 4 2015).



5 **Figure 1-12 Ductility Data, as Measured by RCT, for As-Irradiated Zircaloy-4 and**
 6 **Zircaloy-4 Following Cooling from 400 °C (752 °F) Under Decreasing**
 7 **Internal Pressure and Hoop Stress Conditions (From Billone et al., 2013)**



1 Figure 1-13 Ductility Data, as Measured by RCT, for as-Irradiated ZIRLO and ZIRLO
 2 Following Cooling from 400 °C (752 °F) Under Decreasing Internal Pressure and
 3 Hoop Stress Conditions (From Billone et al., 2013)



1 **Figure 1-14 Ductility Data, as Measured by RCT, for As-Irradiated M5 and M5 Following**
 2 **Cooling from 400 °C (752 °F) Under Decreasing Internal Pressure and Hoop**
 3 **Stress Conditions (From Billone et al., 2013)**

4 The staff recognizes the uncertainties associated with the ductility curve fits of ANL's RCT data
 5 because of the limited number of data points. However, the limited results appeared to support
 6 the following general conclusions: (1) the DTT generally increases with increasing hoop
 7 stresses (i.e., the ductility transition shifts to higher cladding temperature), (2) both the
 8 susceptibility to radial hydride precipitation and ductility changes depend on cladding type and
 9 initial hydrogen content, and (3) depending on the cladding and test conditions, the DTT can
 10 occur at temperatures in the range of 20 °C (68 °F) to 185 °C (365 °F). The results for as-
 11 irradiated Zircaloy-4 are consistent with studies by Wisner and Adamson (1998) and Bai et al
 12 (1994). The staff considered these conclusions when defining limiting conditions for inducing
 13 radial hydrides and conducting fatigue and bending testing of HBU SNF (see Chapter 2).

14 It is important to note that the DTT is not an intrinsic property of a cladding alloy material with a
 15 given homogeneous composition, in the classical metallurgical sense, but it is highly dependent
 16 on the composite microstructure (hydride-zirconium matrix, as determined by reactor operating
 17 conditions), fabrication conditions (degree of cold working, recrystallization) and the operating
 18 conditions during drying-transfer, storage or transportation (peak cladding temperature, peak
 19 hoop stress, temporal cooling profile). Further, the DTT was established based on an arbitrarily-
 20 defined performance criterion (e.g., 50 percent cladding through-wall crack prior to 2-percent
 21 offset strain deformation), and based on a limited number of data points for each cladding alloy.
 22 It is also important to note that, due to the radial and axial temperature gradients in a DSS or
 23 transportation package, it is highly likely that only a small fraction of the cladding in a given
 24 assembly will reach high enough temperatures and hoop stresses to have sufficient hydride
 25 reorientation during cooling. Those hotter axial locations of the cladding will likely be the last to
 26 reach a DTT during transport.

1 1.5.5 Staff's Assessment of Ring Compression Testing Results

2 As previously discussed, the staff has long expected that hydride reorientation would not
3 compromise cladding integrity due to fuel rod bending (i.e., bending expected during normal
4 conditions of storage and transport), since the principal tensile stress field associated with rod
5 bending caused by lateral inertia loads is parallel to both radial and circumferential hydrides
6 (Tang et al., 2015). The staff has considered that any reduced cladding ductility due to hydride
7 reorientation could only potentially compromise the analyzed fuel configuration for pinch loads
8 experienced during drop accident scenarios, if the fuel had significantly cooled during the
9 transportation period. More specifically, the staff had expressed concern that reorientation
10 could decrease failure stresses and strains in response to transportation-induced pinch loads
11 during a 9-m (30-ft) drop scenario as a result of rod-to-grid spacer contact, rod-to-rod contact, or
12 rod-to-basket contact.

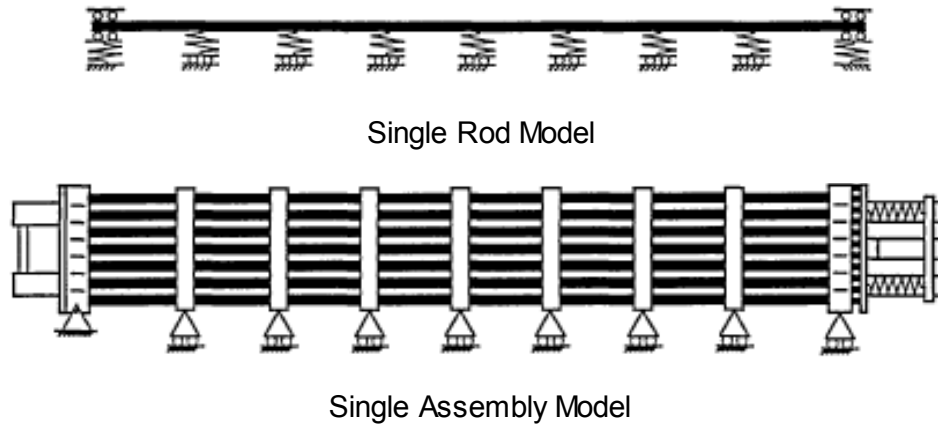
13 To address the concern of reduced ductility during drop accidents, the staff previously proposed
14 varied approaches to demonstrate that the failure limits for as-irradiated cladding as used in the
15 design-basis structural evaluations would continue to be adequate even if hydride reorientation
16 occurred. One of these approaches was based on justifying an RCT-measured DTT for each
17 cladding alloy in the proposed fuel contents, and demonstrating that the minimum cladding
18 temperature remained above the RCT-measured DTT for the entire duration of transport. The
19 minimum cladding temperature assumed for transport operations would need to be bounding to
20 the contents upon consideration of the cold temperature requirement in 10 CFR 71.71(c)(2), i.e.
21 an ambient temperature of -40 °C (-40 °F) in still air and shade. If these conditions were met,
22 then mechanical properties of the as-irradiated cladding material (i.e., material that did not
23 account for the precipitation of radial hydrides), would be considered adequate for the structural
24 evaluation.

25 As an alternative approach, if the applicant could not reasonably demonstrate that sections of
26 the fuel cladding remained above the RCT-measured DTT during the entire duration of
27 transport, the staff proposed that the application provide additional safety analyses assuming
28 hypothetical reconfiguration of the HBU fuel contents. If neither of these two approaches is
29 satisfactory for demonstrating compliance with 10 CFR Part 71 regulations, then the staff would
30 expect that the fuel would be canned and classified as damaged.

31 Since proposing these approaches, the staff has reevaluated whether results from RCT of
32 defueled specimens are accurately representative or if they are overly conservative relative to
33 the actual hoop-loading conditions experienced by the fuel during a 9-m (30-ft) drop. During
34 RCT, the circumferential (hoop) tensile bending stress is perpendicular to the plane of the radial
35 hydrides, which is different from the relative orientation of the applied stress and hydrides under
36 axial tensile bending where the longitudinal (axial) tensile bending stress is always parallel to
37 the plane of both the circumferential and radial hydrides. The orientation of the tensile stress is
38 expected to make a difference in the response of the cladding.

39 The RCT defined a DTT used to determine cladding failure due to pinch loads. However, it is
40 necessary to consider the importance of this failure mode in the determination of cladding
41 integrity in the event of a drop accident. To do this, the RCT must be examined for what it is, a
42 test in which diametrically-opposed concentrated compressive forces are applied to a fuel
43 cladding longitudinal segment that does not contain fuel. During NCT and HAC side drops, the
44 fuel rod is loaded by lateral inertia loads that are resisted by distributed loads applied to the
45 bottom of the rod at the flexible grid spacer springs (Figure 1-15). Further, the inertia load in the

1 rod is transferred to the grid spacer support as a shear force in the cladding (and pellets) not as
2 a concentrated load at the top of the rod.



3 **Figure 1-15 Geometric Models for Spent Fuel Assemblies in Transportation Packages**
4 **(Reproduction, in Part, Of Figure 10 from Sanders et al., 1992)**

5 Given that the forces and displacements in the RCT are measurably different from the actual
6 forces and displacements applied to the rod at the grid spacer support, it is not likely that the
7 pinch-mode of failure will play a significant role in undermining cladding integrity. To quantify
8 the difference between these loading cases, the staff analyzed two ring segments for different
9 loading conditions and the change in diameter calculated. In the first case the ring segment
10 was loaded by diametrically-opposed compressive forces like those of RCT (Case 1, Table 17,
11 Roark and Young (1975)). In the second case the ring segment was supported at the bottom by
12 a concentrated reaction and loaded by a downward load uniformly distributed around the
13 circumference of the ring to simulate a shear loading as in a side drop (Case 13, Table 17,
14 Roark and Young (1975)). In both cases the total applied load was the same. The ratio of the
15 change in diameter of the second case to the first case is 0.48. Thus, the diametrically-opposed
16 compressive forces produced more than twice the displacement when compared to the
17 circumferentially distributed load. In addition, at the pellet-cladding interface, the pellet and
18 cladding are bonded and, thus a gap cannot exist between them. Thus, the staff considers that,
19 under a pinch load, ovalization of the cladding cross-section is very unlikely and any
20 circumferential bending stress that does exist will be negligible. The RCT conducted to date
21 does not account for the rod's resistance to ovalization provided by the pellet.

22 Based on the RCT load-displacement data, ANL defined a figure of merit for cladding ductility
23 (i.e., the transition between ductile and brittle behavior) to be a 2-percent offset strain prior to
24 a crack extending through more than 50 percent of the cladding wall (Billone et al., 2013). If
25 the strains experienced during RCT's diametrically-opposed loads result in twice those that
26 would be experienced during lateral inertial loads, then the DTT is likely to shift to lower
27 temperatures (potentially room temperature or lower). Therefore, the staff considers that the
28 DTT defined by RCT experiments is overly conservative and not representative of actual fuel
29 and stress conditions during NCT and HAC drop scenarios. The DOE is planning on
30 sponsoring a research program in which 25 HBU fuel rods will undergo testing to determine
31 their characteristics, material properties, and rod performance following representative drying-
32 transfer and cooldown (Hanson et al., 2016). The staff expects that material property testing
33 conducted under this program will provide confirmation that the cladding displacements
34 experienced by fueled cladding specimens during RCT will be lower than those measured in

- 1 defueled specimens and that ductility during accident drop scenarios is not compromised.
- 2 Results from the static and fatigue bend testing discussed in Chapter 2 further justify the
- 3 staff's conclusion that the pellet imparts structural support to the mechanical performance of
- 4 the fuel rod.

2 ASSESSMENT OF STATIC BENDING AND FATIGUE STRENGTH RESULTS ON HIGH BURNUP SPENT NUCLEAR FUEL

2.1 Introduction

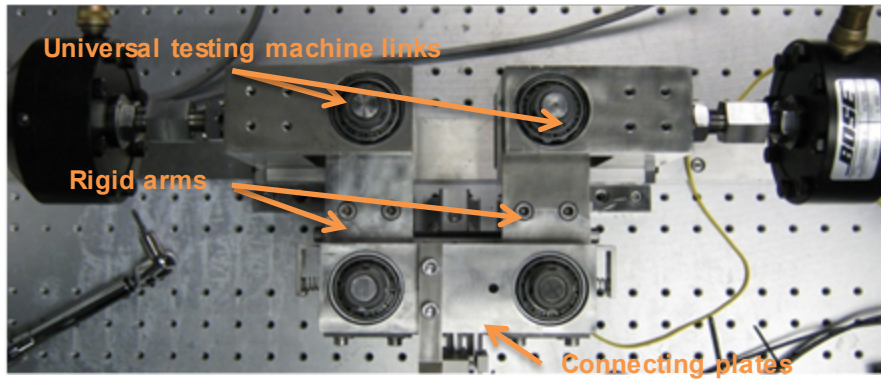
The sealed canister or cask cavity serves as the primary barrier in a dry storage system (DSS) or transportation package for protecting against the release of radioactive solid particles or gases from the loaded spent nuclear fuel (SNF) to the atmosphere. The spent fuel cladding also serves as a confinement or containment barrier for preventing radioactive solid particles and fission gasses from being released into the interior cavity of the DSS or transportation package. The cladding not only provides a barrier for preventing the release of radioactive material but also prevents fuel reconfiguration during storage and transport operations. Therefore, the integrity of the cladding is an essential component of a defense-in-depth strategy to protect the public health and safety.

Until recently, research to understand the structural behavior of spent fuel rods during transportation and storage has focused entirely on obtaining mechanical and strength properties of spent fuel cladding. As a result, the flexural rigidity and structural response of fuel rods during normal and accident events have been based on the mechanical and strength properties of only the cladding. The contribution of the fuel pellets to increasing the flexural rigidity of the rod has been neglected. However, recent research discussed in NUREG/CR-7198, Revision 1, "Mechanical Fatigue Testing of High-Burnup Fuel for Transportation Application," issued October 2017 (NRC, 2017a), on the static bending response and fatigue strength of fuel rods considered as a composite system of cladding and fuel pellets, has begun to provide some of the necessary data to allow a more accurate assessment of the structural behavior of the composite fuel rod system under normal conditions of transport (NCT) and hypothetical accident conditions (HAC), as well as DSS drop and tip-over events.

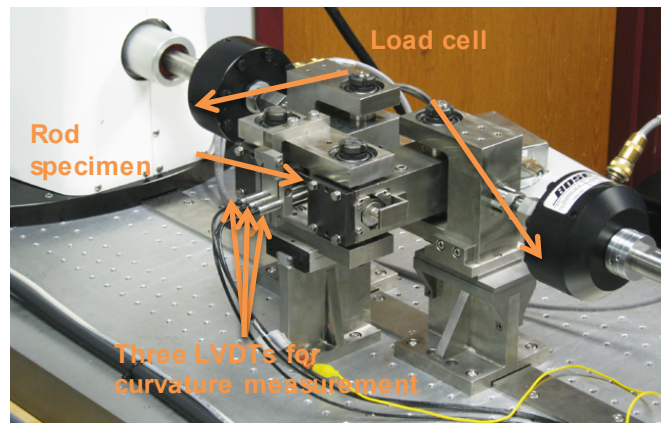
2.2 Cyclic Integrated Reversible Fatigue Tester

In 2009, the U.S. Nuclear Regulatory Commission (NRC) tasked Oak Ridge National Laboratory (ORNL) with investigating the flexural rigidity and fatigue life of high burnup (HBU) SNF (NRC, 2017a). The testing was designed to evaluate the fuel rod as a composite system, including the presence of intact fuel inside the cladding and any pellet/cladding bonding effects. The project proceeded in two phases. Phase I involved testing HBU SNF in the as-irradiated state, where hydrides are expected to be predominantly in the circumferential-axial orientation. Phase II involved testing HBU SNF segments subjected to a treatment designed to reorient the hydrides in the cladding to be predominantly in the radial-axial orientation. All testing was conducted at room temperature, which is expected to result in the most limiting cladding ductility.

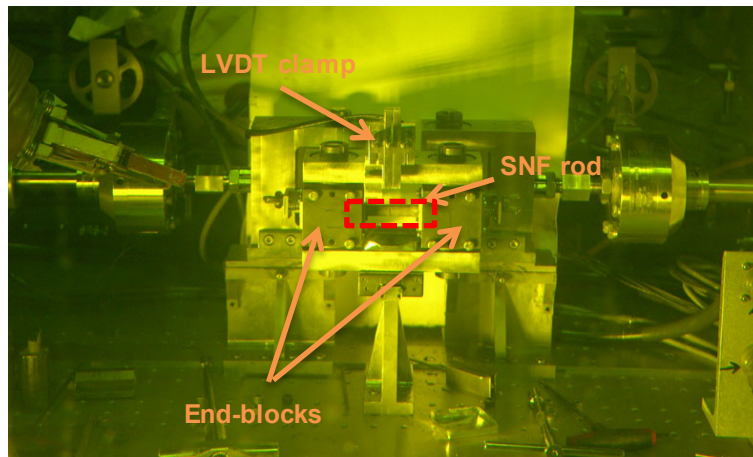
In response to the NRC tasking, in 2011, ORNL proposed a bending fatigue system for testing HBU SNF rods. The system is composed of a U-frame equipped with load cells for imposing pure bending loads on the SNF rod test specimen and measuring the *in-situ* curvature of the fuel rod during bending using a set-up of three linear variable differential transformers (LVDT) (Figure 2-1). Pure bending is a condition of stress in which a bending moment is applied to a beam without the simultaneous presence of axial, shear, or torsional forces.



(top)



(middle)



(bottom)

1 **Figure 2-1** Horizontal Layout of ORNL U-Frame Setup (Top), Rod Specimen and Three
 2 **Lvdt**s for Curvature Measurement (Middle), and Front View of CIRFT
 3 **Installed** in ORNL Hot Cell (Bottom) (Figure 4 from NUREG/CR-7198,
 4 **Revision 1** (NRC, 2017a))

1 On August 19, 2013, a testing system was installed in a hot cell at ORNL's Irradiated Fuels
2 Examination Laboratory and formally named the "cyclic integrated reversible-bending fatigue
3 tester" (CIRFT). After tuning of the test system and performance of benchmark testing in
4 September 2013, Phase I testing began on HBU SNF rod segments with intact Zircaloy-4
5 cladding irradiated in the H.B. Robinson Steam Electric Plant (HBR). ORNL completed four
6 static tests under displacement control at the rate of 0.1 mm/s to a maximum displacement of
7 12.0 mm. In early November 2013, the benchmark and static test results were critically
8 reviewed at a meeting between representatives from the NRC and ORNL. Dynamic testing was
9 then initiated, and 16 cyclic tests were completed in the Irradiated Fuels Examination
10 Laboratory. Load ranges applied to the CIRFT varied, to produce bending moments in the rod,
11 from ± 5.08 to ± 35.56 N·m. There were 12 dynamic tests with rod fracture and 4 tests without
12 rod fracture. One of the cyclic tests reached 1.3×10^7 cycles with no rod fracture. The test was
13 terminated as higher cycles would not be expected during actual transport.

14 Phase II testing began in 2016, again using HBR HBU SNF rods with intact Zircaloy-4 cladding,
15 which had been subjected to an aggressive hydride reorientation treatment (HRT) (see
16 Section 2.3.4). ORNL completed testing on four specimens in the CIRFT following an HRT:
17 one in static loading (hereafter referred to as HR2), and three in dynamic loading (hereafter
18 referred to as HR1, HR3, and HR4). The fatigue lifetime and flexural rigidity of these samples
19 were compared to the results obtained in Phase I for as-irradiated samples.

20 The following observations can be made about the results of the static testing:

- 21 • The HBR HBU SNF rods in the as-irradiated state exhibited a multiple-stage constitutive
22 response, with the two linear stages followed by a nonlinear stage. The flexural rigidity at
23 the initial stage was 63 to 78 N·m², corresponding to an elastic modulus of 101 to
24 125 GPa. The flexural rigidity at the second stage was 55 to 61 N·m², and the
25 corresponding elastic modulus was 88 to 97 GPa.
- 26 • Most HBR HBU SNF rods in the as-irradiated state under static unidirectional loading
27 fractured at a location coincident with the pellet-to-pellet interface, as validated by the
28 posttest examinations showing pellet end faces in most of the fracture surfaces.
29 Fragmentation of the pellets also occurred to a limited degree, along with cladding
30 failure.
- 31 • The static CIRFT results indicate a significant increase in a fueled SNF rod's flexural
32 rigidity compared to a calculated response for cladding only. This applied to both as-
33 irradiated and HRT SNF rods.
- 34 • For the HBR HBU SNF rods, the static CIRFT test results show that at bending moments
35 less than 30 N·m the flexural rigidities of the as-irradiated rods and the HRT HR2 rod are
36 essentially the same.
- 37 • The sample subjected to an HRT and tested under a static bending load showed
38 reduced flexural rigidity at higher loads compared to as-irradiated samples.
39 Nevertheless, material tested in the as-irradiated and HRT state both had higher flexural
40 rigidity than the calculated cladding-only response.
- 41 • The static CIRFT test result for HR2 supports the pretest expectation (hypothesis) that
42 because the tensile bending stress in the cladding is parallel to the plane of both the
43 radial and circumferential hydrides, the presence of radial hydrides would not

1 significantly alter the flexural response when compared to the case where only
2 circumferential hydrides are present.

3 • The methodology developed in this study calculate cladding stress and strain is
4 applicable to all cladding types, and the use of cladding-only properties to calculate
5 cladding stress and strain is always conservative for all cladding types.

6 • The HBR HBU SNF rods in the as-irradiated state survived static unidirectional bending
7 to a maximum curvature of 2.2 to 2.5 m⁻¹, or a maximum moment of 85 to 87 N·m. The
8 maximum static unidirectional bending values were bounded by the CIRFT device
9 displacement capacity. The maximum equivalent strain was 1.2 to 1.4 percent.

10 • Based on the static CIRFT test results, the lower-bound safety margin against fuel rod
11 failure during an HAC side drop event is 2.35 assuming the side drop imparts a 50-g
12 load to the package body (see Section 2.3.4.2).

13 The following observations can be made about the results of the dynamic testing:

14 • The fatigue life of HBR HBU SNF rods in the as-irradiated state in the cyclic tests
15 depended on the level of loading. Under loading with moments of ±8.89 to ±35.56
16 N·m—namely ±0.03 to ±0.38 percent strain—the fatigue life ranged from 5.5 × 10³ to
17 2.3 × 10⁶ cycles.

18 • The ε-N curve of the HBR HBU SNF rods in the as-irradiated state can be described by
19 a power function of $y = 3.839 \cdot x^{-0.298}$, where x is the number of cycles to failure, and y is
20 the strain amplitude (percent).

21 • Maxima of the curvature during dynamic tests in the as-irradiated state ranged from
22 ±0.08 to ±0.78 m⁻¹. The κ-N curve of the HBR HBU SNF rods can be described by a
23 power function of $y = 6.864 \cdot x^{-0.283}$, where x is the number of cycles to failure, and y is the
24 maxima of cladding tensile curvature |κ|_{max} (m⁻¹). A fatigue limit is likely located
25 between 0.08 and 0.13 m⁻¹ if it is defined at 10⁷ cycles (as is typical for material fatigue
26 endurance limits).

27 • The failure of HBR HBU SNF rods under cyclic loading often occurred near pellet-to-
28 pellet interfaces.

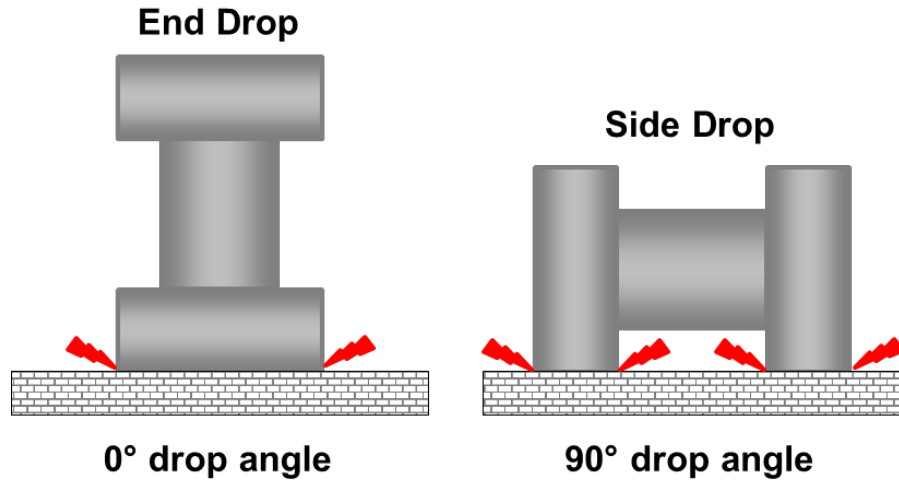
29 • The samples subjected to an HRT showed a slightly reduced lifetime compared to as-
30 irradiated samples in dynamic testing (see Section 2.3.3).

31 The following sections provide an assessment by the NRC staff (the staff) of ORNL's CIRFT
32 data and present conclusions as to the expected structural performance of HBU SNF during dry
33 storage and transportation.

34 **2.3 Application of the Static Test Results**

35 When evaluating the HAC 9-m (30-ft) drop test, as required by Title 10 of the *Code of Federal*
36 *Regulations* (10 CFR) 71.73(c)(1), two drop orientations produce distinctly different structural
37 behaviors in the fuel rods. These orientations are the side drop and the end drop (Figure 2-2).
38 In the side drop, lateral inertia loads are applied to the fuel rods, and bending dominates the
39 structural response. In the end drop, axial compression and the associated buckling of the fuel

1 rod dominates the structural response. For a side-drop event, the CIRFT static bending test
2 results from NUREG/CR-7198, Revision 1 (NRC, 2017a), can be directly applied to quantify the
3 fuel rod structural response. For the end drop, the presence of axial compression in the fuel rod
4 represents a force component that was not present in the CIRFT static bending tests. This,
5 however, does not pose a problem since the CIRFT static test results can be used to
6 conservatively quantify the effect of the fuel pellets on increasing the flexural rigidity of the rods
7 to resist buckling.



8 **Figure 2-2 Schematic Diagram of End and Side Drop Accident Scenarios**
9 **(Revised Figure 5-168 from Patterson and Garzarolli (2015))**

10 2.3.1 Spent Fuel Rod Behavior in Bending

11 The behavior of a fuel rod in bending generally depends on three things: (1) the type of loading,
12 (2) the bond between the cladding and fuel, and (3) the behavior of the pellet-pellet interface.
13 Fundamentally, there are two types of bending—bending without shear and bending with shear.
14 Bending without shear is pure bending (i.e., constant moment or curvature, as exhibited in the
15 ORNL CIRFT tests) and produces no shear stress at the interface between the cladding and
16 fuel pellet. Pure bending is a special case that does not often occur in practice. What occurs
17 more often is the case of a laterally-supported fuel rod subjected to a transverse inertia loading,
18 as in a side drop, where the rod is subjected to both bending and shear forces.¹ Although both
19 bending and shear are acting, the structural response would be expected to be different,
20 depending on whether the cladding is bonded to the fuel pellet.

¹ Because the fuel behaves in a brittle manner while the cladding behaves in a ductile manner, all of the bending tensile stresses will occur in the cladding. The cladding and fuel will resist the shear forces, but for simplicity, it can be conservatively assumed that all of the shear is resisted by the cladding. A simple calculation shows that during a side drop event, the uniformly loaded fuel rod spanning over multiple grid spacers will have maximum tensile stresses due to bending that are more than an order of magnitude greater than the maximum tensile stresses due to shear. Therefore, bending dominates the response of the fuel rod, and this is why the CIRFT tests can accurately represent the behavior of an actual fuel rod during a side drop event.

2.3.2 Composite Behavior of a Spent Fuel Rod

The normal explanation for the structural response of the fueled-rod composite system is as follows. If the pellet is not bonded to the cladding, displacement compatibility is not maintained at the pellet-cladding interface, and composite action does not occur. In this case, the flexural rigidity is given by the following:

$$EI = E_c I_c + E_p I_p \quad (\text{Eqn. 2-1})$$

That is, the flexural rigidity is equal to the sum of the individual flexural rigidities of the cladding and fuel pellets, where E_c and I_c are the elastic modulus and moment of inertia of the cladding, respectively, and E_p and I_p are the elastic modulus and moment of inertia of the pellet, respectively. On the other hand, if the pellet is bonded to the cladding, displacement compatibility is maintained at the pellet-cladding interface and composite action occurs. In this case, the flexural rigidity is calculated by transforming the pellet properties into equivalent cladding properties (i.e., by multiplying the pellet moment of inertia by E_p/E_c). This is the same technique commonly used for reinforced concrete (Winter and Nelson, 1979). As mentioned above, a spent fuel rod is a composite system consisting of cladding and spent fuel. To fully understand the unique behavior of this composite system, the bending behavior of a more general composite beam will be discussed. Consider a composite concrete and steel I-beam where a concrete slab, rectangular in cross-section, is poured onto the top flange of a steel I-beam (Figure 2-3). This type of composite beam is commonly found in highway bridge construction. Assume the concrete and steel beam are simply supported and a concentrated load is applied at mid-span. If the concrete slab and steel beam are not bonded to each other, no shear transfer takes place at the interface between the steel and concrete, and the flexural rigidity (EI) is equal to the sum of the individual flexural rigidities of the concrete slab and steel beam taken separately.

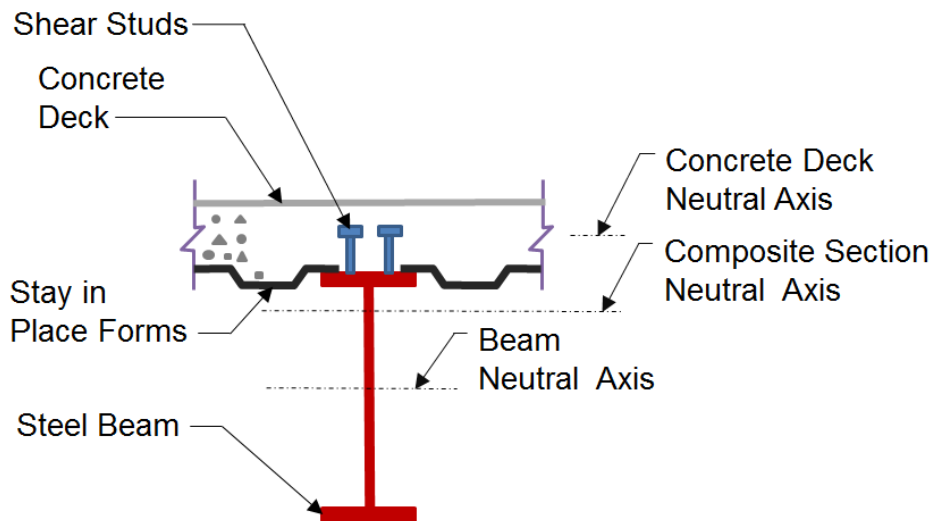
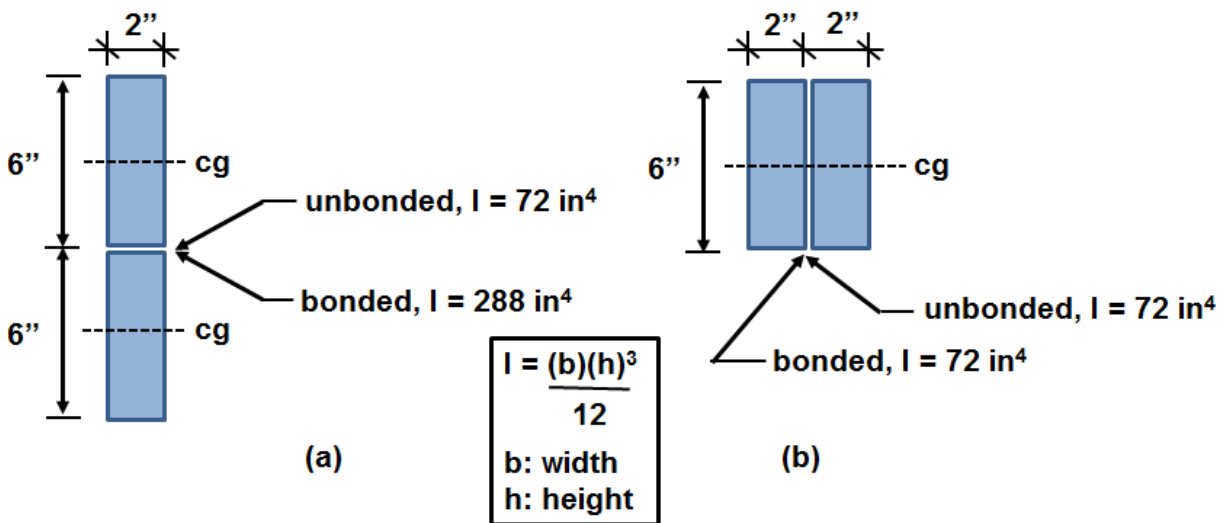


Figure 2-3 Typical Composite Construction of a Bridge

On the other hand, if the concrete slab and steel beam are bonded to each other, as typically done using shear studs, then shear transfer takes place and the concrete slab and steel beam act as a composite section. In this case, the flexural rigidity of the composite beam will be significantly greater than the sum of the individually flexural rigidities taken separately. This

1 example of a concrete slab bonded to the top flange of a steel beam illustrates the behavior of a
 2 composite system where the centers of gravity of each of the two components (i.e., concrete
 3 slab and steel I-beam) are not coincident.

4 For the special case where the centers of gravity of the two components are coincident, the
 5 flexural rigidity of the composite section is always equal to the sum of the flexural rigidities of the
 6 individual components regardless of whether the components are bonded or unbonded. The
 7 following example illustrates this concept. Consider a simply supported span composed of two
 8 beams, each with a rectangular cross-section 2 in. wide, and 6 in. deep (i.e., a "2 × 6"). Let the
 9 2 × 6's be configured one on top of the other, where the centers of gravity (cgs) are not
 10 coincident as shown in Figure 2-4a. If the beams are unbonded, the moment of inertia of the
 11 section ($I = bh^3/12$ per beam), is equal to: $2 \times 2 \text{ in.} \times (6 \text{ in.})^3/12 = 72 \text{ in.}^4$. If they are bonded,
 12 then the moment of inertia of the section is equal to: $2 \text{ in.} \times (2 \times 6 \text{ in.})^3/12 = 288 \text{ in.}^4$.



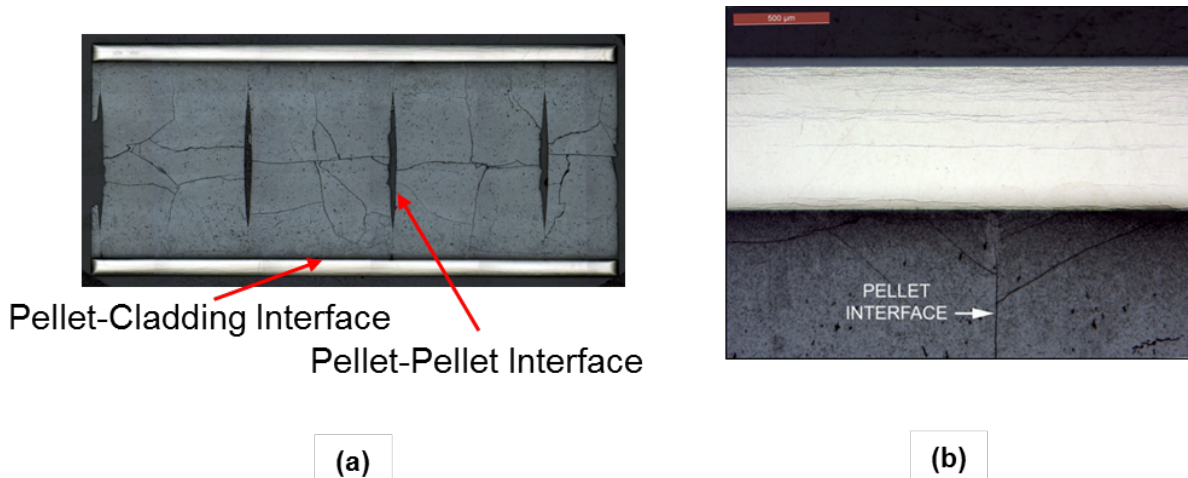
13 **Figure 2-4 Influence of cg Position on Composite Beam Stiffness:**
 14 **(a) cgs Are Not Coincident, (b) cgs Are Coincident**

15 Now let the 2 × 6s be configured as shown in Figure 2-4b, where the cgs are aligned on the
 16 same bending axis (i.e., they are "coincident"). If they are unbonded, the moment of inertia of the
 17 section is: $2 \times 2 \text{ in.} \times (6 \text{ in.})^3/12 = 72 \text{ in.}^4$. If they are bonded $I = 2 \times 2 \text{ in.} \times (6 \text{ in.})^3/12 = 72$
 18 in.^4 . Thus, when the cgs of the 2 × 6's are "coincident" the flexural rigidity of the beam is the
 19 sum of the individual flexural rigidities of the 2 × 6's regardless of whether the 2 × 6s are bonded
 20 or unbonded. While previously unrecognized, this is the situation with a spent fuel rod, where
 21 the cladding cylindrical tube and the spent fuel cylindrical solid section have coincident cgs.
 22 Thus, for a spent fuel rod, where the fuel is a homogenous solid, the flexural rigidity is given by
 23 Equation 2-1, regardless of whether the fuel is bonded to the cladding. All moments of inertia
 24 are taken about the neutral axis of the fuel rod.

25 Calculation of Cladding Strain

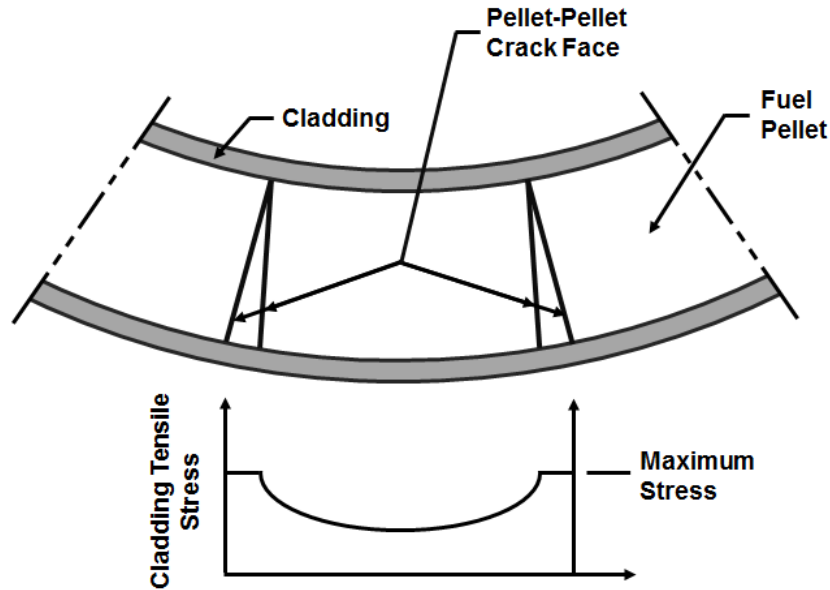
26 The objective of this section is to develop a simple methodology that uses the CIRFT static test
 27 data for fully-fueled composite spent fuel rods to evaluate spent fuel rod cladding strain. The
 28 methodology presented here to determine cladding response (i.e., cladding stresses and
 29 strains) is based on a set of assumptions that are consistent with those made by ORNL in its

1 presentation of CIRFT results in NUREG/CR-7198, Revision 1 (NRC, 2017a). These
2 assumptions, which are discussed in greater detail below, are based on the integrated average
3 response of the fuel rod along its gauge length.



4 **Figure 2-5 Images of Cladding-Pellet Structure in HBU SNF Rod (66.5 Gwd/MTU, 40–**
5 **70 μm Oxide Layer, 500 Wppm H Content in Zircaloy-4): (a) Overall Axial**
6 **Cross Section and (b) Enlarged Area (Revised Figure 33 from NUREG/CR-**
7 **7198, Revision 1 (NRC, 2017a))**

8 The fuel rod composite system (Figure 2-5) is composed of cladding, which exhibits ductile
9 behavior, and the fuel pellet, which exhibits brittle behavior. In a spent fuel rod subject to
10 bending, where the fuel is a homogenous solid, the neutral axis is at the center of the rod cross-
11 section, provided that the brittle fuel does not crack in tension. Once the fuel cracks, the neutral
12 axis will shift toward the compression side of the cross-section. The ORNL tests show that the
13 region of the fuel weakest in tension is at the pellet-pellet interface. When the pellet-pellet
14 interface cracks, the tensile stress in the cladding at the crack face, will increase significantly.
15 On either side of the crack face the shear stress between the cladding and fuel is high and
16 decreases parabolically with distance from the crack (Figure 2-6). The high tensile stress in the
17 cladding at the crack face also decreases parabolically with distance from the crack. Thus, the
18 cladding tensile stresses will vary significantly along the length of the rod; they are highest at the
19 crack face and much lower away from the crack face. Even though this behavior is known to
20 occur, only the average tensile bending stress can be calculated from the static test results
21 because the measured curvature is the integrated average curvature over the measurement
22 length (gauge length) of the rod.



1 **Figure 2-6 Approximate Extreme Fiber Tensile Stresses Between Pellet-Pellet Crack**

2 The LVDTs measure displacements at three locations on the test specimen. The distance
 3 between the first and third probes is the gauge length of the specimen. Because the bending
 4 moment is constant along the gauge length, it would be expected that several pellet-pellet
 5 interface cracks would develop within the gauge length. That being the case, the cladding
 6 tensile stresses and strains along the gauge length will vary significantly. However, this
 7 variation in strain along the gauge length was not, and cannot be, measured. What was
 8 measured is the average curvature along the gauge length. Therefore, only the average tensile
 9 strain (i.e., the smeared tensile strain) can be calculated. The average tensile strain, ϵ , along
 10 the gauge length is equal to the curvature, κ , multiplied by the distance to the neutral axis, y_{max} :

11
$$\epsilon = \kappa \cdot y_{max} \quad (\text{Eq. 2-2})$$

12 However, y_{max} can vary significantly along the gauge length. At a section where the fuel has not
 13 cracked, y_{max} is equal to the outer radius, r . At a pellet-pellet interface crack, y_{max} would be
 14 greater than the radius but less than the diameter. However, because the measured and
 15 calculated results are averages over the gauge length, a convention must be adopted for
 16 calculating cladding strain and this convention must be consistently applied throughout. The
 17 convention used in NUREG/CR-7198, Revision 1 (NRC, 2017a), and adopted in this document
 18 to convert average curvature to average cladding strain, is to assume that the distance from the
 19 tensile face of the cladding to the neutral axis is equal to the outside radius, r .

20 Average cladding tensile stress, σ , should be calculated directly from average cladding strain
 21 using the following equation:

22
$$\sigma = \epsilon \cdot E_c \quad (\text{Eq. 2-3})$$

23 Use Equation 2-3 provides a consistent and compatible relationship between stress and strain.

2.3.3 Calculation of Cladding Strain Using Factored Cladding-Only Properties

The following discussion describes a methodology that can be easily implemented to calculate the cladding tensile strain and stress and fuel rod flexural rigidity using only cladding-only properties. Section 4.2.2 of NUREG/CR-7198, Revision 1 (NRC, 2017a), presents analyses comparing the measured flexural rigidity from the CIRFT static test results to the calculated flexural rigidity values using the validated cladding-only mechanical property models developed by Pacific Northwest National Laboratory (PNNL) (Geelhood et al., 2008). The purpose of the comparison was to investigate the effect of fuel pellets on the fuel rod's flexural rigidity and cladding strain.

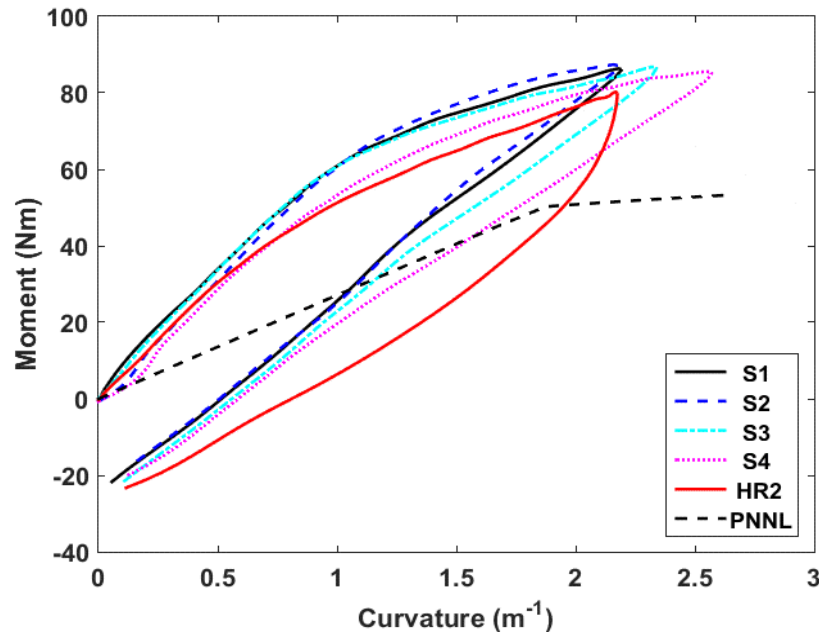
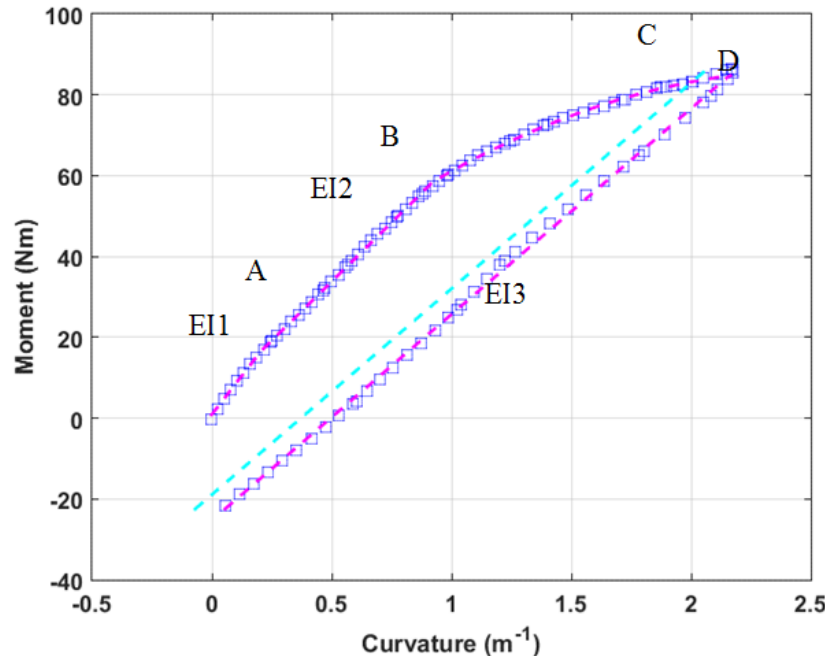


Figure 2-7 Comparison of CIRFT Static Bending Results with Calculated PNNL Moment Curvature (Flexural Rigidity) Derived from Cladding-Only Stress-Strain Curve (Reproduction of Figure 22 from NUREG/CR-7198, Revision 1 (NRC, 2017a)). S1, S2, S3, and S4 Represent the Experimental Results for HBR HBU SNF As-Irradiated Specimens, HR2 Represents the Experimental Results for HBR HBU SNF Hydride-Reoriented Specimen, and PNNL Represents the Results Calculated Using the Validated Cladding-Only Mechanical Property Models Developed by PNNL (From Geelhood et al., 2008)

The CIRFT static test results plotted in Figure 2-7 show the moment-curvature response of the four HBR HBU SNF as-irradiated specimens S1, S2, S3, and S4 and the hydride-reoriented specimen HR2. The loading portion of the moment-curvature response begins at 0 N·m and reaches a maximum at about 80 N·m, at which point the specimens begin to unload. The moment-curvature responses of the four HBR HBU SNF as-irradiated specimens during loading were similar up to a moment of 35 N·m. They are characterized by two distinct linear responses, E11 and E12, followed by a nonlinear response during the loading and a linear response upon unloading (E13) (Figure 2-8).

1 Also shown in Figure 2-7 is the cladding-only moment-curvature loading curve constructed
 2 using the PNNL cladding-only mechanical property models. The static test results for both as-
 3 irradiated and hydride-reoriented specimens show much higher bending moment resistance
 4 during loading compared to the PNNL cladding-only data. The slopes, EI1 and EI2, of the four
 5 HBU fuel rods are greater than the slope of the PNNL data for the cladding-only rod.



7 **Figure 2-8 Characteristic Points on Moment-Curvature Curve. A, B, C, and D are**
 8 **Points on the Curve. EI1 is the Slope of the Loading Curve Between 0 and**
 9 **A. EI2 is the Slope of the Loading Curve Between A and B. EI3 is the Slope**
 10 **of the Unloading Curve Between D and 0. The Cladding-Only Moment-**
 11 **Curvature Loading Curve Constructed Using the PNNL Cladding-Only**
 12 **Mechanical Property Models is not Shown (Reproduction of Figure 21 from**
 13 **NUREG/CR-7198, Revision 1 (NRC, 2017a))**

15 Figure 2-7 also shows that at bending moments during loading less than 35 N·m, the flexural
 16 rigidities of the four as-irradiated rods, which have only circumferential hydrides, and HR2,
 17 which has both circumferential and radial hydrides, are essentially the same. This result
 18 supports the pretest expectation that, because the bending tensile stress in the cladding is
 19 parallel to the plane of both the radial and circumferential hydrides, the presence of radial
 20 hydrides would not significantly alter the flexural response from the case where only
 21 circumferential hydrides are present. The results of tests currently being conducted by the U.S.
 22 Department of Energy (DOE) will further confirm this hypothesis as it applies to other cladding
 23 types.

25 In the CIRFT static test results for HBR HBU SNF rods shown in Figure 2-7, no failures
 26 occurred. The lower-bound maximum moment achieved in the tests is approximately 80 N·m.
 27 In addition, it is important to point out that a bending moment of 80 N·m is significantly greater
 28 than the bending moment an HBR HBU SNF rod will experience during an HAC 9-m (30-ft) side
 29 drop (see Section 2.3.4.1). This means that fuel rod integrity is expected to be maintained
 30 during an HAC drop scenarios, and therefore, fuel rod reconfiguration is very unlikely.

1 For the as-irradiated HBR HBU SNF rods, Table 2-1 shows that in the EI1 region of the
 2 moment-curvature results, the average flexural rigidity is 2.66 (.e., $71.58 \text{ N}\cdot\text{m}^2/26.93 \text{ N}\cdot\text{m}^2$)
 3 times greater than the cladding-only case, and in the EI2 region the average flexural rigidity is
 4 2.16 (i.e., $58.10 \text{ N}\cdot\text{m}^2/26.93 \text{ N}\cdot\text{m}^2$) times greater than the cladding-only case. For the
 5 hydride-reoriented fuel rod, HR2, Table 2-1 shows that in the EI1 region, the average flexural
 6 rigidity is 2.33 (i.e., $62.77 \text{ N}\cdot\text{m}^2 / 26.93 \text{ N}\cdot\text{m}^2$) times greater than the cladding-only case, and in
 7 the EI2 region, the average flexural rigidity is 1.54 (i.e., $41.52 \text{ N}\cdot\text{m}^2 / 26.93 \text{ N}\cdot\text{m}^2$) times greater
 8 than the cladding-only case.

9 **Table 2-1 Comparison of Average Flexural Rigidity Results Between CIRFT Static**
 10 **Testing and PNNL Cladding-Only Data (From Validated Mechanical**
 11 **Property Models in Geelhood et al., 2008)**

	EI1 (N·m ²)	EI2 (N·m ²)	EI3 (N·m ²)
As-Irradiated (S1, S2, S3, and S4)	71.576	58.099	48.133
Hydride-Reoriented (HR2)	62.769	41.517	43.333
Cladding-Only (validated PNNL models)	26.933	-	-

12 **Table 2-2 Characteristic Points and Quantities Based on Moment-Curvature Curves**
 13 **(Reproduction, in Part, of Table 4 from NUREG/CR-7198, Revision 1**
 14 **(NRC, 2017a))**

Spec label	EI1 (N·m ²)	EI2 (N·m ²)	EI3 (N·m ²)	κ_A (m ⁻¹)	κ_B (m ⁻¹)	κ_C (m ⁻¹)	κ_D (m ⁻¹)	M _A (N·m)	M _B (N·m)	M _C (N·m)	M _D (N·m)
S1	78.655	57.33	51.027	0.202	0.968	2.009	2.166	16.695	60.599	83.595	85.413
S2	73.016	60.848	52.699	0.32	1.009	2.001	2.154	20.18	62.133	85.914	87.294
S3	71.517	59.369	47.101	0.311	0.933	2.149	2.308	22.338	59.288	83.728	85.235
S4	63.117	54.849	41.704	0.503	0.862	2.329	2.507	28.54	48.244	81.656	85.02
As- irradiated Avg.	71.576	58.099	48.133	0.334	0.943	2.122	2.284	21.938	57.566	83.723	85.741
As- irradiated Std. Dev.	6.422	2.603	4.886	0.125	0.062	0.154	0.164	4.977	6.322	1.741	1.048
HR2	62.769	41.517	43.333	0.487	1.007	1.585	2.158	30.301	51.884	66.809	79.606

15 In developing a simplified methodology using cladding-only mechanical properties, the staff
 16 considers it conservative to use the flexural rigidity ratio from the EI2 data. More specifically,
 17 using the average minus two standard deviations of the EI2 data from Table 2-2 is $52.90 \text{ N}\cdot\text{m}^2$
 18 (i.e., $58.10 \text{ N}\cdot\text{m}^2 - 2 \cdot (2.60 \text{ N}\cdot\text{m}^2)$), which results in an EI2 ratio of an HBU fuel rod to a
 19 cladding-only rod of 1.96 (i.e., $52.90 \text{ N}\cdot\text{m}^2 / 26.93 \text{ N}\cdot\text{m}^2$). The average minus two standard
 20 deviations has a 98 percent exceedance probability, which means there is a 98 percent chance
 21 that the actual value of the EI ratio will be greater than 1.96. To account for the effects of
 22 hydride reorientation, this result is reduced by 0.713 (i.e., $1.54/2.16$), which is the ratio of the

1 reoriented hydride results to the as-irradiated results that were calculated in the previous
2 paragraph. Multiplying 1.96 by 0.713 results in a factor of 1.40. However, recognizing the
3 limited test data available to calculating the 1.40 factor, the factor has been further reduced to
4 1.25 to account for the additional uncertainty associated with using limited data. Thus, for the
5 purpose of calculating lateral displacements in the simplified methodology, the flexural rigidity of
6 the HBU fuel rod is equal to the flexural rigidity of the cladding-only rod multiplied by the factor
7 1.25:

$$8 \quad (EI)_{\text{HBU rod}} = 1.25 \cdot (EI)_{\text{clad only}} \quad (\text{Eq. 2-4})$$

9 The curvature, κ , of the HBU fuel rod is given by:

$$10 \quad \kappa = M/(EI)_{\text{HBU rod}} \quad (\text{Eq. 2-5})$$

11 or:

$$12 \quad \kappa = M/[1.25 \cdot (EI)_{\text{clad only}}] \quad (\text{Eq. 2-6})$$

13 where M is the bending moment in the rod.

14 The tensile strain is given by:

$$15 \quad \varepsilon = \kappa \cdot y_{\text{max}} \quad (\text{Eq. 2-7})$$

16 where y_{max} is equal to the outer radius, r, of the rod, and the maximum equivalent tensile stress
17 is given by:

$$18 \quad \sigma = \varepsilon \cdot E_c \quad (\text{Eq. 2-8})$$

19 The methodology described above for using cladding-only properties to calculate cladding
20 strains while accounting for the increased flexural rigidity imparted by the fuel pellet can also be
21 applied to cladding alloys other than Zircaloy-4. Once CIRFT static bending results for other
22 HBU SNF rods (i.e., ZIRLO-clad and M5-clad rods) are obtained under planned DOE-sponsored
23 research (Hanson et al., 2016), this methodology can be replicated to obtain a numerical factor
24 that allows for crediting the flexural rigidity of the fuel pellet in those fuel types. Until those
25 results are available, the staff considers the use of cladding-only mechanical properties to
26 calculate cladding stress and strain to be conservative. The staff expects that CIRFT static
27 bending results for other HBU SNF rods obtained by the DOE-sponsored research will confirm
28 this conclusion.

29 2.3.3.1 *Two Alternatives for Calculating Cladding Stress and Strain During Drop* 30 *Accidents*

31 Two alternatives can be used to calculate cladding stress and strain, and cladding flexural
32 rigidity, for the evaluation of drop accident scenarios. The first alternative is to use cladding-
33 only mechanical properties from as-irradiated cladding (which has only circumferential hydrides)
34 or from hydride-reoriented cladding (which would account for radial hydrides precipitated after
35 the drying process). As discussed in Section 2.3.3, the staff considers that the orientation of the
36 hydrides is not a critical consideration when evaluating the adequacy of cladding-only
37 mechanical properties. The properties necessary to implement this alternative are derived from
38 cladding-only uniaxial tensile tests and include modulus of elasticity, yield stress, ultimate

1 tensile strength and uniform strain, and the strain at failure (i.e., the elongation strain).
2 Additional considerations for acceptable cladding-only mechanical properties (i.e., alloy type,
3 burnup, and temperature) may be found in either of the current standard review plans (SRPs)
4 for dry storage of SNF (NUREG-1536, Revision 1, “Standard Review Plan for Spent Fuel Dry
5 Storage Systems at a General License Facility,” issued in July 2010 (NRC, 2010) for the review
6 of applications for Certificates of Compliance under 10 CFR Part 72; and NUREG-1567,
7 “Standard Review Plan for Spent Fuel Storage Facilities,” issued in March 2000 (NRC, 2000a)
8 for the review of applications for specific licenses under 10 CFR Part 72) or transportation
9 (NUREG-1617, “Standard Review Plan for Transportation Packages for Spent Nuclear Fuel,”
10 issued in March 2000 (NRC, 2000b)) – hereafter these documents will be referred to as the
11 current SRPs for dry storage or transportation for SNF.²

12 The second alternative is to use cladding-only mechanical properties that have been modified
13 by a numerical factor to account for the increased flexural rigidity imparted by the fuel pellet.
14 This numerical factor is obtained from static CIRFT static bending results for fully-fueled rods for
15 the particular HBU SNF cladding type and fuel type, as previously discussed. However, this
16 second alternative would be necessary only if the structural evaluation using cladding-only
17 mechanical properties is unsatisfactory. The acceptance criteria for cladding performance
18 following dry storage and transport-related drop accident scenarios can be found in the current
19 SRPs for dry storage and transportation of SNF, respectively.

20 **2.3.4 Applicability to Dry Storage and Transportation**

21 Argonne National Laboratory defined the radial hydride continuity factor (RHCF) as the ratio of
22 the maximum length of continuous radial-circumferential hydrides projected in the radial
23 direction to the cladding thickness within a 150- μm arc length (see Section 1.5.4). This metric
24 can be used to quantify the degree of reorientation induced in the hydride-reoriented specimen
25 that was static-bend tested in the CIRFT instrument (specimen HR2). Figure 2-9 shows a
26 metallographic image of the hydride microstructure of test specimen HR1 (used for CIRFT
27 dynamic testing) after the aggressive hydride reorientation procedure used for HBR HBU SNF
28 rod specimens.³ The HR2 specimen underwent the same radial hydride treatment (Figure 2-10)
29 as HR1, which is considered to be conservative relative to the conditions expected during drying
30 and short-term loading operations (i.e., bounding cladding temperature and hoop stresses,
31 multiple thermal cycling).⁴

32 During the radial hydride treatment, each specimen was pressurized to induce a maximum hoop
33 stress of 140 MPa at a target temperature of 400 °C for 3 hours, cooled at 1 °C/min to 170 °C,
34 and then heated at 1 °C/min to the hold temperature of 400 °C. This thermal cycling was
35 repeated for five cycles (a condition that HBU SNF assemblies would not experience in practice,

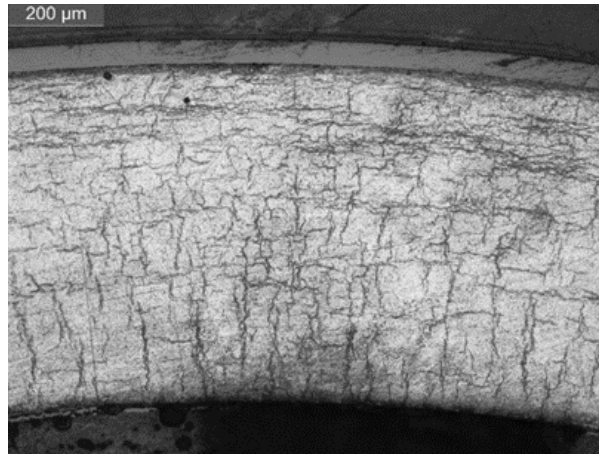
² The current SRPs for dry storage of SNF are being consolidated into a single document, NUREG-2215, “Standard Review Plan for Spent Fuel Dry Storage Systems and Facilities,” Draft Report for Comment issued November 2017 (NRC, 2017b). Similarly, the current SRP for transportation of SNF is being revised and will be reissued as NUREG-2216, “Standard Review Plan for Approval of Transportation Packages” (NRC, 2018). Both documents will incorporate current Interim Staff Review Guidance documents. The new SRPs will be issued for public comment and are expected to be finalized prior to final issuance of this report.

³ Section 3.4.1 of NUREG-7198, Revision 1 (NRC, 2017a), presents a more detailed discussion of the radial hydride treatment used for preparation of the Phase II specimens.

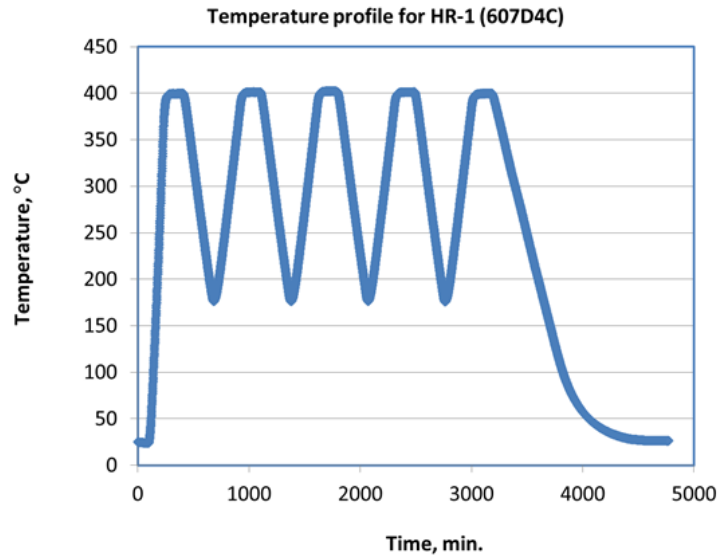
⁴ The cladding alloy in the HR2 test specimen (Zircaloy-4) had a hydrogen content considered representative for cold-worked, stress-relieved alloys (Zircaloy-4, ZIRLO) and considered bounding for recrystallized-annealed alloys (Zircaloy-2, and M5).

1 if drying operations are performed according to the guidance in ISG-11, Revision 3, “Cladding
2 Considerations for the Transportation and Storage of Spent Fuel,” issued November 2003
3 (NRC, 2003a)—see prior Section 1.2 of this report) to further induce a higher fraction of radial
4 hydrides. The specimen was then furnace cooled from 170 °C to room temperature after the
5 last cycle and the pressure was released.

6 The conservative conditions chosen for the radial hydride treatment are evidenced by the high
7 radial hydride fraction observed after metallography following testing. As Figure 2-9 shows, the
8 conservative conditions of the radial hydride treatment induced a near-100-percent RHCF in
9 some sections of the rodlet specimen. Since the radial hydride treatment produced the highest
10 degree of reorientation that could be anticipated, it is therefore expected to provide the most
11 limiting mechanical properties.



12 **Figure 2-9** High Magnification Micrograph Showing Radial Hydrides of a HBR HBU
13 SNF Hydride-Reoriented Specimen Tested Under Phase II (Specimen HR1
14 Results Shown; Hydrogen Content \approx 360–400 Wppm) (Reproduction of
15 Figure 35a in NUREG/CR-7198, Revision 1 (NRC, 2017a))



1 **Figure 2-10 Representative Conditions Used for Radial Hydride Treatment for**
 2 **Preparation of HBR HBU SNF Hydride-Reoriented Specimens Tested Under**
 3 **Phase II. The HBU SNF Specimen Was Pressurized to 140 Mpa at 400 °C**
 4 **With Five Thermal Cycles (Reproduction Of Figure 14 from NUREG/CR-**
 5 **7198, Revision 1 (NRC, 2017a))**

6 The static test results for the hydride-reoriented Zircaloy-4 fuel rod (specimen HR2; Figure 2-7)
 7 show minimal difference in the flexural response compared to the as-irradiated rods up to the
 8 bending moments pertinent to a 9-m (30-ft) drop accident (i.e., bending moments below 35 N·m
 9 – see Section 2.3.4.2 for pertinent calculation). More importantly, the flexural rigidity of the
 10 hydride-reoriented specimen is still markedly higher than the calculated cladding-only response
 11 according to validated PNNL mechanical property models. The major difference between the
 12 response of the hydride-reoriented HR2 specimen and the as-irradiated rods is the slightly lower
 13 flexural resistance of HR2 at higher loads. The slightly lower flexural resistance at higher loads
 14 may be the result of the higher density of hydrides in HR2 or the greater extent to which
 15 debonding occurred between the cladding and pellet away from the pellet-to-pellet crack
 16 interface. However, those loads would not be expected during transportation or dry storage
 17 operations.

18 The static test results for the hydride-reoriented HR2 and the as-irradiated HBR HBU SNF
 19 Zircaloy-4-clad fuel rods support the staff's conclusion that the use of cladding-only mechanical
 20 properties is adequate for the structural evaluation of HAC and NCT drop events. Further, the
 21 HAC drop events required for transportation packages apply inertia loads to the fuel rods that
 22 bound the design basis storage drops (e.g., drops during transfer operations and non
 23 mechanistic tip over). Therefore, this conclusion based on the CIRFT static test results of
 24 Zircaloy-4 can be applied to both transportation and storage.

25 The cladding strains that control the static response of an intact fuel rod are the high tensile
 26 strains at the face of the crack at the pellet-pellet interface. If a pinhole or hairline crack were to
 27 be present at this location, it could have an effect on the static test results because of the strain
 28 concentrations they may create. However, the staff considers the probability that a pinhole or
 29 hairline crack is at the pellet-pellet crack face simultaneously longitudinally and

1 circumferentially to be low. Therefore, it is reasonable that the CIRFT static test results for
2 intact fuel rods can also be applied to undamaged fuel with pinholes or hairline cracks.

3 Since the hydride-reoriented Zircaloy-4 fuel rod had a nearly 100 percent RHCF, the staff
4 considers that the same response should be observed by all modern commercial cladding alloy
5 types that may experience hydride reorientation (i.e., Zircaloy-2, ZIRLO and M5). The staff has
6 also reviewed proprietary and non-proprietary data on end-of-life rod internal pressures for fuel
7 rods with boron-based integral fuel burnable absorbers (see Section 1.5.3) and considers that
8 these rods are also reasonably bound by the maximum rod internal pressure used in the CIRFT
9 radial hydride treatment (i.e., 140 MPa). The staff's expectation is that future DOE-sponsored
10 CIRFT static testing conducted on other cladding alloy types will provide confirmation of this
11 conclusion (Hanson et al., 2016).

12 **2.3.4.1 Use of Static Test Results to Evaluate Safety Margins in an HAC Side Drop**
13 **Event**

14 The CIRFT static test results can be used to determine a lower bound safety margin against fuel
15 rod failure during an HAC side drop event. The safety margin is calculated by dividing the load
16 (or moment) at rod failure by the maximum applied load (or moment) occurring during the side
17 drop event.

18 Figure 2-7 shows that static testing of the HBR HBU SNF rods did not result in rod failures. The
19 lower bound maximum moment achieved in the tests is approximately 80 N·m. Based on the
20 slope of the curves at 80 N·m, it is reasonable to assume that rod failure probably occurs at a
21 moment at or below 100 N·m. Therefore, using 80 N·m provides a conservative basis for
22 calculating safety margin. To quantify the safety margin it is necessary to know the bending
23 moment in the fuel rod as a function of the g-load acting on the rod due to a side drop event.
24 Each fuel rod in the fuel assembly is supported by grid spacers at multiple locations along the
25 rod. Therefore, for the purpose of calculating the maximum bending moment, the rod can be
26 idealized as a uniformly loaded continuous beam.

27 Relationship Between Applied G-Load and Bending Moment

28 For the purpose of evaluating a safety margin, two different fuel rods are initially considered.
29 The first is a fuel rod from a PWR 15 × 15 fuel assembly, and the second is an HBR fuel rod
30 that was tested by ORNL in the CIRFT testing device and reported in NUREG/CR-7198,
31 Revision 1 (NRC, 2017a).

32 The properties of the PWR 15 × 15 rod (Table 2-3) are taken from NUREG-1864, "A Pilot
33 Probabilistic Risk Assessment of a Dry Cask Storage System at a Nuclear Power Plant,"
34 Appendix C, Table C.1, issued March 2007 (NRC, 2007a).

35 **Table 2-3 Properties of PWR 15 × 15 SNF Rod**

Total fuel rod weight	7.011 lb
Fuel length	154 in.
Number of grid spacers	8
Rod length between grid spacers (l)	20.5 in.
Uniform applied load ($w = 7.011 \text{ lb} / 154 \text{ in.}$)	0.0455 lb/in.

1 The maximum moment in a uniformly-loaded continuous beam can be approximated by the
2 maximum moment in a uniformly loaded three-span continuous beam as shown in Eqn. 2-9:

$$3 \quad M_{\max} = 0.100 \cdot w \cdot l^2 \quad (\text{Eqn. 2-9})$$

$$4 \quad \text{i.e., } M_{\max} = (0.100)(0.0455 \text{ lb/in.})(20.5 \text{ in.})^2 = 1.91 \text{ lb}\cdot\text{in.} = 0.216 \text{ N}\cdot\text{m}$$

5 This is the moment resulting from a 1 g-loading. The g-load necessary to produce a moment of
6 $1 \text{ N}\cdot\text{m} = 1 \text{ g} / 0.216 \text{ N}\cdot\text{m} = 4.63 \text{ g} / \text{N}\cdot\text{m}$.

7 For the HBR HBU SNF rod, the weight per unit length is calculated from the weight density of
8 fuel and the weight density of cladding, which can be determined from the information in
9 NUREG-1864, Table C.1 (NRC, 2007a) for a BWR 7 × 7 fuel rod.

$$10 \quad \text{Fuel density} = 0.34 \text{ lb} / \text{in.}^3$$

$$11 \quad (\text{i.e., } 9.60 \text{ lb} / [(\pi)(0.25)^2(144)] = 0.34)$$

$$12 \quad \text{Cladding density} = 0.234 \text{ lb} / \text{in.}^3$$

$$13 \quad (\text{i.e., } 1.98 / [(\pi)(0.535)(0.035)(144)] = 0.234)$$

14 The diameter (outer, inner) and thickness of the cladding of an HBR HBU SNF rod as given in
15 NUREG/CR-7198, Revision 1 (NRC, 2017a) are:

$$16 \quad \text{Outer diameter} = 10.743 \text{ mm} = 0.423 \text{ in.}$$

$$17 \quad \text{Cladding thickness} = 0.748 \text{ mm} = 0.0294 \text{ in.}$$

$$18 \quad \text{Inner diameter} = 0.364 \text{ in.}$$

19 From the HBR HBU SNF rod cross-sectional dimensions and the fuel and cladding densities
20 calculated using the data for the BWR 7 × 7 fuel rods, the fuel and cladding weight per unit
21 length can be calculated as follows:

$$22 \quad \text{HBR fuel weight} = 0.0354 \text{ lb} / \text{in.}$$

$$23 \quad \text{HBR cladding weight} = 0.0085 \text{ lb} / \text{in.}$$

$$24 \quad w = 0.0354 + 0.0085 = 0.0439 \text{ lb} / \text{in.}$$

$$25 \quad l = \text{distance between HBR SNF assembly grid spacers} = 26.2 \text{ in.}$$

$$26 \quad M_{\max} = (0.100)(0.0439)(26.2)^2 = 3.01 \text{ lb}\cdot\text{in} = 0.340 \text{ N}\cdot\text{m}$$

27 This is the moment resulting from a 1 g-loading. The g-load necessary to produce a moment of
28 $1 \text{ N}\cdot\text{m} = 1 \text{ g} / 0.340 \text{ N}\cdot\text{m} = 2.94 \text{ g} / \text{N}\cdot\text{m}$.

29 This example illustrates the fact that the static transverse g-load necessary to produce a
30 bending moment of 1 N·m in a fuel rod supported by multiple grid spacers varies from rod to
31 rod. For the two rods in this example, the static transverse g-load required to produce a

1 bending moment of 1 N·m varied from 2.9 to 5 g depending on the rod cross sectional
2 dimensions and assembly geometry.

3 2.3.4.2 *Dynamic Response of a Fuel Rod*

4 During a HAC 9-m (30-ft) side drop of a transportation package with impact limiters, the cask
5 body will typically experience inertia loads on the order of 50 g. However, the fuel rod is flexible,
6 as are the intervening components that support the rod between the cask body and the rod.
7 Therefore, the rigid body deceleration of the cask body will be amplified during a side drop event
8 by the flexibility of the rod and intervening components, resulting in a g-load in the rod that is
9 higher than the g-load acting on the cask body. This increase in g-load is expressed by a
10 dynamic load factor (DLF), which is the ratio of the deflection due to a dynamically applied load
11 to the deflection that would have resulted from the static application of the load. The DLF will
12 depend on the rod's natural frequency, the duration of the loading, and the shape of the load
13 time history.

14 Since natural frequency, load duration and load time history shape all depend on the physical
15 characteristics of the fuel assembly, the rod and the cask, including impact limiters, a
16 conservative approach will be used to calculate safety margin by using a maximum DLF of 2.0
17 (Biggs, 1964).

18 Thus, the statically equivalent g-load the fuel rod is subjected to is

$$19 \quad (\text{DLF}) \cdot (50 \text{ g}) = 2.0 \cdot (50 \text{ g}) = 100 \text{ g}$$

20 which produces a bending moment in the rod of

$$21 \quad 100 \text{ g} / (2.94 \text{ g/N}\cdot\text{m}) = 34.0 \text{ N}\cdot\text{m}$$

22 The safety margin (SM) against fuel rod failure during a side drop event is then

$$23 \quad \text{SM} = (80 \text{ N}\cdot\text{m}) / (34.0 \text{ N}\cdot\text{m}) = \mathbf{2.35}$$

24 2.3.4.3 *Seismic Response of a Fuel Rod*

25 The seismic response of a fuel rod can be determined using a variety of structural models.
26 These range from simple idealized models, for which hand calculation methods could be used,
27 to very detailed finite element models. The seismic loads can be applied to these models using
28 either the response spectrum method or a time history analysis method. However, regardless
29 of whether the fuel rod is in a DSS or transportation package, seismic loads will not dominate
30 fuel rod response, because the g-loads produced by a seismic event are not large enough. In
31 storage the g-loads applied to the fuel are dominated by the non-mechanistic tipover event and
32 in a transportation package the g-loads applied to the fuel rod are dominated by the HAC. Both
33 of these events produce g-loads on the fuel rod that are approximately an order of magnitude
34 larger than the g-loads produced by a seismic event. In addition, these two events do not occur
35 coincidentally with a seismic event and therefore the seismic event does not add to either of these
36 two events.

1 **2.4 Application of Fatigue Test Results**

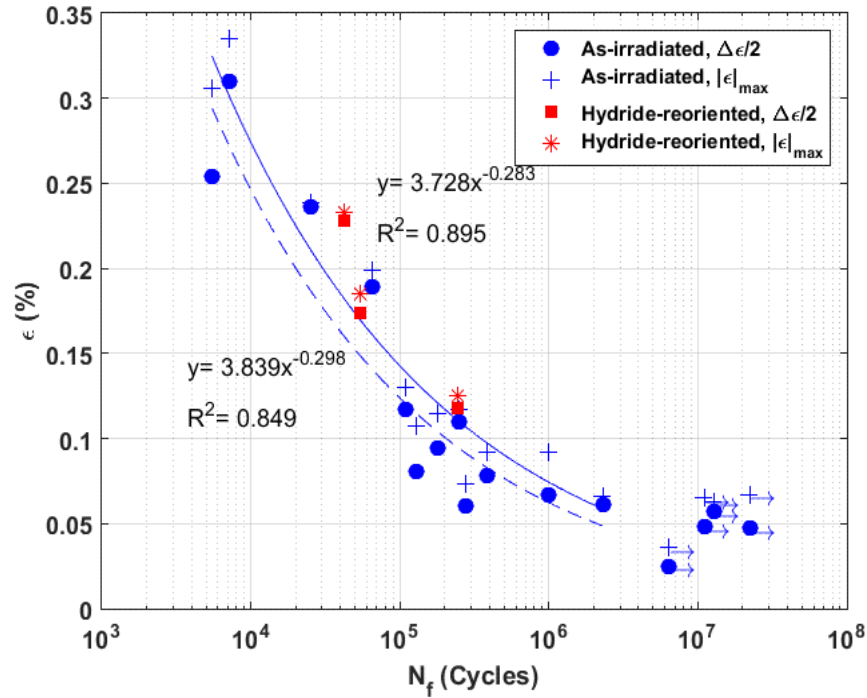
2 **2.4.1 Lower Bound Fatigue S-N Curves**

3 Fatigue strength data are commonly presented in the form of an S-N curve, where S is a
 4 strength parameter, such as stress or strain, and N denotes the number of cycles to failure at a
 5 specific value of the strength parameter. The objective of this section is to develop a lower
 6 bound fatigue S-N curve, that envelopes the HBR HBU Zircaloy-4 fuel rod fatigue data and
 7 includes both as-irradiated rods and rods with reoriented hydrides.

8 Table 2-4 presents the fatigue test data for the HBR HBU fuel rods. In Figure 2-11, half of the
 9 cladding strain range ($\Delta\varepsilon/2$, which is ε_a in Table 2-4) and the maximum strain ($|\varepsilon|_{max}$) are plotted
 10 against the number of cycles required to produce cladding failure at a particular strain
 11 amplitude. The strain range is the average of the strains caused by positive and negative
 12 bending moments, which produce different values of curvature and hence strain. The maximum
 13 strain is the maximum of these two strains.

14 **Table 2-4 Summary of CIRFT Dynamic Test Results for As-Irradiated and Hydride-**
 15 **Reoriented HBR HBU SNF (Reproduction of Table 6 in NUREG/CR-7198,**
 16 **Revision 1 (NRC, 2017a))**

Spec label	Seg. ID	Load amp. (N)	Moment amp. N-m	Number of cycles	Failure	κ_a (m^{-1})	$ \kappa _{max}$ (m^{-1})	σ_a (MPa)	ε_a (percent)	$ \varepsilon _{max}$ (percent)
D0	605D1F	250	24.068	2.50E+04	Yes	0.439	0.444	206.109	0.236	0.239
D1	607C4B	150	14.107	1.10E+05	Yes	0.215	0.24	117.26	0.117	0.13
D2	608C4B	50	4.207	6.40E+06	No	0.046	0.067	35.496	0.025	0.036
D3	605C10A	100	9.17	1.00E+06	Yes	0.125	0.171	77.938	0.067	0.092
D4	605D1C	75	6.726	1.10E+07	No	0.089	0.12	57.596	0.048	0.065
D5	605D1B	90	8.201	2.30E+06	Yes	0.114	0.123	69.706	0.061	0.066
D6	609C4	125	11.624	2.50E+05	Yes	0.205	0.218	99.546	0.11	0.117
D7	609C3	200	18.923	6.50E+04	Yes	0.351	0.37	160.835	0.189	0.199
D8	606C3E	87.5	7.743	1.28E+07	No	0.107	0.118	66.309	0.057	0.063
D9	609C7	350	33.667	7.10E+03	Yes	0.576	0.624	288.308	0.31	0.335
D10	606C3A	125	11.552	1.80E+05	Yes	0.174	0.213	98.185	0.094	0.115
D11	607C4A	300	29.021	5.50E+03	Yes	0.469	0.564	241.223	0.254	0.306
D12	608C4A	110	9.986	3.86E+05	Yes	0.144	0.171	83.617	0.078	0.092
D13	606B3E	135	12.551	1.29E+05	Yes	0.151	0.199	106.677	0.081	0.107
D14	606B3D	87.5	7.842	2.74E+05	Yes	0.112	0.135	66.652	0.06	0.073
D15	606B3C	75	6.639	2.24E+07	No	0.087	0.125	56.426	0.047	0.067
HR1	607D4C	150	15.152	4.19E+04	Yes	0.424	0.433	128.788	0.228	0.233
HR3	608D4A	100	8.982	2.44E+05	Yes	0.219	0.233	76.342	0.118	0.125
HR4	608D4C	160	14.759	5.47E+04	Yes	0.323	0.344	125.449	0.174	0.185

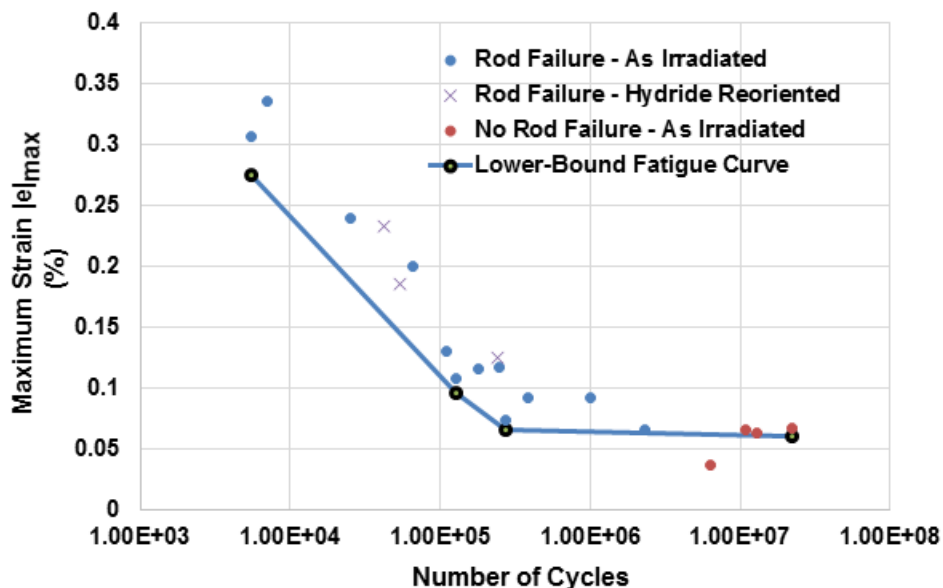


1 **Figure 2-11 Plots of Half of the Cladding Strain Range ($\Delta\epsilon/2$) and the Maximum Strain**
 2 **($|\epsilon|_{Max}$) as a Function of Number of Cycles to Failure. Markers with Arrows**
 3 **Indicate that the Tests Were Stopped Without Failure. (Reproduction of**
 4 **Figure 31b In NUREG/CR 7198, Revision 1 (NRC, 2017a))**

5 The lower bound enveloping S-N curve for the HBR HBU SNF rods is composed of three
 6 straight line segments when plotted on a linear-log scale. To account for uncertainty with
 7 respect to future test results and the influence of higher test temperatures, the equivalent strain
 8 amplitude of all segments has been reduced by a factor of 0.9. The 0.9 is justified to account
 9 for uncertainty with respect to future test results particularly at higher temperatures. Each
 10 segment's beginning and end point labels from Table 2-4 coordinates (equivalent strain
 11 amplitude percent, number of cycles to failure) are given in Table 2-5 and plotted in Figure 2-12.

12 **Table 2-5 Coordinates for Lower-Bound Enveloping S-N Curve for the HBR HBU SNF**
 13 **Rods (Equivalent Strain Amplitude Percent, Number of Cycles to Failure)**

Segment	Beginning Point	End Point
1 (D11 to D13)	(0.275, 5.50E+3)	(0.096, 1.29E+5)
2 (D13 to D14)	(0.096, 1.29E+5)	(0.066, 2.74E+5)
3 (D14 to D15)	(0.066, 2.74E+5)	(0.060, 2.24E+7)



1 **Figure 2-12 CIRFT Dynamic (Fatigue) Test Results for As-Irradiated and Hydride-**
 2 **Reoriented H.B. Robinson Zircaloy-4 HBU Fuel Rods. The Calculated**
 3 **Lower-Bound Fatigue Endurance Curve is also Shown**

4 Fatigue data for reoriented cladding alloys other than Zircaloy-4 (i.e., Zircaloy-2, ZIRLO and M5)
 5 are not yet available. However, the staff believes the methodology described above for
 6 developing a lower-bound fatigue curve can be used to construct a lower-bound fatigue curve
 7 for other cladding alloys once the as-irradiated fatigue data become available. The fatigue data
 8 plotted in Figure 2-11 show that at the same number of cycles all of the Zircaloy-4 fuel rods
 9 with reoriented hydrides failed at nearly the same strains as the as-irradiated Zircaloy-4 fuel rods.
 10 Rod specimen D2, which did not fail, was tested at a very low moment amplitude resulting in a
 11 very low maximum strain amplitude. The test was also terminated prematurely at 6.4×10^6
 12 cycles. Based on the results for the other test specimens that did not fail, it would be expected
 13 that specimen D2 would not have failed until 1×10^8 cycles or beyond. Therefore, rod specimen
 14 D2 is not included in the development of the lower bound curve since it would have
 15 inappropriately skewed the results. Therefore, the staff considers that a lower-bound fatigue
 16 curve developed from as-irradiated data for other cladding alloys is adequate for assessing the
 17 fatigue life of alloys with reoriented hydrides. Additional fatigue data for hydride-reoriented
 18 specimens for other cladding alloys to be obtained under DOE-sponsored research are
 19 expected to confirm these expectations.

20 **2.4.2 Fatigue Cumulative Damage Model**

21 During NCT if a fuel rod were to vibrate at a constant strain amplitude, all that would be
 22 necessary to predict the fatigue life of the rod is the S-N curve. However, fuel rod vibration
 23 during NCT is expected to have a series of many cycles encompassing a range of strain
 24 amplitudes and with each cycle, damage to the fuel rod cladding is continuously accumulating.
 25 A fatigue damage model can be used to express how damage from these cycles accumulates.
 26 To date, more than 50 fatigue damage models have been proposed, but unfortunately none of
 27 these models enjoys universal acceptance, and the applicability of each model varies from case
 28 to case. Unlike the aerospace industry, which has conducted extensive research on the

1 accumulation of fatigue damage to materials, such as steel, aluminum, and titanium, no
2 research has been conducted on fatigue damage to HBU spent fuel cladding. Nevertheless, for
3 many metals, the simple linear damage rule developed by Miner (Gaylord and Gaylord, 1979)
4 appears to provide a simple and reasonably reliable prediction of fatigue behavior under random
5 loadings, and therefore, will be used to evaluate fatigue damage accumulation in HBU SNF rods
6 during NCT.

7 For failure, the linear damage rule is, the following:

$$8 \quad \sum_i n_i/N_i = n_1/N_1 + n_2/N_2 + n_3/N_3 + \dots = 1 \quad (\text{Eqn 2-9})$$

9 where:

10 n_i = number of strain cycles at strain level ϵ_i

11 N_i = number of strain cycles to produce failure at ϵ_i .

12 To apply this simple linear damage rule it is assumed that the NCT loading history can be
13 reduced to a series of different strain levels where the number of cycles associated with each
14 strain level, i , is, n_i . To account for uncertainty in using a simple linear damage rule to describe
15 the accumulated fatigue damage in HBU fuel, the right side of the above equation should be set
16 equal to 0.7. This value is considered an approximate lower bound for the uncertainty in Miner's
17 damage model (Hashin, 1979).

18 **2.4.3 Applicability to Storage and Transportation**

19 The CIRFT fatigue tests were conducted under conditions that produced a uniform bending
20 moment in the fuel rod. Thus, these results apply only to loading conditions that produce
21 longitudinal bending stresses in the cladding of the fuel. Such loading conditions occur when
22 fuel rods vibrate during NCT. Fluctuating loads can also occur during storage when the
23 cladding experiences thermal cycles because of daily and seasonal fluctuations in ambient
24 temperature. These thermal cycles will induce cyclic stresses on the cladding due to changes in
25 fission and decay gas pressure, which will result in fluctuations in cladding hoop stresses. As
26 explained above, however, the fatigue test results apply only to loading conditions that produce
27 longitudinal bending stresses in the cladding of the fuel. The fatigue test results are not
28 applicable to loading conditions that produce fluctuations in hoop stress. Therefore, the fatigue
29 test results cannot be applied to thermal fatigue during storage.

30 In the CIRFT static and fatigue tests the fuel rods were subjected to a constant bending moment
31 which resulted in a longitudinal bending stress in the cladding. However, in an actual spent fuel
32 rod there is internal gas pressure, which creates hoop stress on the order of 100 MPa – see
33 Section 1.5.3.3. The presence of the hoop stresses creates a non-proportional biaxial stress
34 state in the cladding. The stress state is non-proportional because the hoop stress remains
35 constant while the longitudinal bending stress fluctuates. Recent research on the effect of
36 proportional biaxial stress fields on fatigue crack growth shows no significant effect of the biaxial
37 stress field on fatigue crack propagation behavior (Pickard, 2015). It is expected that the same
38 result would also hold for non-proportional biaxial stress fields. Based on these results, the staff
39 considers that the presence of a biaxial stress field in a spent fuel rod does not need to be
40 considered. Therefore, only the longitudinal bending stresses in the cladding need to be
41 considered when using the ORNL static and fatigue test data.

1 During storage or transportation, it is possible that a seismic event could occur. Typically the
2 strong motion duration of a seismic event is approximately 10 seconds. A fuel rod generally
3 responds to seismic input in the 10 to 30 hertz (Hz) frequency range. This means that the
4 number of fatigue cycles associated with a seismic event would be no more than about 300
5 cycles (10 seconds x 30 Hz = 300 cycles). In addition, it is expected that the seismic load
6 applied to the rod would be less than 10-g. Based on the results summarized at the end of
7 Section 2.3.4.1, a 10-g load would produce a bending moment in the rod of about 3.5 N·m.
8 From Table 2-4, a bending moment of 3.5 N·m would result in a maximum cladding strain of
9 about 0.03%. From an event that produced 300 bending cycles at a maximum strain of
10 0.03%, Figures 2-11 and 2-12 show that virtually no fatigue damage would be expected.
11 Therefore, seismic events during storage or transportation are not expected to compromise
12 the fuel integrity.

3 DRY STORAGE OF HIGH BURNUP SPENT NUCLEAR FUEL

3.1 Introduction

The U.S. Nuclear Regulatory Commission (NRC) staff (the staff) has developed example licensing and certification approaches for dry storage of high burnup (HBU) spent nuclear fuel (SNF). Applicants may use these approaches to provide reasonable assurance of compliance with Title 10 of the *Code of Federal Regulations* (10 CFR) Part 72, "Licensing Requirements for the Independent Storage of Spent Nuclear Fuel, High-Level Radioactive Waste, and Reactor Related Greater Than Class C Waste," during normal, off-normal and accident conditions of storage. The staff developed these example approaches according to the conclusions of the engineering assessment in Chapter 2. Figure 3-1 provides a high-level diagram of these approaches, which vary based on (1) the condition of the fuel (undamaged or damaged), and (2) the length of time the fuel has been in dry storage. Section 3.2.2. discusses considerations for additional analyses expected for non-leaktight dry storage system (DSS) designs. An applicant may consider and demonstrate other approaches that may be acceptable.

As required by 10 CFR 72.24(b) and 10 CFR 72.236(a), an application for a specific license for an independent spent fuel storage installation (ISFSI) or an application for a Certificate of Compliance (CoC) for a DSS design, respectively, should identify the allowable SNF contents and condition of the assembly and rods per the design bases. The allowable cladding condition for the SNF contents is generally defined in the Technical Specifications of the specific license (10 CFR 72.44(c)) or CoC (10 CFR 72.236(a)), and the nomenclature may vary between different DSS designs. For example, the terms "intact" and "undamaged" have both been historically used to describe cladding without any known gross cladding breaches. In accordance with 10 CFR 72.212(a)(1) and 10 CFR 72.212(b)(3), users of DSSs (general licensees) are to comply with the Technical Specifications of the CoC by selecting and loading the appropriate fuel, and are to maintain records that reasonably demonstrate that loaded fuel was adequately selected, in accordance with their approved site procedures and Quality Assurance Program.

Interim Staff Guidance (ISG)-1, Revision 2, "Classifying the Condition of Spent Nuclear Fuel for Interim Storage and Transportation Based on Function," issued in May 2007 (NRC, 2007b), provides guidance for developing the technical basis supporting the conclusion that the SNF (both rods and assembly) to be loaded in a DSS are intact or undamaged.¹ This would include considering whether the material properties, and possibly the configuration, of the SNF assemblies can be altered during the requested dry storage period. If the alteration is significant enough to prevent the fuel or assembly from performing its intended functions, then the fuel assembly should be classified as damaged.

Damaged SNF is generally defined in terms of the characteristics needed to perform functions to ensure compliance with fuel-specific and DSS-related regulations. A fuel-specific regulation defines a characteristic or performance requirement of the SNF assembly. Examples of such regulations include 10 CFR 72.122(h)(1) and 10 CFR 72.122(l). A DSS-related regulation defines a performance requirement placed on the fuel so that the DSS can meet its regulatory requirements. Examples of such regulations include 10 CFR 72.122(b) and 10 CFR 72.124(a).

¹ The current revisions of all ISG documents will be rolled into revised standard review plans (SRPs) for dry storage and transportation, as appropriate, and will then be removed from the public domain. The revised SRPs will be issued for public comment prior to being finalized.

1 The glossary in this report provides the staff's definitions of intact, undamaged, and damaged
2 fuel. For additional information, refer to the current standard review plans (SRPs) for dry
3 storage of SNF (NUREG-1536, Revision 1, "Standard Review Plan for Spent Fuel Dry Storage
4 Systems at a General License Facility," issued in July 2010 (NRC, 2010) for the review of
5 applications for Certificates of Compliance under 10 CFR Part 72, and NUREG-1567, "Standard
6 Review Plan for Spent Fuel Storage Facilities," issued in March 2000 (NRC, 2000a) for the
7 review of applications for specific licenses under 10 CFR Part 72) – hereafter, these documents
8 will be referred to as the current SRPs for dry storage SNF.²

² The current SRPs for dry storage of SNF are being consolidated into a single document, NUREG-2215, "Standard Review Plan for Spent Fuel Dry Storage Systems and Facilities," Draft Report for Comment issued November 2017 (NRC, 2017b), which will incorporate current Interim Staff Review Guidance documents. NUREG-2215 has been issued for public comment and is expected to be finalized prior to final issuance of this report.

Dry Storage of High Burnup Spent Nuclear Fuel
Normal, Off-Normal, and Accident Conditions

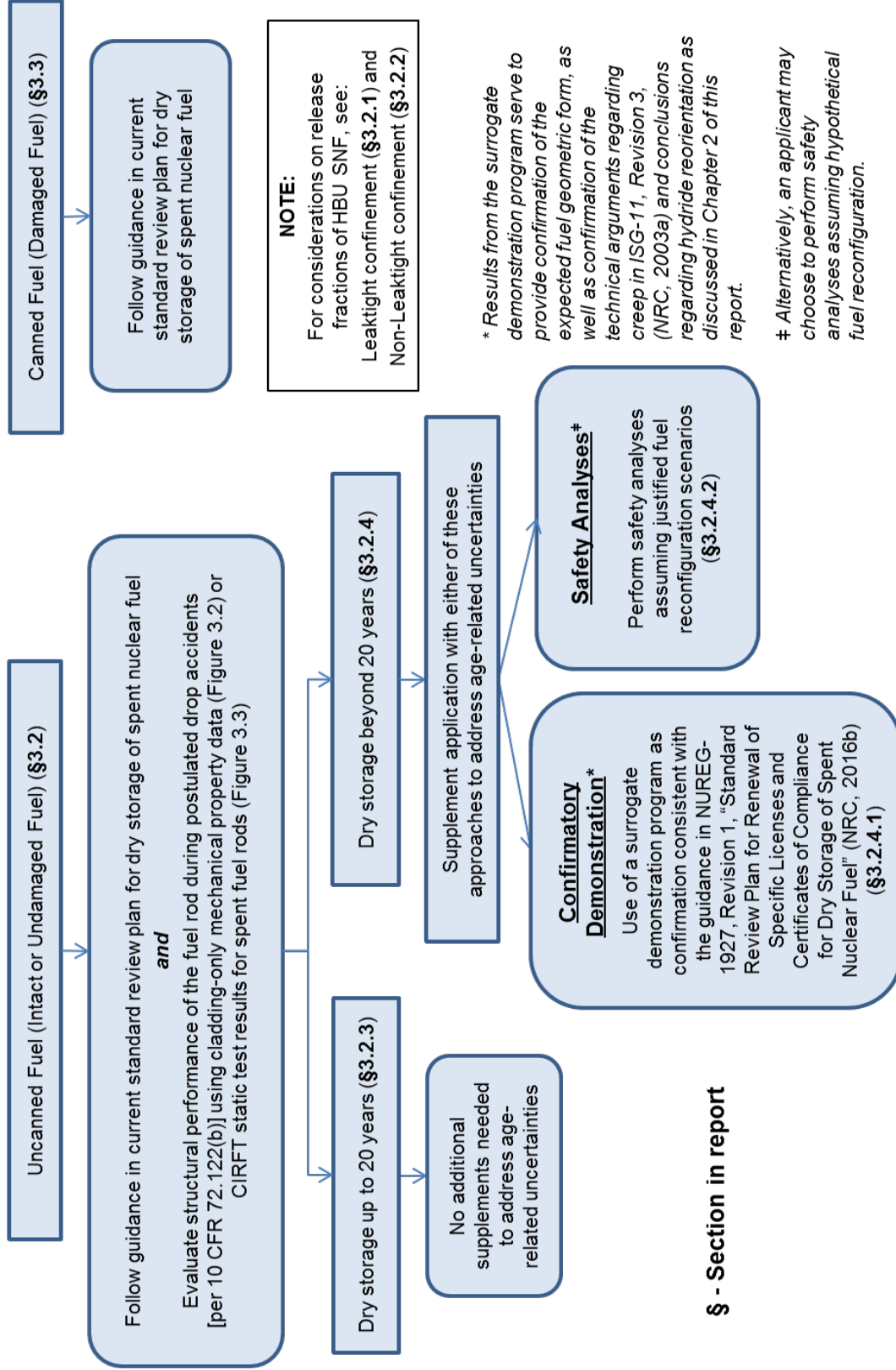


Figure 3-1 Example Licensing and Certification Approaches for Dry Storage of High Burnup Spent Nuclear Fuel

1 Consistent with the guidance in (ISG)-1, Revision 2 (NRC, 2007b), HBU SNF assemblies with
2 any of the following characteristics, as identified during the fuel selection process, are generally
3 classified as damaged unless an adequate justification is provided for not doing so:

4 • There is visible deformation of the rods in the HBU SNF assembly. This does not refer
5 to the uniform bowing that occurs in the reactor; instead, this refers to bowing that
6 significantly opens up the lattice spacing.

7 • Individual fuel rods are missing from the assembly. The assembly may be classified as
8 intact or undamaged if the missing rod(s) do not adversely affect the structural
9 performance of the assembly, or radiological and criticality safety (e.g., there are no
10 significant changes to rod pitch). Alternatively, the assembly may be classified as intact
11 or undamaged if a dummy rod that displaces a volume equal to, or greater than, the
12 original fuel rod is placed in the empty rod location.

13 • The HBU SNF assembly has missing, displaced, or damaged structural components
14 such that either:

15 – Radiological and/or criticality safety is adversely affected (e.g., significant change
16 in rod pitch),

17 – The structural performance of the assembly may be compromised during normal,
18 off-normal, and accident conditions of storage, or

19 – The assembly cannot be handled by normal means (i.e., crane and grapple), if
20 the design bases relies on ready retrieval of individual fuel assemblies.

21 • Reactor operating records or fuel classification records indicate that the HBU SNF
22 assembly contains fuel rods with gross rupture.

23 • The HBU SNF assembly is no longer in the form of an intact fuel bundle (e.g., consists
24 of, or contains, debris such as loose fuel pellets or rod segments).

25 Defects such as dents in rods, bent or missing structural members, small cracks in structural
26 members, and missing rods do not necessarily render an assembly as damaged, if the intended
27 functions of the assembly are maintained; i.e., the performance of the assembly does not
28 compromise the ability to meet fuel-specific and DSS-related regulations.

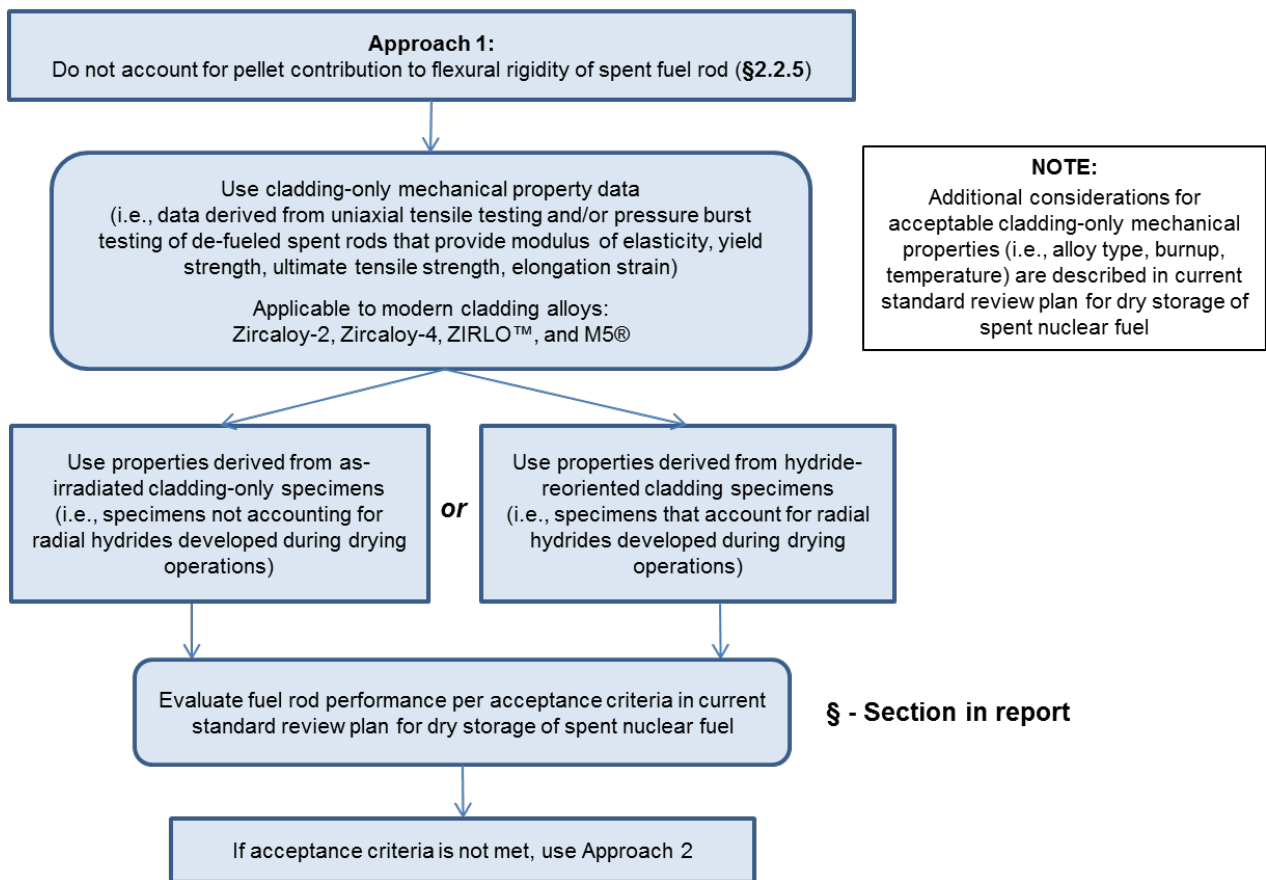
29 **3.2 Uncanned Fuel (Intact and Undamaged Fuel)**

30 Undamaged HBU SNF can be stored in the DSS without the need for a separate fuel can (i.e., a
31 separate metal enclosure sized to confine damaged fuel particulates) to maintain a known
32 configuration inside the DSS confinement cavity. This fuel includes rods that are either intact
33 (i.e., no breaches of any kind) or that contain small cladding defects (i.e., pinholes or hairline
34 cracks) that may permit the release of gas from the interior of the fuel rod. Cladding with gross
35 ruptures that may permit the release of fuel particulates may not be considered undamaged. The
36 configuration of undamaged HBU SNF may be demonstrated to be maintained if loading and
37 transport operations are designed to prevent and/or mitigate degradation of the cladding and
38 other assembly components, as discussed in ISG-22, "Potential Rod Splitting Due to Exposure to
39 an Oxidizing Atmosphere during Short-Term Cask Loading Operations in LWR or Other Uranium
40 Oxide Based Fuel," issued May 2006 (NRC, 2006).

1 Following the approaches delineated in Figure 3-1, an application for dry storage of undamaged
 2 HBU SNF would include a structural evaluation of the fuel rods under design-bases drop
 3 accident scenarios. The evaluation serves to demonstrate that the uncanned fuel remains in a
 4 known configuration after a drop accident scenario.

5 Two alternatives may be used to calculate cladding stress and strain, and cladding flexural
 6 rigidity, for the aforementioned evaluation of drop accident scenarios. The first alternative,
 7 shown in Figure 3-2, is to use cladding-only mechanical properties from as-irradiated cladding
 8 (i.e., cladding with circumferential hydrides, primarily), or hydride-reoriented cladding (i.e.,
 9 cladding that accounts for radial hydrides precipitated after the drying process).

Evaluation of Design-Bases Drop Accidents during Dry Storage
 (i.e., drops during transfer operations and non-mechanistic tip over)



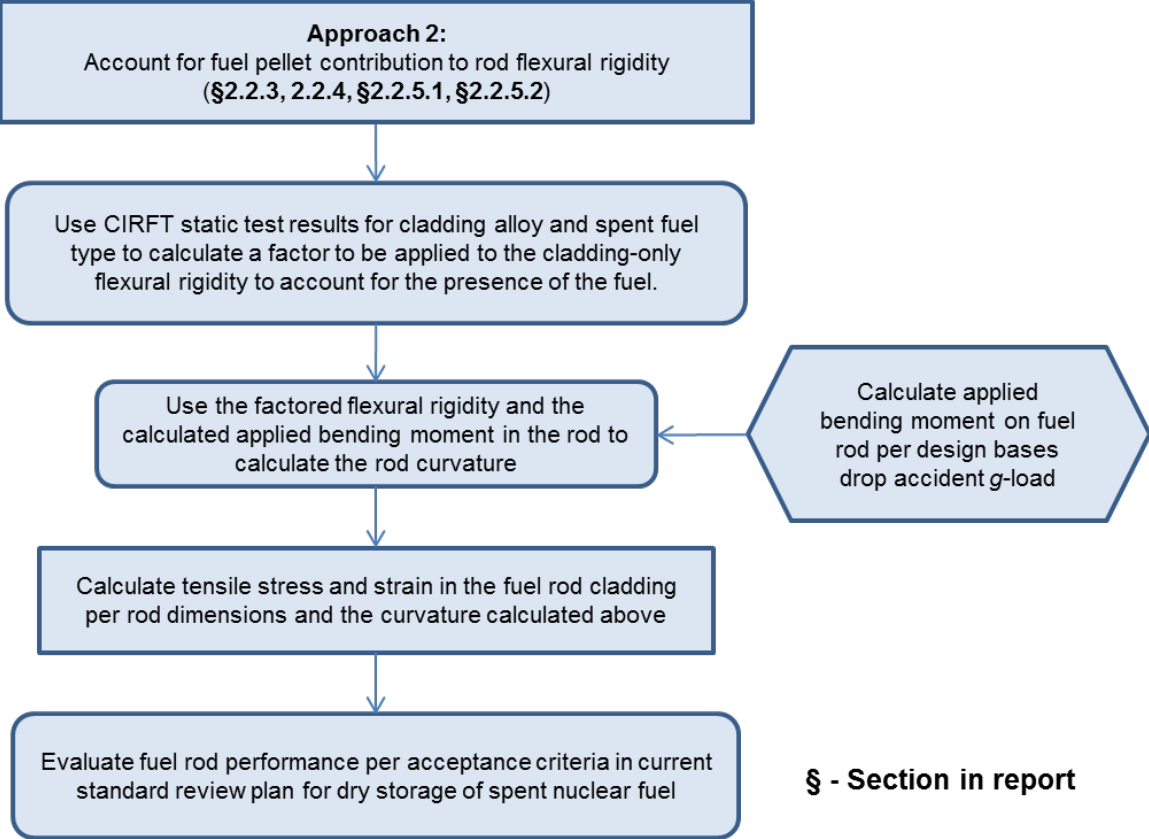
10 **Figure 3-2 First Approach for Evaluating Design-Bases Drop Accidents During Dry**
 11 **Storage**

12 As discussed in Section 2.3.3, the staff considers the orientation of the hydrides not to be critical
 13 when evaluating the adequacy of cladding-only mechanical properties. Therefore, the properties
 14 necessary to implement this first alternative may be derived from cladding-only uniaxial tensile
 15 tests and include modulus of elasticity, yield stress, ultimate tensile strength and uniform strain,
 16 and the strain at failure (i.e., the elongation strain). Refer to the current SRPs for dry storage of
 17 SNF for additional considerations for acceptable cladding-only mechanical properties (i.e., alloy

1 type, burnup, and temperature) and the acceptance criteria for cladding performance during dry
2 storage operations.

3 A second alternative, shown in Figure 3.3, is to use cladding-only mechanical properties that
4 have been modified by a numerical factor to account for the increased flexural rigidity imparted
5 by the fuel pellet. This numerical factor is obtained from static test data from the cyclic
6 integrated reversible-bending fatigue tester (CIRFT) for fully-fueled rods for the particular
7 cladding type and fuel type (see Section 2.3.3). However, this second alternative would be
8 necessary only if the structural evaluation using cladding-only mechanical properties is
9 unsatisfactory. Refer to the current SRP for dry storage of SNF for acceptance criteria on
10 cladding performance during dry storage operations.

Evaluation of Design-Bases Drop Accidents during Dry Storage
(i.e., drops during transfer operations and non-mechanistic tip over)



11 **Figure 3-3 Second Approach for Evaluation of Design-Bases Drop Accidents During**
12 **Dry Storage**

13 **3.2.1 Leaktight Confinement**

14 Consistent with the guidance in the current SRPs for dry storage of SNF, an application for a
15 DSS for HBU SNF is expected to define the maximum allowable leakage rate for the entire
16 confinement boundary. The maximum allowable leakage rate is based on the quantity of
17 radionuclides available for release and is evaluated to meet the confinement requirements for

1 maintaining an inert atmosphere within the DSS confinement cavity and compliance with the
2 regulatory limits of 10 CFR 72.104, “Criteria for Radioactive Materials in Effluents and Direct
3 Radiation from an ISFSI or MRS,” and 10 CFR 72.106, “Controlled Area of an ISFSI or MRS.”
4 Leakage rate testing is performed on the entire confinement boundary (over the course of
5 fabrication and loading) and ensures that the package can maintain a leak rate below the
6 maximum allowable leakage rate per ANSI N14.5 (2014).

7 If the entire DSS confinement boundary, including its closure lid, is designed and tested to be
8 “leaktight” as defined in American National Standards Institute (ANSI) N14.5 – 2014, “American
9 National Standard for Radioactive Materials—Leakage Tests on Packages for Shipment” and the
10 current SRPs for dry storage of SNF, then the application is not expected to include additional
11 dose calculations based on the allowable leakage rate that demonstrate compliance with the
12 regulatory limits of 10 CFR 72.104(a) and 10 CFR 72.106(b). In addition, the structural analysis
13 of the package is to demonstrate that the confinement boundary will not fail under the postulated
14 drop scenarios and that the confinement boundary will remain leaktight under all conditions of
15 storage. Refer to the current SRPs for dry storage of SNF for additional guidance on
16 demonstrating compliance with the leaktight criterion.

17 **3.2.2 Non-Leaktight Confinement**

18 For those DSS designs not tested to a “leaktight” confinement criterion, the application is
19 expected to include dose calculations based on the allowable leakage rate to demonstrate
20 compliance with the regulatory limits of 10 CFR 72.104(a) and 10 CFR 72.106(b). Leakage rate
21 testing is performed on the entire confinement boundary (over the course of fabrication and
22 loading) and ensures that the package can maintain a leak rate below the maximum allowable
23 leakage rate per ANSI N14.5 (2014).

24 To determine the dose rate for the confinement boundary, an application for a non-leaktight
25 DSS is expected to provide a technical basis for the assumed bounding HBU fuel failure rates
26 for normal, off-normal, and accident conditions of storage. If an application is not able to
27 provide and justify its bounding fuel failure rates, then the fuel failure rates below can be
28 assumed as bounding values for normal, off-normal, and accident conditions of storage:

- 29 • Normal conditions of storage: 1 percent
- 30 • Off-normal conditions of storage: 10 percent
- 31 • Accident conditions of storage: 100 percent

32 Bounding Release Fractions for High Burnup Spent Nuclear Fuel

33 HBU SNF fuel has different characteristics than low burnup (LBU) SNF with respect to cladding
34 oxide thickness, hydride content, radionuclide inventory and distribution, heat load, fuel pellet
35 grain size, fuel pellet fragmentation, fuel pellet expansion and fission gas release to the rod
36 plenum [See Appendix C.5 to NUREG/CR-7203, “A Quantitative Impact Assessment of
37 Hypothetical Spent Fuel Reconfiguration in Spent Fuel Storage Casks and Transportation
38 Packages,” issued September 2015 (NRC, 2015) for additional details on HBU SNF]. These
39 characteristics may affect the mechanisms by which the fuel can breach and the amount of fuel
40 that can be released from failed fuel rods. Hence, the staff evaluated open literature on HBU
41 fuel rod failure rates and release fractions of Chalk River unknown deposits (CRUD), fission
42 gases, volatiles, and fuel fines to assist in the review of applications for non-leaktight

1 confinement boundaries. Table 3-1 provides release fractions that may be considered
 2 reasonably bounding for HBU SNF. If the release fractions are not used, justification of the
 3 proposed release fractions of the source terms is expected to include an adequate description
 4 of burnup for the test specimen, number of tests, collection method for quantification of
 5 respirable release fractions, test specimen pressure at the time of fracture, and source
 6 collection system (sophisticated enough to gather the bounding respirable release fractions).

7 **Table 3-1 Fractions of Radioactive Materials Available for Release from HBU SNF**
 8 **Under Conditions of Dry Storage (for both Pressurized Water Reactor and**
 9 **Boiling Water Reactor Fuels)**

Variable	Normal Conditions	Off-Normal Conditions	Accident-Fire Conditions	Accident-Impact Conditions
Fraction of Fuel Rods Assumed to Fail	0.01	0.1	1.0	1.0
Fraction of Fission Gases Released Due to a Cladding Breach	0.15	0.15	0.15	0.35
Fraction of Volatiles Released Due to a Cladding Breach	3×10^{-5}	3×10^{-5}	3×10^{-5}	3×10^{-5}
Mass Fraction of Fuel Released as Fines Due to a Cladding Breach	3×10^{-5}	3×10^{-5}	3×10^{-3}	3×10^{-5}
Fraction of CRUD Spalling Off Cladding	0.15	0.15	1.0	1.0

10 CRUD

11 The average CRUD thickness in HBU SNF cladding has been estimated to be similar to that
 12 observed on LBU SNF cladding. A review of data in the literature (NRC, 2000c; Einziger and
 13 Beyer, 2007) indicates that a release (spalling off) of 15 percent of cladding CRUD may be
 14 assumed as reasonably bounding to both normal and off-normal conditions of storage, and a
 15 release of 100 percent of the cladding CRUD is conservatively bounding to both postulated fire
 16 and impact accidents during storage (NRC, 2014).

17 Fission Gases

18 The NRC's FRAPCON steady-state fuel performance code has been previously used to assess
 19 release fractions of fission gases during transportation (NRC, 2011). The seven most common
 20 fuel designs were evaluated using FRAPCON's modified Forsberg-Masih model (8×8, 9×9,
 21 and 10×10 fuel for boiling water reactors (BWRs) and 14×14, 15×15, 16×16, and 17×17 for
 22 pressurized-water reactors (PWRs). For each fuel design, a number of different power histories
 23 aimed at capturing possible realistic reactor irradiations were modeled. The fission gas content
 24 within the free volume of the rods was evaluated for a total of 243 different cases (39 for each of
 25 the BWR fuel designs; 37 for 14×14 and 16×16 PWR fuel designs, and 26 for 15×15 and 17×17
 26 PWR fuel designs). A review of the results indicates that a release of 15 percent of fission

1 gases may be assumed as reasonably bounding to normal conditions of transport scenarios for
2 rod average burnups up to 62.5 GWd/MTU. The same release fraction may be reasonably
3 assumed for both normal and off-normal conditions of storage.

4 During a fire accident scenario in storage, the fuel is not expected to reach temperatures high
5 enough that fission gases can diffuse out of the pellet matrix or grain boundaries to the rod
6 plenum. The thermal rupture tests showed that release occurred at higher temperatures than
7 those experienced during a transportation fire accident (NRC, 2000c). The same behavior is
8 expected during a postulated fire accident condition of storage. Therefore, the same release
9 fraction of 15 percent of fission gases during normal/off-normal conditions of storage may be
10 assumed to be reasonably bounding to the fire scenario under accident conditions of storage.

11 In the case of postulated impact accident (drop) scenarios (e.g., during transfer or retrieval
12 operations), the pellet may be conservatively assumed to crumble. In this scenario, fission
13 gases retained within the pellet grain boundaries may be released in addition to those already
14 released from the fuel rod free volume (i.e., from the fuel-cladding gap and plenum). The
15 FRAPFGR model in FRAPCON may be used to predict the location of the fission gases within
16 the fuel pellet (NRC, 2011). The model has been validated with experimental data obtained
17 using an electron probe micro analyzer. The FRAPFGR model was used to calculate the
18 maximum fraction of the pellet-retained fission gases that may be released during a drop
19 impact, which was determined to be 20 percent. Therefore, assuming all fission gases within
20 the pellet grain boundaries are released, a 35 percent (15 percent + 20 percent) maximum
21 release fraction may be assumed to be reasonably bounding to a postulated accident fire
22 scenario during storage. This value accounts for the 15 percent maximum fission gases
23 released from the fuel rod free volume (as calculated with the modified Forsberg- Massih model)
24 and the 20 percent maximum fission gases released from the fuel pellet grain boundaries (as
25 calculated with the FRAPFGR model). These release fraction estimates are consistent with
26 previous NRC estimates (NRC, 2000c; NRC, 2007; Einziger and Beyer, 2007).

27 Volatiles

28 Most of the volatile release fractions originate from cesium-based compounds in the form of
29 oxides or chlorides (NRC, 2000c; NRC, 2014). These volatiles exhibit a different release
30 behavior in comparison to fission gases. Volatiles tend to migrate and aggregate at the rim on
31 the outer surface of the fuel pellet during reactor irradiation, which is characteristic of burnups
32 near or exceeding 60 GWd/MTU. The pellet rim is characterized by a fine crystalline grain
33 structure (0.1—0.3 μm or submicron in characteristic size) (Spino et al., 2003; Einziger and
34 Beyer, 2007), a high porosity that may exceed 25 percent, and a high concentration of actinides
35 relative to the inner pellet matrix.

36 Sandia National Laboratories assessed the maximum release fraction of volatiles (cesium and
37 other ruthenium-based compounds) under drop and fire accident scenarios of transportation,
38 and determined it to be 0.003 percent (3×10^{-5}) (NRC, 2000c). This assessment included
39 modeling and analyses using various data from the literature. The volatile release fraction
40 during a fire accident scenario was determined to be lower than the release fraction during a
41 drop accident scenario (NRC, 2014; NRC, 2000c). Therefore, a volatile release fraction of
42 0.003 percent (3×10^{-5}) may be assumed to be reasonably bounding to normal, off-normal, and
43 accident conditions of storage. This release fraction estimate is also consistent with an
44 independent estimate by Einziger and Beyer (2007).

45

1 Fuel Fines

2 Release fractions from SNF fines during storage and transportation have been previously
3 documented (NRC, 2000c; NRC, 2007; Benke et al., 2012; NRC, 2014). HBU SNF has a
4 different pellet microstructure than LBU SNF, which is characterized by an inner matrix and an
5 outer pellet rim layer. The thickness of the outer pellet rim layer increases with higher fuel
6 burnup. Therefore, differences in microstructure between the inner pellet matrix and the outer
7 pellet rim should be considered when evaluating release fractions of fuel fines from HBU SNF.

8 Although there is no reported literature on HBU SNF rim fracture as a function of impact energy,
9 other data can be used to indirectly assess the contribution of the rim layer to the release
10 fractions of fuel fines. Spino et al (1996) estimated the fracture toughness of the rim layer from
11 micro-indentation tests. Compared to the inner SNF matrix, the rim layer showed an increase of
12 fracture toughness. The increase of fracture toughness implies a decrease of release fraction.
13 Hirose et al (2015) also discussed results of axial dynamic impact tests simulating accident
14 conditions during transport, which are expected to be bounding to postulated drop scenarios
15 during dry storage. The dispersed particles from pellet breakage following impact were
16 collected and correlated to impact energy. The staff has compared the measured release
17 fraction of fuel fines from Hirose et al (2015) with previous NRC estimates of release fraction
18 versus impact energy for SNF and other brittle materials (depleted UO_2 , glass and Synroc) (see
19 Figure 3 of NUREG 1864, "A Pilot Probabilistic Risk Assessment of a Dry Cask Storage System
20 at a Nuclear Power Plant" (NRC 2007)). Based on these analyses, the staff concludes that
21 there is no indication that pellet rim layer contributes to increased release fractions.

22 Since the outer HBU fuel pellet rim does not appear to contribute to additional release fractions,
23 previous NRC estimates for release fractions of fuel fines may continue to be used (NRC,
24 2000c; NRC, 2007; Benke, et al., 2012; Ahn et al., 2012; NRC, 2014). Per the range of
25 estimates in the literature, a release fraction for fuel fines of 0.003 percent (3×10^{-5}) may be
26 assumed to be reasonably bounding to normal, off-normal, and accident (drop impact)
27 conditions of storage. During a fire accident scenario, fuel oxidation is conservatively assumed
28 to increase the release fraction of fuel fines by a factor of 100 (NRC, 2000c; Ahn et al 2012).
29 Therefore, a 0.3 percent (3×10^{-3}) release fraction of fuel fines may be assumed as reasonably
30 bounding to fire accident conditions of storage.

31 The staff recognizes that various international cooperative research programs are currently
32 investigating release fractions from HBU SNF. Once those data are available to the public, the
33 staff will review and determine whether the conservative estimates in the above discussion
34 should be revisited.

35 **3.2.3 Dry Storage Up To 20 Years**

36 Section 1.2 discussed the staff's review guidance for the licensing and certification of dry
37 storage of HBU SNF for a period of up to 20 years. The technical basis referenced in that
38 guidance supports the staff's conclusion that creep is not expected to result in gross rupture if
39 cladding temperatures are maintained below 400 °C (752 °F).

40 Chapter 2 also provided an assessment of the effects of hydride reorientation per static and
41 fatigue bending test results on HBU SNF specimens. Those test results provide a technical
42 basis for the staff's conclusion that the use of cladding mechanical properties (with either as-
43 irradiated or hydride- reoriented microstructure) is adequate for the structural evaluation of HBU
44 SNF when evaluating postulated drops during dry storage (e.g., drops during transfer

1 operations, non-mechanistic DSS cask tipover). Refer to the current SRPs for dry storage of
2 SNF for staff review guidance on additional considerations for acceptable cladding-only
3 mechanical properties (i.e., alloy type, burnup, temperature), on acceptable references for
4 cladding mechanical properties and on acceptance criteria for the structural evaluation of the
5 HBU fuel assembly for the drop accident scenarios. As indicated in Figure 3-1, supplemental
6 safety analyses are not expected for HBU SNF in dry storage for periods not exceeding 20
7 years.

8 **3.2.4 Dry Storage Beyond 20 Years**

9 As indicated in Figure 3-1, to address age-related uncertainties related to the extended dry
10 storage of HBU SNF (i.e., dry storage beyond 20 years), the application is expected to be
11 supplemented with either results from a surrogate demonstration program or supplemental
12 safety analyses assuming justified hypothetical fuel reconfiguration scenarios. The results from
13 a surrogate demonstration program are meant to provide field-obtained confirmation that the
14 fuel has remained in the analyzed configuration after 20 years of dry storage. If confirmation is
15 not provided, the safety analyses for the DSS should be supplemented to assume reconfigured
16 fuel. Consistent with the requirements in 10 CFR Part 72, the supplemental information may be
17 provided in either the initial license or CoC application (per 10 CFR 72.40(a) and
18 10 CFR 72.238, "Issuance of an NRC Certificate of Compliance") or in a renewal application
19 (10 CFR 72.42(a) and 10 CFR 72.240(a)).

20 The NRC has approved the licensing and certification of HBU SNF for an initial 20-year-term per
21 the technical basis in the staff's review guidance, as discussed in Section 1.2. However, the
22 staff has recognized that the technical basis is based on short-term accelerated creep testing
23 (i.e., laboratory scale testing up to a few months), which results in increased uncertainties when
24 extrapolated to long periods of dry storage – see Appendix D to NUREG-1927, Revision 1
25 (NRC, 2016b). Although the staff has confidence based on this short-term testing that creep-
26 related degradation of the HBU fuel will not adversely affect its analyzed configuration for
27 storage periods beyond 20 years, there is no operational field-obtained data to confirm this
28 expectation, as was done in the prior demonstration on LBU fuel described in NUREG/CR-6745,
29 "Dry Cask Storage Characterization Project—Phase 1; CASTOR V/21 Cask Opening and
30 Examination," issued September 2001 (NRC, 2001),; and NUREG/CR 6831, "Examination of
31 Spent PWR Fuel Rods after 15 Years in Dry Storage," issued September 2003 (NRC, 2003b).

32 In addition, the staff also acknowledges that while the CIRFT results obtained to-date (as
33 discussed in Chapter 2) provide an adequate technical basis for assessing the separate effects
34 of hydride reorientation, the results do not account for potential synergistic effects of various
35 physical and chemical phenomena occurring during extended dry storage (e.g., cladding creep,
36 hydride reorientation, irradiation hardening, oxidation, hydriding caused by residual water
37 hydrolysis, etc. – see NUREG-2214, "Managing Aging Processes in Storage (MAPS) Report,"
38 issued October 2017 (NRC, 2017c) for discussions on these phenomena). Therefore, the staff
39 considers it prudent to gather and review evidence that HBU fuel in dry storage beyond 20
40 years has maintained its analyzed configuration be gathered and reviewed.

41 **3.2.4.1 Supplemental Results from Confirmatory Demonstration**

42 A demonstration program, like that conducted for LBU SNF (NRC, 2003; NRC, 2001; NRC,
43 2003b), may be used to confirm the results from separate-effects testing, which has provided
44 the technical bases for dry storage of HBU SNF beyond 20 years.

1 3.2.4.1.1 *Initial Licensing or Certification*

2 Consistent with 10 CFR 72.42(a) and 10 CFR 72.238, an applicant may request approval for dry
3 storage of HBU SNF for periods up to 40 years. These applications are not required to provide
4 aging management programs (AMPs), as these programs are expected only in renewal
5 applications. Instead, for initial licenses and CoC approvals for dry storage beyond 20 years (up
6 to 40 years), the application may describe the activities to obtain and evaluate confirmatory data
7 from a demonstration program under the aegis of a maintenance plan. The maintenance plan
8 would be implemented after the initial 20 years of dry storage. Applicants may refer to
9 Appendices B and D to NUREG-1927, Revision 1 (NRC, 2016b) when developing the
10 description of activities to assess data from the confirmatory demonstration.

11 3.2.4.1.2 *Renewal Applications*

12 Consistent with 10 CFR 72.42(a) and 10 CFR 72.240(a), a renewal application for a specific
13 license or CoC, may describe the activities to obtain and evaluate confirmatory data to be
14 performed under the aegis of an AMP. Applicants may refer to Appendices B and D to NUREG-
15 1927, Revision 1 (NRC, 2016b) when developing the description of activities to assess data
16 from the confirmatory demonstration.

17 3.2.4.2 *Supplemental Safety Analyses*

18 As an alternative approach to a confirmatory demonstration for HBU SNF, an application may
19 supplement the design bases with safety analyses that demonstrate the DSS can still meet the
20 pertinent regulatory requirements by assuming hypothetical reconfiguration of the HBU fuel
21 contents into justified geometric forms. This alternative approach would demonstrate that the
22 design-bases fuel, even if reconfigured, can still meet the 10 CFR Part 72 requirements for
23 thermal, confinement, criticality safety and shielding during normal, off-normal, and accident
24 conditions. For renewal applications, a separate license amendment or CoC amendment may
25 be required if the changes in the supplemental safety analyses do not meet the acceptance
26 criteria in 10 CFR 72.48, “Changes, Tests, and Experiments.”.

27 In NUREG/CR-7203 (NRC, 2015), ORNL Oak Ridge National Laboratory (ORNL) evaluated the
28 impact of a wide range of postulated fuel reconfiguration scenarios under non-mechanistic
29 causes of fuel assembly geometry change with respect to criticality, shielding (dose rates),
30 containment, and thermal. The study considered three fuel reconfiguration categories , which
31 were characterized by either category 1, cladding failure; category 2, rod/assembly deformation
32 without cladding failure; or category 3 changes to assembly axial alignment without cladding
33 failure. Within configurations in both Category 1 and Category 2, the study identified various
34 scenarios:

- 35 • Category 1: cladding failure
- 36 – Scenario 1(a): breached rods
- 37 – Scenario 1(b): damaged rods

38

39

- 1 • Category 2: rod/assembly deformation without cladding failure
- 2 – Scenario 2(a): configurations associated with side drop
- 3 – Scenario 2(b): configurations associated with end drop
- 4 • Category 3: changes to assembly axial alignment without cladding failure

5 The analyses in NUREG/CR-7203 (NRC, 2015) considered representative SNF transportation
6 packages, and a range of fuel initial enrichments, discharge burnup values, and decay times.
7 Two package designs were analyzed: a general burnup credit (GBC)-32 package containing 32
8 PWR fuel assemblies and a GBC-68 package containing 68 BWR fuel assemblies. Although
9 NUREG/CR-7203 did not evaluate reconfiguration in DSSs, the scenarios and analytical
10 methods may also be applicable to those designs, as the loads experienced during transport
11 conditions (normal, hypothetical accident) are expected to bound those experienced during
12 storage (normal, off-normal and accident). The results in NUREG/CR-7203 should not be
13 assumed to be generically applicable as fuel reconfiguration may have different consequences
14 for a DSS design other than the generic models evaluated in the study. However, the following
15 sections discuss considerations in developing supplemental safety analyses for other DSS
16 designs according to the reconfiguration scenarios considered in NUREG/CR-7203.

17 3.2.4.2.1 *Materials and Structural*

18 An application relying on supplemental safety analyses based on hypothetical reconfiguration of
19 the HBU SNF contents should provide a structural evaluation for the package and its fuel
20 contents using any of the approaches discussed in Section 3.2. The staff will review the
21 structural evaluation and the assumed material mechanical properties, including any changes
22 due to higher temperatures resulting from fuel reconfiguration, in a manner consistent with the
23 guidance in the current SRP for dry storage of SNF.

24 3.2.4.2.2 *Confinement*

25 An application relying on supplemental safety analyses based on hypothetical reconfiguration of
26 the HBU SNF is expected to demonstrate that the DSS design meets the regulatory
27 requirements for confinement if data from a surrogate demonstration program, used for
28 confirmatory demonstration following the guidance in NUREG-1927, Revision 1 (NRC, 2016b),
29 is not available before the renewal of the license for previously dry-stored fuel for periods longer
30 than 20 years.

31 However, if the thermal, structural, and material analyses, together with aging management
32 activities for the DSS subcomponents supporting confinement (i.e., confinement boundary)³, are
33 used to provide assurance that the allowable leak rate is maintained even after hypothetical
34 reconfiguration of the fuel under normal, off-normal and accident-level conditions, supplemental
35 safety analysis for the confinement performance of the DSS design are not expected. Thermal
36 analyses demonstrate that all DSS subcomponents supporting confinement (i.e., confinement

³ Aging management activities may be conducted under either the aegis of an NRC-approved AMP (for renewal applications) or a maintenance plan (for initial license or CoC applications requesting approval for periods exceeding 20 years).

1 boundary) will be able to withstand their maximum operating temperatures and pressures under
2 normal, off-normal and accident-level conditions.

3 3.2.4.2.3 *Thermal*

4 Fuel reconfiguration can affect the efficiency of heat removal from the fuel because of changes
5 in (1) thermo-physical properties of the canister gas space stemming from release of fuel rod
6 inert gas and fission product gases, (2) heat source location within the canister, and (3) changes
7 in flow area (convection), conduction lengths (conduction) and radiation view factors (thermal
8 radiation). As part of a defense-in-depth approach for addressing age-related uncertainties for
9 uncanned and undamaged HBU fuel in dry storage beyond 20 years, the thermal analyses
10 would be expected to analyze scenarios for normal, off-normal, and accident conditions of
11 storage by assuming the fuel may become substantially altered. NUREG/CR-7203 (NRC, 2015)
12 describes the impact on the DSS canister pressure and the fuel cladding and DSS component
13 temperatures for various scenarios of fuel geometry changes. These are examined below. In
14 general, the results in NUREG/CR-7203 should not be considered generically applicable. The
15 thermal analyses of the application are expected to consider scenarios discussed in
16 NUREG/CR-7203 to determine consistency in the analytical methods, scenario phenomena,
17 and results. The thermal analyses are expected to assess the impact of the fuel reconfiguration
18 on the fuel cladding and DSS component temperatures and the canister pressure for the
19 particular DSS design.

20 For Scenario 1(a) in Category 1 (see Section 3.2.4.2) , the fuel rods are assumed to breach in
21 such a manner that the cladding remains in its nominal geometry (no fuel reconfiguration), but
22 depending on the canister orientation (horizontal or vertical), the release of fuel rod fill gas and
23 fission product gases can cause a change to component peak temperatures. For Scenario 1(b)
24 in Category 1, for configurations where an assembly (or assemblies) is represented as a debris
25 pile(s) inside its basket cell, fuel reconfiguration has a larger impact on the component
26 temperatures for the vertical orientation than for the horizontal orientation, but the packing
27 fraction of the debris bed has minor impact on the component temperatures. For both
28 Scenarios 1(a) and 1(b), release of the fuel rod gaseous contents increases the number of
29 moles of gas and therefore increases the canister pressure. The canister pressure is expected
30 to increase with the increased fuel rod release fractions.

31 For Scenarios 2(a) and 2(b), the fuel rods are assumed to remain intact without gaseous
32 leakage into the canister space. The changes of the fuel assembly lattice (contraction in
33 Scenario 2(a) and expansion in Scenario 2(b)) could cause either an increase or decrease in
34 the component temperatures of the storage system depending on the initial assembly geometry
35 and whether the storage system relies on convection for heat transfer. In general, scenarios
36 Scenario 2(a) and Scenario 2(b) have minor impact on the fuel cladding and DSS component
37 temperatures and canister pressure. For Category 3, the fuel rods are assumed to remain intact
38 without gaseous leakage into the canister space, but the axial shifting of the assembly changes
39 the heat source location within the canister. Changes in assembly axial alignment within the
40 basket cells are expected to have minor impact on the component temperatures and the
41 canister pressure.

42 Normal, Off-Normal, and Accident Conditions of Storage

43 Based on the thermal phenomena described above and NUREG/CR-7203 (NRC, 2015), an
44 approach acceptable to staff would evaluate the impact of Scenarios 1(a) and 1(b) on the
45 canister pressure and the fuel cladding and package component temperatures assuming

1 rupture of 1 percent, 10 percent and 100 percent of the fuel rods for normal, off-normal, and
2 accident conditions, respectively.

3 Although Scenarios 2(a) and 2(b) in Category 2 and Category 3 are not expected to have a
4 significant impact on DSS thermal performance under normal, off-normal and accident
5 conditions, because the fuel rods in Scenarios 2(a), 2(b) and 3 are assumed to remain intact
6 without gaseous leakage into the canister space, the applicant may need to provide a thermal
7 evaluation due to specifics of the DSS design.

8 3.2.4.2.4 *Criticality*

9 An application may demonstrate that a DSS meets the regulatory requirements for criticality
10 safety for the period beyond 20 years by assuming hypothetical reconfiguration of the HBU
11 SNF into a bounding geometric form. This approach is one way to ensure compliance with
12 10 CFR 72.124, "Criteria for Nuclear Criticality Safety," or 10 CFR 72.236(c) during normal, off-
13 normal, and accident conditions, if the structural evaluation does not adequately define the
14 mechanical properties of the cladding.

15 As mentioned previously, ORNL examined hypothetical fuel reconfiguration for various
16 scenarios and the impacts on the criticality safety of a DSS and documented the results in
17 NUREG/CR-7203. This study, considers burnup up to 70 GWd/MTU for criticality evaluations.
18 NUREG/CR-7203 provides some insight into the reactivity trends for various reconfiguration
19 scenarios; however the results in NUREG/CR-7203 (NRC, 2015) should not be considered
20 generically applicable with respect to criticality safety analyses.

21 Criticality is not a concern for dry SNF systems, as SNF requires moderation to reach criticality.
22 Although DSS casks are expected to remain dry while in storage, cask users may be allowed to
23 load and unload a cask in a wet environment. The criticality analyses in NUREG/CR-7203 are
24 performed with an assumption of fully flooded conditions and any conclusions adopted are
25 applicable to analyses that support wet loading and unloading. The following considerations for
26 criticality evaluations for reconfigured fuel are applicable only to DSS scenarios where there
27 may be flooding within the canister. Otherwise, the staff does not find reconfiguration to pose a
28 criticality safety concern for a dry system.

29 All of the criticality safety analyses presented in NUREG/CR-7203 take credit for burned fuel
30 nuclides (burnup credit) and the conclusions may not be applicable to criticality analyses that
31 assume a fresh fuel composition. In its review of the burnup credit methodology and code
32 benchmarking used to support a criticality safety evaluation, the staff will follow the guidance in
33 ISG-8, Revision 3, "Burnup Credit in the Criticality Safety Analyses of PWR Spent Fuel in
34 Transportation and Storage Casks," issued in September 2012 (NRC, 2012) to review the
35 burnup credit analyses. ISG-8, Revision 3, does not endorse any particular methodology for
36 BWR fuel burnup credit. The staff does not necessarily endorse the methodology described in
37 NUREG/CR-7203 for BWR fuel DSS, and considers it to be for illustration only.

38 For criticality safety analyses using burnup credit, NUREG/CR-7203 (NRC, 2015) shows that
39 reactivity increases for longer decay times (e.g., analyses supporting storage beyond 20 years)
40 would need to use an appropriate decay time within the criticality evaluations. The enrichment
41 and burnup values assumed within the criticality evaluations in NUREG/CR-7203 may differ
42 from those allowed within another storage system. However NUREG/CR-7203 states that no
43 significant differences were observed in trends between configurations that evaluated fuel at
44 44.25 GWd/MTU and 70 GWd/MTU.

1 The following sections discuss information from NUREG/CR-7203 that may be applicable when
2 performing reconfiguration analyses within a criticality evaluation for HBU fuel under normal, off-
3 normal, and accident conditions of storage.

4 Normal Conditions of Storage

5 In an approach acceptable to the staff, the applicant's criticality safety analyses would consider
6 the reactivity impact of 3-percent fuel failure during normal conditions of storage. The most
7 applicable scenario from NUREG/CR-7203 (NRC, 2015) is Scenario 1(a) (See Section 3.2.4.2
8 above for a description of the scenarios).

9 ORNL created Scenario 1(a) to represent breached rods. ORNL assumed that a percentage of
10 the rods were breached and that cladding from these rods failed completely and then removed
11 this percentage of fuel rods from the system. This is conservative as SNF systems are
12 undermoderated and replacing fuel with moderator typically causes reactivity to increase. Using
13 a fresh fuel composition for PWR fuel, ORNL's models in NUREG/CR-7203 showed that
14 reactivity decreases when removing rods. Therefore, this type of analysis may not be
15 appropriate for PWR analyses that assume a fresh fuel composition. The location assumed for
16 failed or removed rods can significantly effect reactivity. ORNL showed in Section A.1.1 of
17 NUREG/CR-7203 that removing rods from the center of the assembly causes reactivity to
18 increase the most.

19 In NUREG/CR-7203, ORNL also showed the number of rods removed that produces the
20 maximum reactivity. For the systems studied, NUREG/CR-7203 shows that the maximum
21 reactivity occurs when a number of rods far greater than 1-percent is removed from the system.

22 NUREG/CR-7203 also presents the results of a sensitivity study showing that reactivity increases
23 even more for Scenario 1(a) when it is assumed that the failed fuel relocates to a location outside
24 of the absorber plate. This is based on the generic systems modeled for the study. A different
25 system may allow relocation of the failed rod material outside of the absorber plate material to a
26 different extent.

27 Off-Normal Conditions of Storage

28 In an approach acceptable to the staff, the applicant's criticality safety analyses would consider
29 the reactivity impact of 10-percent fuel failure under off-normal conditions of storage. The
30 methods discussed in the previous section on normal conditions of storage also apply to off-
31 normal conditions of storage; however the applicant would consider fuel failure up to 10 percent
32 rather than 1 percent. Scenario 1(a) can be used to represent rod failure via removing rods
33 from the system. In this case an applicant would remove 10-percent of the rods rather than 1-
34 percent. The applicant would remove rods in such a way that it produces maximum reactivity
35 and consider relocation of the fuel to outside of the absorber plates.

36 Accident Conditions of Storage

37 In an approach acceptable to the staff, the applicant's criticality safety analyses would consider
38 the reactivity impact of 100-percent fuel failure under accident conditions of storage. The
39 damaged fuel models in Section A.1.2 for Scenario 1(b) from NUREG/CR-7203 are applicable
40 when representing 100 percent failed fuel.

1 Scenario 1(b) from NUREG/CR-7203 considers reconfiguration of damaged fuel. With 100-
2 percent compromise in cladding integrity, reconfiguration is considered to the maximum extent.
3 Section A.1.2 of NUREG/CR-7203 shows that a model assuming an “ordered pellet array” is
4 more reactive than a homogenous mixture of fuel, cladding materials and water.

5 3.2.4.2.5 *Shielding*

6 An application may demonstrate that a DSS continues to meet the regulatory dose limits for the
7 period beyond 20 years by assuming hypothetical reconfiguration of the HBU SNF into a
8 justified bounding geometric form under normal, off-normal, and accident conditions. This
9 method is one way to demonstrate compliance with 10 CFR 72.104, 10 CFR 72.106, or 10 CFR
10 72.236(d).

11 To assess the impacts of various fuel geometry changes on the shielding designs of DSSs and
12 ISFSIs, ORNL analyzed various scenarios of fuel geometry changes and the impact on the
13 annual dose at the ISFSI boundary and dose rates near the cask and presented the results in
14 NUREG/CR-7203 (NRC, 2015).

15 Appendix B to NUREG/CR-7203 (provides some insight into the effects on external dose for
16 various reconfiguration scenarios; however the results in NUREG/CR-7203 should not be
17 considered generically applicable with respect to external dose and dose rate evaluations. A
18 DSS designer would assess the impacts of fuel reconfiguration on external dose and dose rates
19 for its particular design.

20 This section discusses an approach acceptable to the staff for addressing the impacts on
21 external dose and dose rates when considering possible reconfiguration of HBU fuel for a period
22 of storage beyond 20 years. This discusses the scenarios from NUREG/CR-7203 most
23 applicable to the reconfiguration under normal, off-normal, and accident conditions of storage as
24 well as the analytical assumptions likely to result in bounding dose and dose rates based on the
25 results from NUREG/CR-7203. The NUREG has considered burnup up to 65 GWd/MTU within
26 its dose and dose rate evaluations. As discussed in Section B.5 of NUREG/CR-7203, different
27 nuclides become important to external dose and dose rate based on the decay time.

28 Since reconfiguration is to be considered after 20 years of storage, and this length of cooling
29 time is generally much longer than cooling times used to establish loading tables, applicants
30 may be able to make the justification that increases to external dose due to reconfiguration are
31 bounded by the additional cooling time the assemblies will experience.

32 NUREG/CR-7203 also indicates that fuel assembly type, (i.e., PWR vs BWR), may have a
33 significant impact on the surface dose rate and controlled area boundary dose under fuel
34 reconfiguration scenarios. Tables 13 and 14 of NUREG/CR-7203 show the difference in dose
35 rate increase for BWR and PWR SNF. A DSS system may permit storage of other fuel
36 assemblies, with different allowable burnup and enrichments to which the results of
37 NUREG/CR-7203 (NRC, 2015) do not apply. The burnup profile and depletion parameters used
38 to create the source term within NUREG/CR-7203 may also not be generically applicable.

39 Normal Conditions of Storage

40 In an approach acceptable to the staff, the applicant’s external dose and dose rate evaluation
41 would consider the impact of 3-percent fuel failure during normal conditions of storage. The
42 most applicable scenario from NUREG/CR-7203 is Category 1, fuel failure, Scenario, 1(a). If

1 cladding is breached and the fuel fails, this could lead to source relocation or change of the
2 geometric shape of the source. Based on NUREG/CR-7203, the impact on the controlled-area
3 boundary dose caused by source relocation resulting from 1-percent fuel failure is insignificant.
4 For a different DSS, the application may need to discuss potential fuel failure and source
5 reconfiguration and the potential impact on controlled-area boundary doses as required by 10
6 CFR 72.104 and 10 CFR 72.106.

7 Depending on the DSS and the resultant fuel geometry, the dose rate may increase significantly
8 as the detector moves close to the cask. Although it may not cause a significant change to the
9 dose and therefore may not constitute a significant concern for people at the controlled area
10 boundary, the changes of source term geometry will affect the doses of occupational workers
11 who need to perform necessary work around the casks. In general, an application should
12 consider the impact of HBF failure on the near cask dose rate and potential impacts on radiation
13 protection associated with ISFSI surveillance and maintenance operations.

14 Off-Normal Conditions of Storage

15 In an approach acceptable to the staff, the applicant's external dose and dose rate evaluation
16 for HBF would consider the impact of 10-percent fuel failure under off-normal conditions of
17 storage. If cladding is breached and fails, the fuel, and hence the source, may relocate to
18 different parts of the fuel basket. The impact of HBF failure on dose at the controlled-area
19 boundary for storage under off-normal conditions of dry storage operations should be examined.

20 A 10-percent fuel failure is similar to Scenario 1(a) in NUREG/CR-7203 (NRC, 2015). For
21 Scenario 1(a), breached rods, ORNL assumed the rods turned to rubble and calculated the
22 dose rate when the fuel mixture relocated to the bottom of the fuel assembly. ORNL assumed
23 failure of 10-percent of fuel rods collected into the available free volume within the assembly
24 lower hardware region. Section B.4.1 of NUREG/CR-7203 discusses the implementation in
25 detail. ORNL reduced the source strength and density of the active fuel zone by the failure
26 percentage and relocated this source to the bottom of the fuel assembly and increased the
27 source strength and density accordingly. The storage system in NUREG/CR-7203 is modeled
28 as a vertically-oriented storage system. Fuel would likely not relocate this way in a horizontal
29 storage system, and the models is not necessarily applicable to a horizontal system.

30 In Section B.5.5 of NUREG/CR-7203, ORNL discuss the results of the study performed on the
31 individual storage, which shows that there could be significant increases in the dose rate near
32 the cask. It concludes that fuel configuration changes can cause significant dose rate increases
33 relative to the nominal intact fuel configuration in the cask outer regions that face air vent
34 locations. NUREG/CR-7203 states that the change in radiation dose rate away from air vent
35 locations is either small or negligible.

36 Similar to normal conditions of storage, the changes in source term geometry will impact the
37 doses of occupational workers who need to perform necessary surveillance and maintenance
38 work around the casks. To assess the impacts on radiation protection, an applicant may need
39 to evaluate the surface dose rate increase resulting from reconfiguration.

40 Accident Conditions of Storage

41 In an approach acceptable to the staff, the applicant's external dose and dose rate evaluation
42 for HBF would consider the impact of 100-percent fuel failure during normal conditions of
43 storage. If cladding is breached and the fuel fails, this may cause the fuel, and hence the

1 source, to relocate to different parts of the fuel basket. Based NUREG/CR-7203 (NRC, 2015),
2 the impacts on the controlled-area boundary dose caused by source relocation resulting from
3 100 percent fuel failure will result in significant increases in the dose rate near the cask and
4 annual dose on the controlled area boundary. Scenarios 1(b) and 2 in NUREG/CR 7203 can
5 represent 100-percent fuel failure.

6 At the controlled area boundary, 100-percent fuel reconfiguration can have a significant impact
7 on the annual dose. It can also significantly affect the dose rate near the cask and the radiation
8 protection associated with ISFSI remediation operations. Tables B.9 and B.10 of Appendix B to
9 NUREG/CR-7203 (NRC, 2015) show the relative changes in dose rates at 1 meter from a
10 sample PWR fuel cask and a sample BWR fuel cask, respectively. Table B.11 of Appendix B to
11 NUREG/CR-7203 shows the estimated relative impact on controlled-area boundary dose from
12 fuel reconfiguration. The data presented in these tables show that the impacts on the dose
13 rates at the cask side, particularly the dose rate near the vent ports are significant.

14 In Scenario 1(b), ORNL assumed that the assembly and basket plate material is homogenized,
15 placed it at the bottom of the cask, and determined that the limiting packing fraction is 0.58.
16 This scenario did not produce an increase in site boundary dose; however, it did show an
17 increase in local dose rates. The location of the “bottom” of the cask would depend on whether
18 the DSS is vertical or horizontal. Homogenizing the basket material with the fuel rubble may be
19 overly conservative for a horizontal configuration, and applicants may choose to maintain basket
20 integrity similar to the Scenario S2 model in Section B.4.2 of NUREG/CR-7203 when evaluating
21 dose or dose rates for a horizontal system or a tip-over scenario.

22 For Scenario 1(b), ORNL also assumed that the fuel and basket material forms a homogenized
23 rubble that is distributed throughout the canister cavity. This scenario produced an increase in
24 site boundary dose.

25 **3.3 Canned Fuel (Damaged Fuel)**

26 10 CFR 72.122(h)(1) requires SNF, including HBU, with gross ruptures (i.e., classified as
27 damaged) be placed in a can designed for damaged fuel or in an acceptable alternative. The
28 staff will follow the guidance in the current SRPs for dry storage of SNF in its review of an
29 application for a DSS with damaged HBU SNF contents.

4 TRANSPORTATION OF HIGH BURNUP SPENT NUCLEAR FUEL

4.1 Introduction

The U.S. Nuclear Regulatory Commission (NRC) staff (the staff) has developed example approaches for approval of transportation packages with high burnup (HBU) spent nuclear fuel (SNF). Applicants may use these approaches to provide reasonable assurance of compliance with Title 10 of the *Code of Federal Regulations* (10 CFR) Part 71, “Packaging and Transportation of Radioactive Material,” during normal conditions of transport and hypothetical accident conditions. The staff developed these example approaches based on the conclusions of the engineering assessment in Chapter 2. Figure 4-1 provides a high-level diagram of these approaches, which vary based on (1) the condition of the fuel (undamaged or damaged), and (2) the length of time the fuel has been in prior dry storage. Considerations for additional analyses expected for non-leaktight transportation packages are also provided (see Section 4.2.2). An applicant may consider and demonstrate other approaches to be acceptable.

As required by 10 CFR 71.33(b), an application for a transportation package should identify allowable SNF contents and condition of the assembly and rods. The allowable cladding condition for the SNF contents is generally defined in the certificate of compliance (CoC), and the nomenclature may vary between different transportation packages. For example, the terms “intact” and “undamaged” have both been used to describe cladding without any known gross cladding breaches. In accordance with 10 CFR 71.17(c)(2) (for NRC licensees) and 49 CFR 173.471 (for non-NRC licensees), users of transportation packages must comply with the CoC by selecting and loading the appropriate fuel, and, in accordance with 10 CFR 71.91, “Records,” must maintain records that reasonably demonstrate that loaded fuel was adequately selected, in accordance with their approved site procedures and Quality Assurance Program.

Interim Staff Guidance (ISG)-1, Revision 2, “Classifying the Condition of Spent Nuclear Fuel for Interim Storage and Transportation Based on Function,” issued in May 2007 (NRC, 2007b), provides guidance for developing the technical basis supporting the conclusion that the HBU SNF (both rods and assembly) to be shipped are intact or undamaged.¹ This would include considering whether the material properties, and possibly the configuration, of the SNF assemblies may have been altered during prior dry storage. If the alteration is not within the bounds of the approved contents for the transportation package, then an application must be submitted to revise the CoC. This application must show that, with the altered condition of the SNF, the package can still meet the regulations in 10 CFR Part 71.

Damaged SNF is generally defined in terms of the characteristics needed to perform functions to assure compliance with fuel-specific and package-related regulations. A fuel-specific regulation defines a characteristic or performance requirement of the SNF assembly (e.g., 10 CFR 71.55(d)(2)). A package-related regulation defines a performance requirement placed on the fuel so that the transportation package can meet a regulatory requirement (e.g., 10 CFR 71.55(e)). The glossary provides the staff’s definitions of intact, undamaged, and damaged fuel. For additional information, refer to the current standard review plan (SRP) for transportation of SNF (NUREG-1617, “Standard Review Plan for Transportation Packages for Spent Nuclear

¹ The current revisions of all ISG documents will be rolled into revised standard review plans (SRPs) for dry storage and transportation, as appropriate, and will then be removed from the public domain. The revised SRPs will be issued for public comment prior to being finalized.

1 fuel,” issued in March 2000 (NRC, 2000b)) – hereafter referred to as the current SRP for
2 transportation SNF.²

² The current SRP for transportation of SNF is being consolidated with current revisions of all ISG documents into a single document, NUREG-2216, “Standard Review Plan for Approval of Transportation Packages,” Draft Report for Comment to be issued in 2018 (NRC, 2018).

Transportation of High Burnup Spent Nuclear Fuel
Normal Conditions of Transport (NCT) and Hypothetical Accident Conditions (HAC)

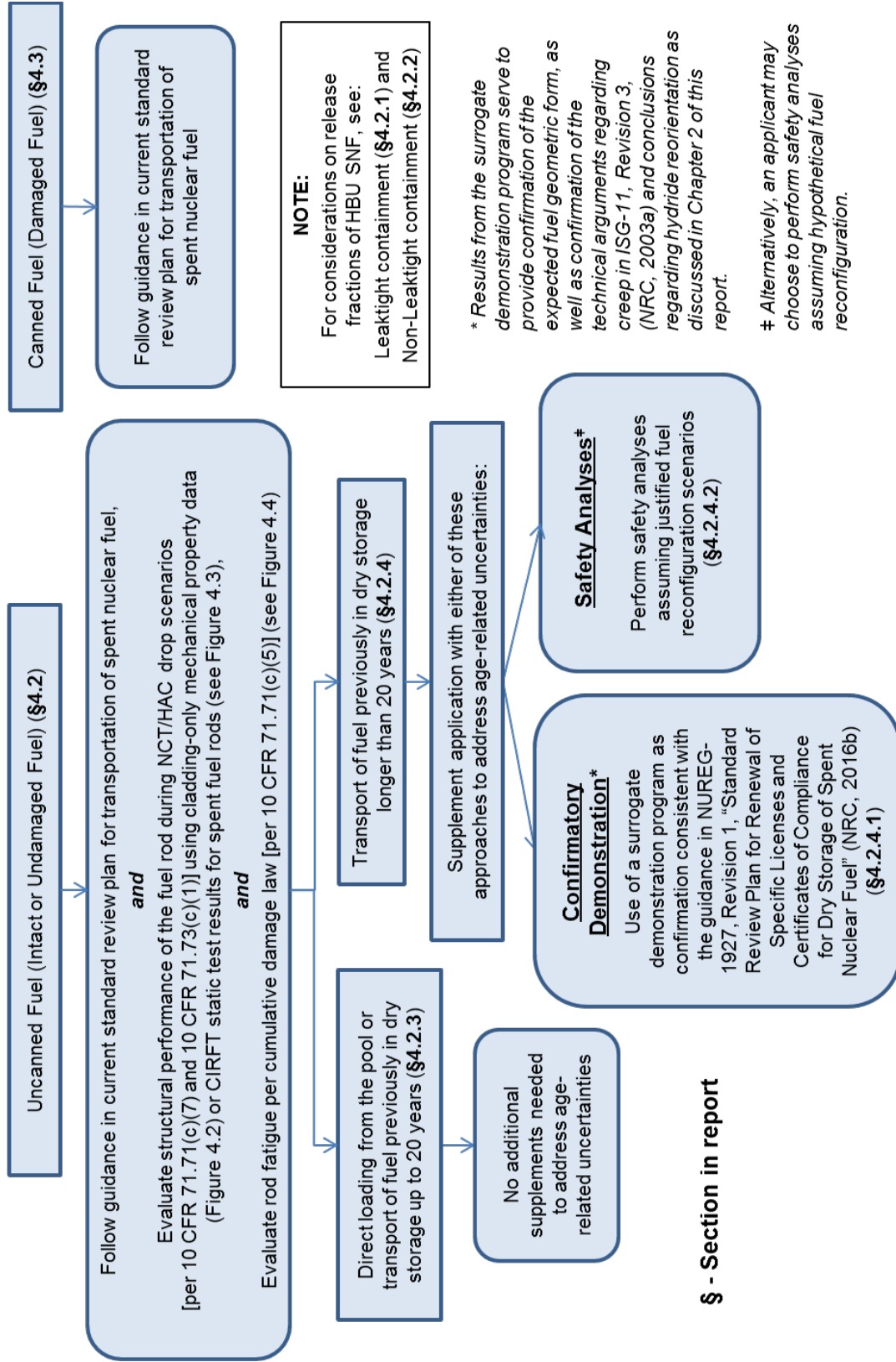


Figure 4-1 Example Approaches for Approval of Transportation Packages with High Burnup Spent Nuclear Fuel

1 Consistent with the guidance in (ISG)-1, Revision 2 (NRC, 2007b), SNF assemblies with any of
2 the following characteristics, as identified during the fuel selection process, are generally
3 classified as damaged unless an adequate justification is provided that shows otherwise:

4 • There is visible deformation of the rods in the HBU SNF assembly. This is not referring
5 to the uniform bowing that occurs in the reactor; instead, this refers to bowing that
6 significantly opens up the lattice spacing.

7 • Individual fuel rods are missing from the assembly. The assembly may be classified as
8 intact or undamaged if the missing rod(s) do not adversely affect the structural
9 performance of the assembly, and radiological and criticality safety (e.g., there are no
10 significant changes to rod pitch). Alternatively, the assembly may be classified as intact
11 or undamaged if a dummy rod that displaces a volume equal to, or greater than, the
12 original fuel rod is placed in the empty rod location.

13 • The HBU SNF assembly has missing, displaced, or damaged structural components
14 such that either: of the following occurs:

15 – Radiological and/or criticality safety is adversely affected (e.g., significantly
16 changed rod pitch)

17 – The structural performance of the assembly may be compromised during normal
18 conditions of transport (NCT) or hypothetical accident conditions (HAC).

19 • Reactor operating records or fuel classification records indicate that the HBU SNF
20 assembly contains fuel rods with gross ruptures.

21 • The HBU SNF assembly is no longer in the form of an intact fuel bundle (e.g., it consists
22 of, or contains, debris such as loose fuel pellets or rod segments).

23 Defects such as dents in rods, bent or missing structural members, small cracks in structural
24 members, and missing rods do not necessarily render an assembly damaged, if the intended
25 functions of the assembly are maintained (i.e., if the performance of the assembly does not
26 compromise the ability to meet fuel-specific and package-related regulations).

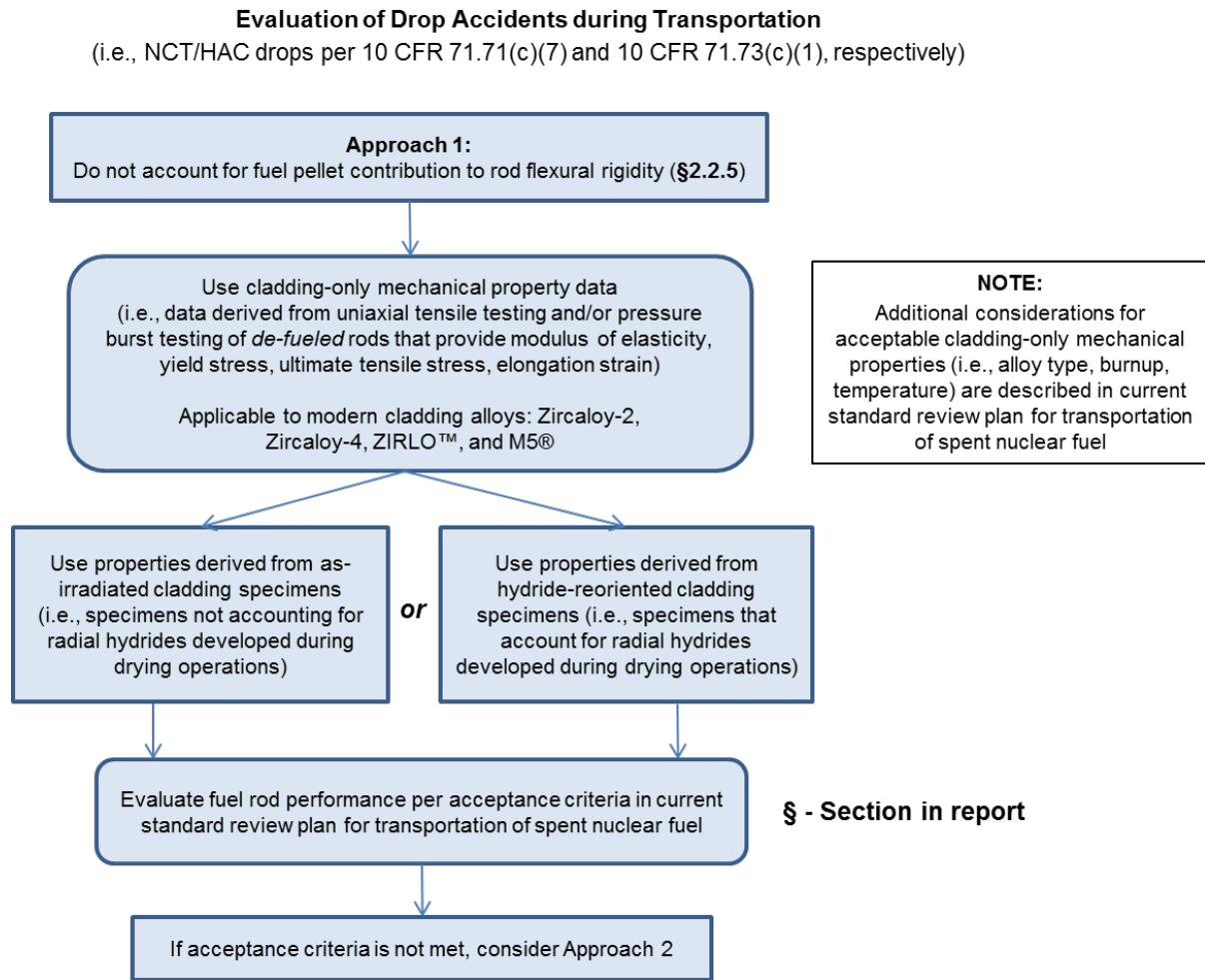
27 **4.2 Uncanned Fuel (Intact and Undamaged Fuel)**

28 Undamaged HBU SNF can be transported without the need for a separate can for damaged fuel
29 (i.e., a separate metal enclosure sized to confine damaged fuel particulates) to maintain a
30 known configuration inside the package containment cavity. This fuel includes rods that are
31 either intact (i.e., there are no breaches of any kind) or that contain small cladding defects (i.e.
32 pinholes or hairline cracks), which may permit the release of gas from the interior of the fuel rod.
33 Cladding with gross ruptures that may permit the release of fuel particulates may not be
34 considered undamaged. The configuration of undamaged HBU SNF may be demonstrated to
35 be maintained if loading and transport operations are designed to prevent or mitigate
36 degradation of the cladding and other assembly components, as discussed in ISG-22, "Potential
37 Rod Splitting Due to Exposure to an Oxidizing Atmosphere during Short-Term Cask Loading
38 Operations in LWR or Other Uranium Oxide Based Fuel," issued May 2006 (NRC, 2006)..

39 As the approaches delineated in Figure 4-1 show, an application for a CoC for a package that
40 includes undamaged HBU SNF would include a structural evaluation of the fuel rods under NCT

1 and HAC drop accident scenarios. The evaluation serves to demonstrate that the uncanned fuel
2 remains in a known configuration after a drop accident scenario.

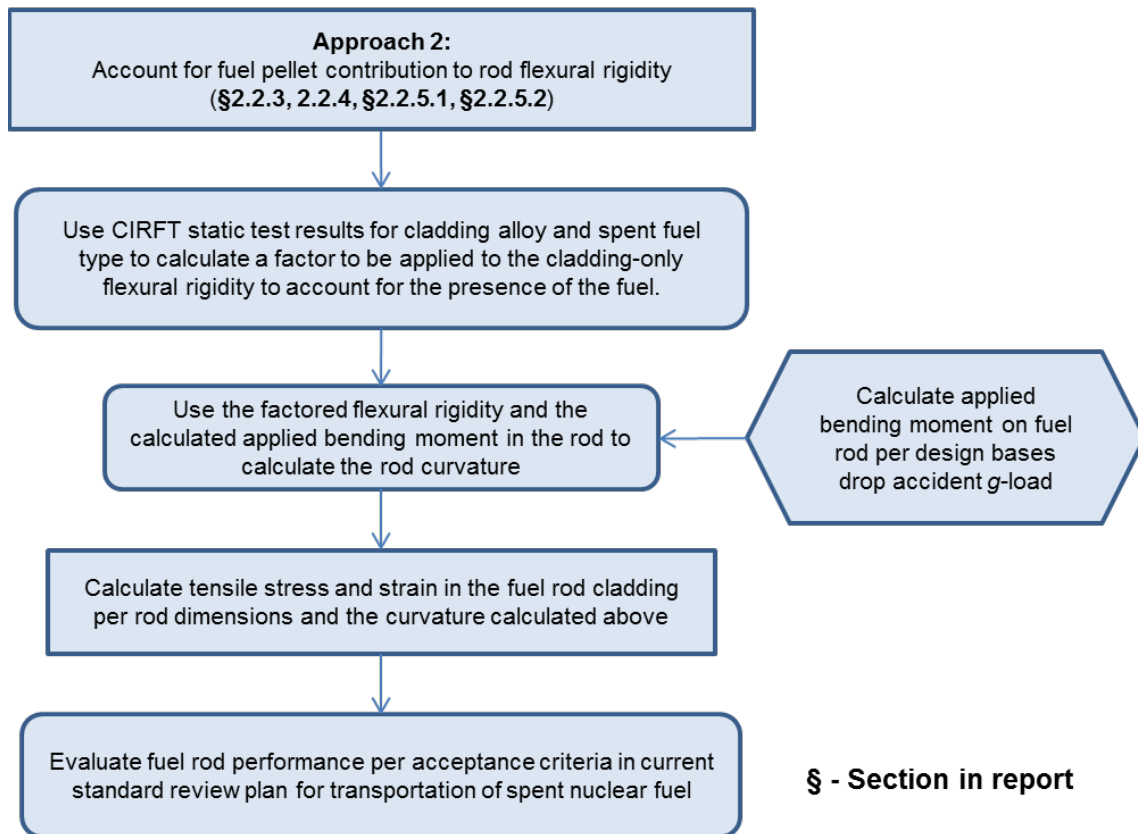
3 Two alternatives may be used to calculate cladding stress and strain, and cladding flexural
4 rigidity, for the aforementioned evaluation of drop accident scenarios. The first alternative,
5 shown in Figure 4-2, is to use cladding-only mechanical properties from as-irradiated cladding
6 (i.e., cladding with circumferential hydrides, primarily), or hydride-reoriented cladding (i.e.,
7 cladding that accounts for radial hydrides precipitated after the drying process). As indicated in
8 the discussion in Section 2.3.3, the staff considers that the orientation of the hydrides is
9 not critical in evaluating the adequacy of cladding-only mechanical properties during drop
10 accident scenarios. The properties necessary to implement this alternative may be derived from
11 cladding-only uniaxial tensile tests and include modulus of elasticity, yield stress, ultimate
12 tensile strength and uniform strain, and the strain at failure (i.e., the elongation strain). Refer to
13 the current SRP for transportation of SNF for additional considerations on acceptable cladding-
14 only mechanical properties (i.e., alloy type, burnup, and temperature) and the acceptance criteria
15 for cladding performance during transport operations can be found in are described in.



16 **Figure 4-2 First Approach for Evaluation of Drop Accidents During Transport**

1 The second alternative, outlined in Figure 4-3, is to use cladding-only mechanical properties that
 2 have been modified by a numerical factor to account for the increased flexural rigidity imparted
 3 by the fuel pellet. This numerical factor is obtained from static test data from the cyclic integrated
 4 reversible-bending fatigue tester (CIRFT) for fully-fueled rods for the particular cladding type and
 5 fuel type (see Section 2.3.3). However, this second alternative would be necessary only if the
 6 structural evaluation using cladding-only mechanical properties is unsatisfactory. Refer to the
 7 current SRP for transportation of SNF for acceptance criteria on cladding performance following
 8 NCT and HAC drop scenarios.

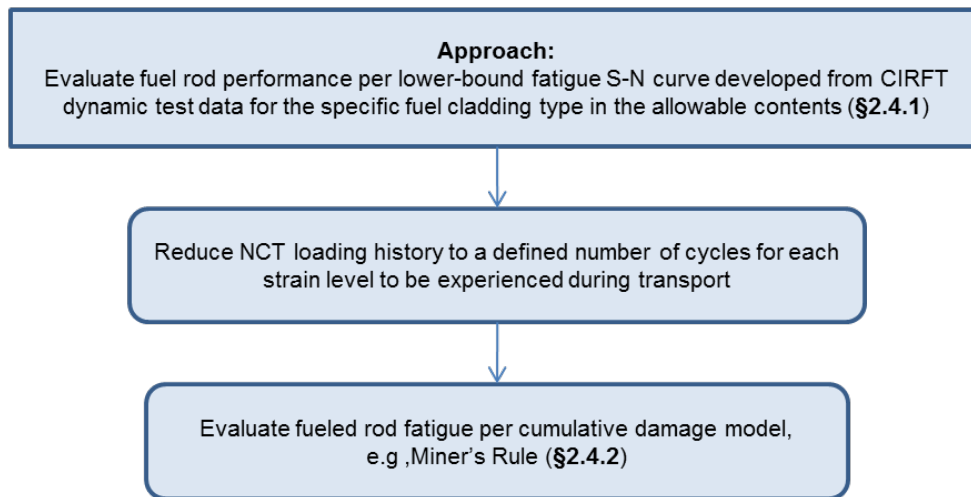
Evaluation of Drop Accidents during Transportation
 (i.e., NCT/HAC drops per 10 CFR 71.71(c)(7) and 10 CFR 71.73(c)(1), respectively)



9 **Figure 4-3 Second Approach for Evaluation of Drop Accidents During Transport**

10 In addition to the structural evaluation for NCT and HAC drop accident scenarios, the
 11 application would contain a fatigue evaluation for NCT using the cumulative damage approach
 12 described in Section 2.3. The satisfactory performance under fatigue would serve to
 13 demonstrate compliance with the requirement in 10 CFR 71.71(c)(5).

Evaluation of Rod Fatigue during Transportation
(i.e., vibration normally incident to transport per 10 CFR 71.71(c)(5))



§ - Section in report

1 **Figure 4-4 Evaluation of Vibration Normally Incident to Transport**

2 **4.2.1 Leaktight Containment**

3 An application for a transportation package CoC with HBU SNF as contents is expected to
4 define the maximum allowable leakage rate for the entire containment boundary. The maximum
5 allowable leakage rate is based on the quantity of radionuclides available for release and is
6 evaluated to meet the containment requirements for maintaining an inert atmosphere within the
7 containment cavity and compliance with the regulatory release limits of 10 CFR 71.51,
8 “Additional Requirements for Type B Packages.” The leakage rate testing is performed on the
9 entire containment boundary (over the course of fabrication and loading) and ensures that the
10 package can maintain a leakage rate below the maximum allowable leakage rate per ANSI
11 N14.5-2014.

12 If the entire containment boundary of the transportation package, including its closure lid, is
13 designed and tested to be “leaktight” as defined in American National Standards Institute (ANSI)
14 N14.5-2014, “American National Standard for Radioactive Materials — Leakage Tests on
15 Packages for Shipment,” and the current SRP for transportation of SNF, then the application is
16 not expected to include release calculations that demonstrate compliance with the regulatory
17 release limits of 10 CFR 71.51. In addition, the structural analyses of the package
18 demonstrates that the containment boundary will not fail under the tests for NCT and HAC and
19 that the containment boundary will remain leaktight under all conditions of transport. Refer to
20 the current SRP for transportation of SNF for additional guidance on demonstrating compliance
21 with the leaktight criterion.

22 **4.2.2 Non-Leaktight Containment**

23 Transportation packages certified to transport HBU SNF must satisfy the release limits of
24 10 CFR 71.51. For those packages not tested to a “leaktight” criterion, the application is

1 expected to include release calculations and identify the allowable NCT and HAC volumetric
2 leakage rates in accordance with ANSI N14.5. The standard provides an acceptable method to
3 determine the maximum permissible volumetric leakage rates based on the allowed regulatory
4 release limits under both NCT and HAC. Refer to the current SRP for transportation of SNF for
5 additional guidance on demonstrating compliance with 10 CFR 71.51 for non-leaktight packages.
6 The leakage rate testing is performed on the entire containment boundary (over the course of
7 fabrication and loading) and ensures that the package can maintain a leakage rate below the
8 maximum allowable leakage rate per ANSI N14.5. In order to determine the release rates for the
9 primary containment boundary, an application for certification of a non-leaktight package should
10 provide a technical basis for the assumed bounding HBU fuel failure rates for both NCT and
11 HAC. If an application is not able to provide and justify its bounding HBU fuel failure rates, then
12 the fuel failure rates below may be assumed as bounding values for NCT and HAC:

- 13 • NCT: 3 percent
- 14 • HAC: 100 percent

15 *Bounding Release Fractions for High Burnup Fuel*

16 HBU SNF has different characteristics relative to low burnup (LBU) SNF with respect to cladding
17 oxide thickness, hydride content, radionuclide inventory and distribution, heat load, fuel pellet
18 grain size, fuel pellet fragmentation, fuel pellet expansion and fission gas release to the rod
19 plenum (See Appendix C.5 to NUREG/CR-7203, "A Quantitative Impact Assessment of
20 Hypothetical Spent Fuel Reconfiguration in Spent Fuel Storage Casks and Transportation
21 Packages," issued September 2015 (NRC, 2015) for additional details on HBU SNF).
22 Differences in these characteristics affect the mechanisms by which the fuel can breach and the
23 amount of fuel that can be released from failed fuel rods. Hence, the staff evaluated open
24 literature on HBU fuel rod failure rates and release fractions (Chalk River unknown deposits
25 (CRUD), fission gases, volatiles, and fuel fines) to assist in the review of applications for non-
26 leaktight containment boundaries. Table 4-1 provides release fractions that may be considered
27 reasonably bounding for HBU SNF. A justification of the proposed release fractions of the
28 source terms would be expected to include an adequate description of burnup for the test
29 specimen, number of tests, collection method for quantification of respirable release fractions,
30 test specimen pressure at the time of fracture, source collection system (sophisticated enough
31 to gather the bounding respirable release fractions), etc.

1 **Table 4-1 Fractions Of Radioactive Materials Available for Release from HBU SNF**
 2 **Under Conditions of Transport (for Both Pressurized Water Reactor and**
 3 **Boiling Water Reactor Fuels)**

Variable	NCT	HAC-Fire Conditions	HAC-Impact Conditions
Fraction of Fuel Rods Assumed to Fail	0.03	1.0	1.0
Fraction of Fission Gases Released Due to a Cladding Breach	0.15	0.15	0.35
Fraction of Volatiles Released Due to a Cladding Breach	3×10^{-5}	3×10^{-5}	3×10^{-5}
Mass Fraction of Fuel Released as Fines Due to a Cladding Breach	3×10^{-5}	3×10^{-3}	3×10^{-5}
Fraction of CRUD Spalling Off Cladding	0.15	1.0	1.0

4 CRUD

5 The average CRUD thickness on HBU SNF cladding has been estimated to be similar to that
 6 observed on LBU SNF cladding. A review of data from the literature (NRC, 2000c; Einziger and
 7 Beyer, 2007) indicates that a release (spalling off) of 15 percent of cladding CRUD may be
 8 assumed as reasonably bounding to NCT scenarios, and a release fraction of 100 percent of
 9 the cladding CRUD, that spalls off, is conservatively bounding to HAC scenarios (NRC, 2014).

10 Fission Gases

11 NRC's FRAPCON steady-state fuel performance code has been previously used to assess
 12 release fractions of fission gases during transportation (NRC, 2011). The seven most common
 13 fuel designs were evaluated using FRAPCON's modified Forsberg-Masih model (8×8 , 9×9 ,
 14 and 10×10 fuel for BWR; and 14×14 , 15×15 , 16×16 , and 17×17 for PWR). For each fuel
 15 design, a number of different power histories aimed at capturing possible realistic reactor
 16 irradiations were modeled. The fission gas content within the free volume of the rods was
 17 evaluated for a total of 243 different cases (39 for each of the BWR fuel designs; 37 for 14×14
 18 and 16×16 PWR fuel designs, and 26 for 15×15 and 17×17 PWR fuel designs). A review of
 19 the results indicates that a release of 15 percent of fission gases may be assumed as
 20 reasonably bounding to NCT scenarios for rod average burnups up to 62.5 GWd/MTU.

21 During an HAC fire scenario, per 10 CFR 71.73(c)(4), the fuel is not expected to reach
 22 temperatures high enough that fission gases can diffuse out of the pellet matrix or grain
 23 boundaries to the rod plenum. The thermal rupture tests showed that release occurred at
 24 higher temperatures than those experienced during HAC (NRC, 2000c). Therefore, the same
 25 release fraction of 15 percent of fission gases during NCT scenarios may also be assumed to
 26 be reasonably bounding to the HAC fire scenario.

1 In the case of HAC drop (impact) conditions, the pellet may be conservatively assumed to
2 crumble. In this scenario, fission gases retained within the pellet grain boundaries may be
3 released in addition to those already released from the fuel rod free volume (i.e., from the fuel-
4 cladding gap and plenum). The FRAPFGR model in FRAPCON may be used to predict the
5 location of the fission gases within the fuel pellet (NRC, 2011). The model has been validated
6 with experimental data obtained using an electron probe micro analyzer. The FRAPFGR model
7 was used to calculate the maximum fraction of the pellet-retained fission gases that may be
8 released during a drop impact, which was determined to be 20 percent. Therefore, assuming all
9 fission gases within the pellet grain boundaries are released, a 35-percent (15-percent + 20-
10 percent) maximum release fraction may be assumed to be reasonably bounding to the HAC fire
11 scenario. This value accounts for the 15-percent maximum fission gases released from the fuel
12 rod free volume (as calculated with the modified Forsberg- Massih model) and the 20-percent
13 maximum fission gases released from the fuel pellet grain boundaries (as calculated with the
14 FRAPFGR model). These release fraction estimates are consistent with previous NRC
15 estimates (NRC, 2000c; NRC, 2007; Einziger and Beyer, 2007).

16 Volatiles

17 The majority of the volatile release fractions originate from cesium-based compounds in the
18 form of oxides or chlorides (NRC, 2000c; NRC, 2014). These volatiles exhibit a different
19 release behavior in comparison to fission gases. Volatiles tend to migrate and aggregate at the
20 rim on the outer surface of the fuel pellet during reactor irradiation, which is characteristic of
21 burnups near or exceeding 60 GWd/MTU. The pellet rim is characterized by a fine crystalline
22 grain structure (0.1-0.3 μm in characteristic size) (Spino et al., 2003; Einziger and Beyer, 2007),
23 a high porosity that may exceed 25-percent, and a high concentration of actinides relative to the
24 inner pellet matrix.

25 Sandia National Laboratories determined the maximum release fraction of volatiles (cesium and
26 other ruthenium-based compounds) under HAC drop and fire scenarios to be 0.003 percent (3
27 $\times 10^{-5}$) (NRC, 2000c). The assessment included modeling and analyses using various data from
28 the literature. The volatile release fraction during an HAC fire scenario was determined to be
29 lower than the release fraction during an HAC impact scenario (NRC, 2014; NRC, 2000c).
30 Therefore, a volatile release fraction of 0.003 percent (3×10^{-5}) may be assumed to be
31 reasonably bounding to NCT, HAC fire, and HAC impact scenarios. This release fraction
32 estimate is also consistent with an independent estimate by Einziger and Beyer (2007).

33 Fuel Fines

34 Release fractions from SNF fines during storage and transportation have been previously
35 documented (NRC, 2000c; Benke et al., 2012; NRC, 2007; NRC, 2014). HBU SNF has a
36 different pellet microstructure relative to LBU SNF, which is characterized by an inner matrix
37 and an outer pellet rim layer. The thickness of the outer pellet rim layer increases with higher
38 fuel burnup. Therefore, differences in microstructure between the inner pellet matrix and the
39 outer pellet rim should be considered when evaluating release fractions of fuel fines from HBU
40 SNF.

41 Although there is no reported literature on HBU SNF rim fracture as a function of impact energy,
42 other data can be used to indirectly assess the contribution of the rim layer to the release
43 fractions of fuel fines. Spino et al (1996) estimated the fracture toughness of the rim layer from
44 micro-indentation tests. Relative to the inner SNF matrix, the rim layer showed an increase of
45 fracture toughness. The increase of fracture toughness implies a decrease of release fraction.

1 Hirose et al (2015) also discussed results of axial dynamic impact tests simulating accident
2 conditions during transport. The dispersed particles due to pellet breakage following impact
3 were collected and correlated to impact energy. The staff has compared the measured release
4 fraction of fuel fines from Hirose et al (2015) with previous NRC estimates of release fraction
5 versus impact energy for SNF and other brittle materials (depleted UO₂, glass and Synroc) (see
6 Figure 3 of NUREG-1864 (NRC (2007))). Based on these analyses, the staff concludes that
7 there is no indication that pellet rim layer contributes to increased release fractions for HBU
8 SNF.

9 Since the outer HBU fuel pellet rim does not appear to contribute to additional release fractions,
10 previous NRC estimates for release fractions of fuel fines may continue to be used (NRC,
11 2000c; NRC, 2007; Benke et al., 2012; Ahn et al., 2012; NRC, 2014). Based on the range of
12 estimates in the literature, a release fraction for fuel fines of 0.003 percent (3×10^{-5}) may be
13 assumed to be reasonably bounding to both NCT and HAC (drop impact) scenarios. During an
14 HAC fire scenario, fuel oxidation is conservatively assumed to increase the release fraction of
15 fuel fines by a factor of 100 (NRC, 2000c; Ahn et al, 2012). Therefore, a 0.3 percent (3×10^{-3})
16 release fraction of fuel fines may be assumed as reasonably bounding to an HAC fire scenario.

17 The staff recognizes that various international cooperative research programs are currently
18 investigating release fractions from HBU SNF. Once the data is available to the public, the staff
19 will review and determine if the conservative estimates in the above discussion should be
20 revisited.

21 **4.2.3 Direct Shipment from the Spent Fuel Pool and Shipment of Previously Dry-** 22 **Stored Fuel (Up To 20 Years Since Fuel Was Initially Loaded)**

23 Section 1.2 discussed the staff's review guidance for the licensing and certification of dry
24 storage of HBU SNF for a period up to 20 years. The technical basis referenced in that
25 guidance has supported the staff's conclusion that creep is not expected to result in gross
26 ruptures if cladding temperatures are maintained below 400 °C (752 °F). Creep is a time-
27 dependent mechanism. Therefore, the short transportation period (relative to dry storage) is not
28 expected to compromise the integrity of HBU SNF, if the cladding temperatures remain below
29 400 °C (752 °F).

30 Chapter 2 also provided an assessment of the effects of hydride reorientation per static and
31 fatigue bending test results on HBU SNF specimens. Those results provide a technical basis
32 for the staff's conclusion that the use of best-estimate cladding mechanical properties (with
33 either as-irradiated or hydride-reoriented microstructure) is adequate for the structural
34 evaluation of HBU SNF. This finding applies to the evaluation of the drop tests for NCT (per
35 10 CFR 71.71(c)(7)) and HAC (per 10 CFR 71.73(c)(1)). Refer to the current SRP for
36 transportation of SNF for staff review guidance on additional considerations for acceptable
37 cladding-only mechanical properties (i.e., alloy type, burnup, temperature), on acceptable
38 references for cladding mechanical properties and on acceptance criteria for the structural
39 evaluation of the HBU fuel assembly following the drop tests. As Figure 4-1 shows,
40 supplemental safety analyses are not expected for dry storage of HBU SNF directly loaded
41 from the spent fuel pool or HBU SNF that has previously been in dry storage for periods not
42 exceeding 20 years.

1 **4.2.4 Shipment of Previously Dry-Stored Fuel (Beyond 20 Years Since Fuel Was**
2 **Initially Loaded)**

3 To address age-related uncertainties related to the transportation of HBU SNF previously in dry
4 storage for extended periods (i.e., periods of storage exceeding 20 years), the application
5 should be supplemented with either results from a surrogate demonstration program or
6 supplemental safety analyses assuming justified hypothetical fuel reconfiguration scenarios (see
7 Figure 4-1). The results from a surrogate demonstration program can provide field-obtained
8 confirmation that the fuel has remained in the analyzed configuration after 20 years of dry
9 storage, if that is the approved configuration for the transportation package. If confirmation is
10 not provided, the safety analyses for the transportation package should be revised to assume
11 reconfigured fuel.

12 The licensing and certification of storage containers for HBU SNF has been approved for an
13 initial 20-year-term per the technical basis for the evaluation of creep, as discussed in Chapter
14 1. However, the staff has recognized that the technical basis is based on short-term
15 accelerated creep testing (i.e., laboratory scale testing up to a few months), which results in
16 increased uncertainties when extrapolated to long periods of dry storage (see Appendix D to
17 NUREG-1927, Revision 1, "Standard Review Plan for Renewal of Specific Licenses and
18 Certificates of Compliance for Dry Storage of Spent Nuclear Fuel," issued June 2016 (NRC,
19 2016b). Although the staff has confidence based on this short-term testing that creep-related
20 degradation of the HBU fuel will not adversely affect its analyzed configuration for storage
21 periods beyond 20 years, there is no operational field-obtained data to confirm this expectation,
22 as in the prior demonstration for LBU fuel (NRC, 2001; NRC, 2003b).

23 In addition, the staff also acknowledges that, while the CIRFT results obtained to date (as
24 discussed in Chapter 2) provide an adequate technical basis for assessing the separate effects
25 of hydride reorientation, the results do not account for potential synergistic effects of various
26 physical and chemical phenomena occurring during extended dry storage (e.g., cladding creep,
27 hydride reorientation, irradiation hardening, oxidation, hydriding caused by residual water
28 hydrolysis (see NUREG-2214, "Managing Aging Processes in Storage (MAPS) Report," issued
29 October 2017 (NRC, 2017c) for discussions on these phenomena). Therefore, evidence that
30 HBU fuel in dry storage beyond 20 years has maintained its analyzed configuration is expected
31 prior to transport, if that is the approved configuration for the transportation package.

32 **4.2.4.1 Supplemental Data from Confirmatory Demonstration**

33 One example approach for approval of a transportation package with HBU SNF previously in
34 dry storage for periods exceeding 20 years (e.g., 40 years) involves supplementing the
35 application with results from a surrogate demonstration program. Such a program could provide
36 field obtained confirmation that the fuel configuration has been maintained before transport.
37 The applicant may refer to Appendices B and D to NUREG-1927, Revision 1 (NRC, 2016b),
38 which describe attributes and acceptance criteria of an acceptable surrogate demonstration
39 program.

40 **4.2.4.2 Supplemental Safety Analyses**

41 As an alternative approach to relying on a surveillance and monitoring program for the
42 transportation of HBU SNF previously in dry storage for longer than 20 years, an application
43 may demonstrate that a transportation package can still meet the pertinent regulatory
44 requirements by assuming hypothetical reconfiguration of the fuel contents into justified

1 geometric forms. This alternative approach would include supplemental safety analyses to
2 demonstrate that the HBU SNF contents, even if reconfigured, can still meet the pertinent 10
3 CFR Part 71 regulations for containment, thermal performance, criticality safety and shielding
4 after the required tests for NCT and HAC.

5 In NUREG/CR-7203 (NRC, 2015), Oak Ridge National Laboratory (ORNL) evaluated the impact
6 of a wide range of postulated fuel reconfiguration scenarios under non-mechanistic causes of
7 fuel assembly geometry change with respect to criticality, shielding (dose rates), containment,
8 and thermal performance. The study considered three fuel reconfiguration categories, which
9 were characterized by either (1) cladding failure, (2) rod/assembly deformation without cladding
10 failure or (3) changes to assembly axial alignment without cladding failure. Within
11 configurations in both Category 1 and Category 2, various scenarios were identified:

- 12 • Category 1: cladding failure
 - 13 – Scenario 1(a): breached spent fuel rods
 - 14 – Scenario 1(b): damaged spent fuel rods
- 15 • Category 2: rod/assembly deformation without cladding failure
 - 16 – Scenario 2(a): configurations associated with side drop
 - 17 – Scenario 2(b): configurations associated with end drop
- 18 • Category 3: changes to assembly axial alignment without cladding failure

19 The analyses in NUREG/CR-7203 (NRC, 2015) considered representative SNF transportation
20 packages, and a range of fuel initial enrichments, discharge burnup values, and decay times.
21 The analyses examined two package designs: a general burnup credit (GBC)-32 package
22 containing 32 PWR fuel assemblies and a GBC-68 package containing 68 BWR fuel
23 assemblies. The results in NUREG/CR-7203 should not be assumed to be generically
24 applicable, as fuel reconfiguration may have different consequences for a transportation
25 package other than the generic models evaluated in NUREG/CR-7203, however, the following
26 sections discuss considerations in developing supplemental safety analyses for other packages
27 according to the reconfiguration scenarios considered in NUREG/CR-7203.

28 4.2.4.2.1 *Materials and Structural*

29 An application for package certification relying on supplemental safety analyses based on
30 hypothetical reconfiguration of the HBU SNF contents should still provide a structural evaluation
31 for the package and its fuel contents using any of the approaches discussed in Section 4.2. The
32 staff will follow the guidance in the current SRP for transportation of SNF in its review of the
33 structural evaluation and the assumed material mechanical properties, including any changes
34 caused by higher temperatures resulting from fuel reconfiguration.

35 4.2.4.2.2 *Containment*

36 An application relying on supplemental safety analyses based on hypothetical reconfiguration of
37 the HBU SNF is expected to demonstrate that the transportation package design meets the
38 regulatory requirements for containment if data from a surrogate demonstration program, used

1 for confirmatory demonstration consistent with the guidance in NUREG-1927 (NRC, 2016b), are
2 not available before shipment of fuel in prior dry storage for periods longer than 20 years.

3 Thermal, structural, and material analyses, together with aging management activities for the
4 DSS subcomponents supporting confinement (i.e., confinement boundary) during prior dry
5 storage,¹ serve to provide assurance that the allowable leak rate is maintained even after
6 hypothetical reconfiguration of the fuel under NCT and HAC. Supplemental thermal analyses
7 should demonstrate that the containment boundary will be able to withstand their maximum
8 operating temperatures and pressures under NCT and HAC. If the canister serves as the
9 confinement boundary at the future storage location, then the canister is expected to be leak-
10 tested while it is within the transportation package after it reaches its new storage location.

11 4.2.4.2.3 *Thermal*

12 Fuel reconfiguration can affect the efficiency of heat removal from the fuel because of changes
13 in (1) thermo-physical properties of the container gas space resulting from the release of fuel
14 rod fill gas and fission product gases, (2) heat source location within the container, and (3)
15 changes in flow area (convection), conduction lengths (conduction) and radiation view factors
16 (thermal radiation). As part of a defense-in-depth approach to addressing age-related
17 uncertainties for uncanned or undamaged HBU SNF in shipment for fuel previously in dry
18 storage for periods longer than 20 years, the thermal analyses would be expected to analyze
19 the spent fuel at NCT and HAC by assuming the fuel has become substantially altered.
20 NUREG/CR-7203 (NRC, 2015) describes impacts on canister pressure and fuel cladding, and
21 package component temperatures for various scenarios of fuel geometry changes. These
22 impacts are examined below. In general, the results in NUREG/CR-7203 (NRC, 2015) should
23 not be considered generically applicable. The thermal analyses of the application should
24 consider scenarios discussed in NUREG/CR-7203 to determine consistency in the analytical
25 methods, scenario phenomena, and results. The thermal analyses would be expected to
26 assess the impact of fuel reconfiguration on the fuel cladding and component temperatures and
27 the internal pressure for the particular transportation package design.

28 For Scenario 1(a) of Category 1 (see list of scenarios in Section 4.2.4.2 of this report) from
29 NUREG/CR-7203, the fuel rods are assumed to breach in such a manner that the cladding
30 remains in its nominal geometry (no fuel reconfiguration), but the release of fuel rod backfill gas
31 and fission product gases can cause a change to the package component peak temperatures.
32 For Scenario 1(b) of Category 1, for configurations where an assembly (or assemblies) is
33 represented as a debris pile(s) inside its basket cell, fuel reconfiguration has a larger impact on
34 the component temperatures for the vertical orientation than for the horizontal orientation, but
35 the packing fraction of debris bed has minor impact on the component temperatures. For both
36 Scenario 1(a) and Scenario 1(b), release of the fuel rod gaseous contents increases the number
37 of moles of gas and thus the package container pressure. The canister pressure is expected to
38 increase with the increased fuel rod failure fractions.

39 For Category 2 (Scenarios 2(a) and 2(b)), the fuel rods are assumed to remain intact without
40 gaseous leakage into the canister space. The changes of the fuel assembly lattice (contraction
41 in Scenario 2(a) and expansion in Scenario 2(b)) could cause either an increase or decrease in
42 the package component temperatures depending on the initial assembly geometry and whether

³ Aging management activities maybe conducted under the aegis of an NRC-approved AMP (for renewal applications) or a maintenance plan (for initial license or CoC applications requesting approval for periods exceeding 20 years).

1 the package relies on convection for heat transfer. In general, the impact from Scenarios 2(a)
2 and 2(b) is expected to be minor for the package component temperatures and canister
3 pressure.

4 For Category 3, the fuel rods are assumed to remain intact without gaseous leakage into the
5 canister space, but the axial shifting of the assembly changes the heat source location within
6 the packaging. It is expected that changes in assembly axial alignment within the basket cells
7 have minor impact on the component temperatures and canister pressure.

8 Normal Conditions of Transport

9 Based on the thermal phenomena described in Section 4.2.4.2.3 and NUREG/CR-7203 (NRC,
10 2015), an application should evaluate the impact of Scenarios 1(a) and 1(b) of Category 1 on
11 the canister pressure and the fuel cladding and package component temperatures for 3-percent
12 fuel rod failure for NCT thermal evaluation.

13 For Scenarios 2(a) and 2(b) in Category 2 and Scenario 3 in Category 3, although the impact of
14 hypothetical fuel reconfiguration on package thermal performance (e.g., temperature and
15 pressure) is not expected to be significant because the fuel rods are assumed to remain intact
16 without gaseous leakage into the canister space, the applicant may need to provide thermal
17 analyses due to the specifics of the package design.

18 Hypothetical Accident Conditions

19 Based on thermal phenomena described in Section 4.2.4.2.3 and NUREG/CR-7203 (NRC,
20 2015), an application should evaluate the impact of Scenarios 1(a) and 1(b) of Category 1 on
21 the canister pressure and the fuel cladding and package component temperatures for 100
22 percent fuel rod failure for HAC thermal evaluation.

23 For Scenarios 2(a) and 2(b) in Category 2 and Scenario 3 in Category 3, although the impact of
24 fuel reconfiguration on package thermal performance (e.g., temperature and pressure) is not
25 expected to be significant because the fuel rods are assumed to remain intact without gaseous
26 leakage into the canister space, the applicant may need to provide thermal analyses due to
27 specifics of the package design.

28 4.2.4.2.4 *Criticality*

29 An application may demonstrate that a transportation package meets the regulatory
30 requirements for criticality safety by assuming hypothetical reconfiguration of the HBU SNF into
31 justified bounding geometric forms. If data from a surrogate demonstration program are not
32 available before the shipment of fuel previously dry-stored for periods longer than 20 years, this
33 approach is one way to provide additional assurance of compliance with 10 CFR 71.55,
34 "General Requirements for Fissile Material Packages," and 10 CFR 71.59, "Standards for
35 Arrays of Fissile Material Packages," during NCT and HAC.

36 To assess the impacts of hypothetical fuel reconfiguration, ORNL performed criticality safety
37 analyses for various scenarios and examined the impacts on the reactivity of a package. The
38 results were described in NUREG/CR-7203 (NRC, 2015) which considers burnup up to 70
39 GWd/MTU for criticality evaluations. The study characterized the assumed hypothetical
40 reconfiguration scenarios were categorized depending on the nature of the assembly damage,
41 as described previously.

1 With respect to criticality safety analyses, NUREG/CR-7203 (NRC, 2015) provides some insight
2 on the reactivity effects of some reconfiguration scenarios; however the values in the results are
3 not generically applicable. Fuel reconfiguration may have different reactivity effects on a
4 transportation package other than the generic models used in NUREG/CR-7203.

5 Criticality is not a concern for dry SNF transportation packages, as SNF requires moderation to
6 reach critical. The criticality analyses in NUREG/CR-7203 (NRC, 2015) assume fully-flooded
7 conditions, and any conclusions adopted are applicable only to analyses that include moderator
8 intrusion. The staff will follow the guidance in ISG-19, "Moderator Exclusion under Hypothetical
9 Accident Conditions and Demonstrating Subcriticality of Spent Fuel under the Requirements of
10 10 CFR 71.55(e)," issued in May 2003 (NRC, 2003), to review an application for moderator
11 exclusion. The following considerations for criticality evaluations for reconfigured fuel apply
12 only to transportation packages that do not employ moderator exclusion.

13 All of the criticality safety analyses presented in NUREG/CR-7203 (NRC, 2015) take credit for
14 burned fuel nuclides (burnup credit) and the results may not apply to analyses that assume a
15 fresh fuel composition. To review the staff will follow the guidance in ISG-8, Revision 3, "Burnup
16 Credit in the Criticality Safety Analyses of PWR Spent Fuel in Transportation and Storage
17 Casks," issued in September 2012 (NRC, 2012), to review the the burnup credit methodology
18 and code benchmarking used to support a criticality safety evaluation. ISG-8, Revision 3 does
19 not endorse any particular methodology for BWR fuel burnup. The staff does not necessarily
20 endorse the methodology used to perform the study presented in NUREG/CR-7203 for BWR
21 fuel DSS, and considers it to be for illustration only.

22 For criticality safety analyses using burnup credit, NUREG/CR-7203 (NRC, 2015) shows that
23 reactivity increases for longer decay times. Therefore, analyses supporting storage beyond 20
24 years would need to use an appropriate decay time in the criticality evaluations. The
25 enrichment and burnup values assumed in the criticality evaluations in NUREG/CR-7203 may
26 differ from the values allowed in another transportation package. However NUREG/CR-7203
27 states that no significant differences were observed in trends between configurations that
28 evaluated fuel at 44.25 GWd/MTU and 70 GWd/MTU.

29 The following sections discuss an approach acceptable to the staff for addressing increases in
30 reactivity resulting from the potential reconfiguration for HBU fuel under NCT and HAC. These
31 sections identify the most applicable information from NUREG/CR-7203 to address each of
32 these specific conditions.

33 Normal Conditions of Transport

34 In an approach acceptable to the staff, the applicant's criticality safety evaluations would
35 consider the reactivity impact of 3-percent fuel failure under NCT. Based on NUREG/CR-7203
36 (NRC, 2015), the impacts on the package k_{eff} resulting from 3-percent fuel failure may become
37 significant. Applicants for transportation packages may need to consider the 3-percent fuel
38 failure for both single package and array analyses under NCT.

39 The scenario most applicable to 3-percent fuel failure under NCT is Category 1, Scenario 1(a)
40 from NUREG/CR-7203. ORNL created this scenario to represent breached rods. ORNL
41 assumed that a percentage of the rods were breached, and that cladding from these rods failed
42 completely. ORNL then removed this percentage of fuel rods from the system. This is
43 conservative as SNF is undermoderated and replacing fuel with moderator typically causes
44 reactivity to increase. Using a fresh fuel composition for PWR fuel, NUREG/CR-7203 shows

1 that reactivity decreases when removing rods and therefore this type of analysis may not be
2 appropriate for PWR analyses that assume a fresh fuel composition. The location assumed for
3 failed or removed rods can have a significant effect on reactivity. NUREG/CR-7203 shows in
4 Section A.1.1 that removing rods from the center of the assembly causes reactivity to increase
5 the most.

6 In NUREG/CR-7203 (NRC, 2015), ORNL also determines the number of rods removed that
7 produces the maximum reactivity. For the systems studied in NUREG/CR-7203 the maximum
8 reactivity occurs when more than 3-percent of the rods are removed from the system.

9 NUREG/CR-7203 (NRC, 2015) also presents the results of a sensitivity study that shows
10 increased reactivity for an alternative Category 1, Scenario 1(a), which assumed that the failed
11 fuel relocates to a location outside of the absorber plate. This is based on the generic system
12 modeled in NUREG/CR-7203. A different package may allow relocation of the failed rod
13 material outside of the absorber plate material to a different extent, and an applicant would
14 evaluate an alternative scenario for the specific transportation package being evaluated.

15 Hypothetical Accident Conditions

16 In an approach acceptable to the staff, the applicant's criticality safety evaluations would
17 consider the reactivity impact of 100-percent fuel failure under HAC. Based on NUREG/CR-
18 7203 (NRC, 2015), the impacts on the package k_{eff} resulting from 100-percent fuel failure may
19 be significant. Applicants for transportation packages may need to consider the 100 percent
20 fuel failure for both single package and array analyses under HAC.

21 The applicable scenarios from NUREG/CR-7203 (NRC, 2015) for the hypothetical case of 100
22 percent fuel failure are a combination of Category 1 Scenario 1(b), Category 2 Scenarios,
23 Category 3 Scenarios.

24 In Scenario 1(b) in Section A.1.2 of NUREG/CR-7203 (NRC, 2015), ORNL considered
25 reconfiguration of damaged fuel. With 100-percent compromise in cladding integrity,
26 reconfiguration is considered to the maximum extent. Section A.1.2 of NUREG/CR-7203 shows
27 that a model assuming an "ordered pellet array" is more reactive than a homogenous mixture of
28 fuel, cladding materials, and water.

29 In Scenario 2 in Section A.2 of NUREG/CR-7203 (NRC, 2015), ORNL considered rod/assembly
30 deformation from side and end impact events. ORNL investigated the effects on birdcaging and
31 bottlenecking by changing the pitch uniformly and non-uniformly. For all pitch contraction
32 cases, ORNL calculated a decrease in k_{eff} from the nominal pitch. For the uniform pitch
33 expansion ORNL found that the maximum pitch increase possible within the basket cell resulted
34 in the highest k_{eff} . For the non-uniform pitch expansion, ORNL increased the pitch of the inner
35 fuel rods/pins by decreasing the space between the outer rods/pins. The results in NUREG/CR-
36 7203 show that non-uniform pitch expansion produces k_{eff} values higher than uniform pitch
37 expansion for all cases except the unchanneled BWR fuel.

38 In Scenario 3 in Section A.3 of NUREG/CR-7203 (NRC, 2015), ORNL considered reactivity
39 effects of changes in assembly axial alignment. Neutron absorber panels may not extend the
40 full length of the basket and it may be possible for fuel to reconfigure outside of the neutron
41 absorber panels. ORNL investigated the change in reactivity resulting from the displacement of
42 intact fuel assemblies outside of the neutron absorber panels. NUREG/CR-7203 shows that the
43 maximum reactivity increase results when displacing the assemblies to the maximum extent at

1 the top, versus the bottom, because there is less burnup at the top of the assembly. The
2 amount of displacement possible depends on the particular transportation package and may be
3 different from that of the package(s) analyzed in NUREG/CR-7203. Higher burnup assemblies
4 show the largest change in k_{eff} upon displacement; however, the increase in k_{eff} caused by the
5 displacement may be bounded by the k_{eff} from a non-displaced lower burned assembly.

6 4.2.4.2.5 *Shielding*

7 An application may demonstrate that a transportation package meets the regulatory
8 requirements for shielding safety by showing that, with reconfiguration of the HBU SNF, the
9 package meets the dose rate limits under NCT and HAC. If a confirmatory demonstration is not
10 applicable or available, this approach is one way to provide additional assurance of compliance
11 with 10 CFR 71.47, "External Radiation Standards for All Packages"; 10 CFR 71.51(a)(1) for
12 NCT, and 10 CFR 71.51(a)(2) under HAC.

13 To assess the impacts of various fuel geometry changes on the calculated external dose rates
14 of an SNF transportation package, ORNL evaluated the external dose rate for various scenarios
15 of fuel geometry changes and show the results in NUREG/CR-7203 (NRC, 2015) for example
16 BWR and PWR transportation packages.

17 With respect to external dose rate analyses, the results in NUREG/CR-7203 (NRC, 2015)
18 should not be considered generically applicable. The impacts of fuel reconfiguration on the
19 maximum external dose rates may be different based on the package design.

20 Since reconfiguration is to be considered for transportation packages shipped after 20 years of
21 storage, and this length of cooling time is generally much longer than cooling times used to
22 establish loading tables, applicants may be able to justify that increases to external dose
23 resulting from reconfiguration are bounded by the additional cooling time the assemblies will
24 experience. As discussed in Section B.5 of NUREG/CR-7203 (NRC, 2015), based on the decay
25 time different nuclides become important in the evaluations.

26 NUREG/CR-7203 (NRC, 2015) also indicates that fuel assembly type (i.e., PWR vs BWR) may
27 have a significant impact on the external dose rate under fuel reconfiguration scenarios. Table
28 9 12 of NUREG/CR-7203 shows the difference in dose rate increase for BWR and PWR SNF. In
29 addition, a transportation package may allow transport of other fuel assemblies, with different
30 allowable burnup and enrichments. The burnup profile and depletion parameters used to create
31 the source term within NUREG/CR-7203 may also not be generically applicable. Appendix B to
32 NUREG/CR-7203 presents details of the analyses.

33 The following sections discuss an approach acceptable to the staff for addressing increases in
34 external dose rate resulting from the potential reconfiguration of HBU fuel under NCT and HAC.
35 These sections identify the most applicable information from NUREG/CR-7203 (NRC, 2015) to
36 address each of these specific conditions.

37 Normal Conditions of Transport

38 In an approach acceptable to the staff, the applicant's external dose rate evaluations would
39 evaluate the impact of 3-percent fuel failure under NCT. Based on NUREG/CR-7203 (NRC,
40 2015), source relocation resulting from 3 percent fuel failure may have a significant impact on
41 the dose rates prescribed in 10 CFR 71.47(b) due to . The most applicable scenario from
42 NUREG/CR-7203 is Category 1 (fuel failure), Scenario, 1(a). The results show that the dose

1 rate changes are sensitive to the number of fuel rod breaches and available space for fuel to
2 move in the cavity.

3 For Category 1 Scenario 1(a), breached rods, ORNL assumed that when the cladding is
4 breached, the rods turn to rubble and calculated the dose rate when the rubbleized fuel mixture
5 relocated within the fuel assembly. ORNL assumed failure of 10 and 25-percent of PWR fuel
6 rods and 11-percent of BWR fuel rods failed. Section B.4.1 of NUREG/CR-7203 (NRC, 2015)
7 discusses the implementation in detail. ORNL reduced the source strength and density of the
8 active fuel zone by the failure percentage, relocated this source to a different part of the fuel
9 assembly and increased the source strength and density accordingly. ORNL calculated
10 external dose rates using models with the fuel rubble mixture relocated to varied locations of the
11 package (top, middle, bottom). The limiting location for the relocated fuel rubble would be
12 based on the characteristics of the transportation package being analyzed.

13 Hypothetical Accident Conditions

14 In an approach acceptable to the staff, the applicant's external dose rate evaluations would
15 consider the impact of 100-percent fuel failure under HAC. The applicable scenarios from
16 NUREG/CR-7203 (NRC, 2015) are Category 1 Scenarios, Category 2 Scenarios and Category
17 3 Scenarios. ORNL assumed that there was no neutron shield present for the HAC models.
18 This is a typical assumption in HAC dose rate evaluations as it is difficult to predict the condition
19 of the neutron shield after the HAC fire event. Therefore source terms with high neutron
20 radiation, such as HBU fuel, tend to be limiting for HAC.

21 Based on NUREG/CR-7203 (NRC, 2015), source relocation resulting from 100-percent fuel
22 failure can have a significant impact on external dose rates under HAC. Tables 11 and 12 of
23 NUREG/CR-7203 show the relative changes for the example packages under HAC. These
24 dose rate change ratios are for dose rates at 1 m from the package as required by 10 CFR
25 71.51(a)(2).

26 For Category 1 Scenarios (cladding failure), ORNL assumed in the analyses in NUREG/CR-
27 7203 (NRC, 2015) that when the cladding fails the rods turn to rubble, and created a model with
28 a homogenized fuel and basket material. ORNL determined that the limiting mass packing
29 fraction for rubbleized fuel and basket material is 0.58. When evaluating dose rates for a
30 package in the vertical orientation, the damaged fuel model from the Category 1 Scenario 1(b)
31 in NUREG/CR-7203 is applicable. For a package in a horizontal orientation, the Category 2
32 Scenario from NUREG/CR-7203 would be more applicable. In this scenario, ORNL analyzed
33 the dose rates when the fuel is kept within its respective basket cell but pushed to the side walls
34 as shown in Section B.4.2 of NUREG/CR-7203. The limiting scenarios for any given
35 transportation package would depend on the specific characteristics of that package.

36 In the Category 3 Scenario in NUREG/CR-7203 (NRC, 2015), ORNL evaluates the dose rate
37 increase when an intact fuel assembly is pushed to the bottom or top of the package, thus
38 increasing dose rates at the bottom or top, or radially if the source becomes aligned with an
39 area of the package where there is streaming. The results from NUREG/CR-7203 generally
40 show a smaller increase in dose rates for this scenario than for Category 1 Scenarios and the
41 Category 2 Scenario and are likely to be bounded by the results for those situations. However,
42 there may be specific features from a particular package that may cause this scenario to be
43 worth considering.

1 **4.3 Canned Fuel**

2 HBU SNF that has been classified as damaged should be placed in a can designed for
3 damaged fuel or in an acceptable alternative. The staff will follow the guidance in the current
4 SRP for transportation of SNF when reviewing an application for a transportation package with
5 damaged HBU SNF contents.

5 CONCLUSIONS

1

2 The information in this report provides technical background information on the mechanical
3 performance of high burnup (HBU) spent nuclear fuel (SNF) after drying operations for storage
4 and transportation. The report also provides an engineering assessment of the test results for
5 HBU SNF discussed in NUREG/CR-7198, Revision 1, "Mechanical Fatigue Testing of
6 High-Burnup Fuel for Transportation Applications," issued October 2017 (NRC, 2017a), and
7 proposes example approaches for licensing and certification of HBU SNF for dry storage (under
8 Title 10 of the *Code of Federal Regulations* (10 CFR) Part 72, "Licensing Requirements for the
9 Independent Storage of Spent Nuclear Fuel and High-Level Radioactive Waste, and Reactor-
10 Related Greater Than Class C Waste," and transportation (under 10 CFR Part 71, "Packaging
11 and Transportation of Radioactive Material") based on the engineering assessment.

12 Until recently, experimental testing on the structural behavior of SNF rods during transportation
13 and storage has focused primarily on obtaining mechanical and strength properties of the
14 cladding. As a result, the flexural rigidity and structural response of fuel rods during normal and
15 accident events have been assessed only in terms of the mechanical and strength properties of
16 the cladding. Historically, the contribution of the fuel pellet to the flexural rigidity of the rod has
17 been ignored because of the lack of bending test data. Recent research sponsored by the U.S.
18 Nuclear Regulatory Commission (NRC) on the static bending response and fatigue strength of
19 HBU SNF rods (i.e., rods with burnup exceeding 45 GWd/MTU) with the presence of the fuel
20 pellets, has provided some of the data necessary to more accurately assess the structural
21 behavior of the composite HBU SNF rod system (NRC, 2017a). This staff has examined the
22 results from this research to assess the expected behavior of HBU SNF under normal
23 conditions of transport (NCT) and hypothetical accident conditions (HAC), as well as DSS drop
24 and tip-over accident scenarios.

25 The results in NUREG/CR-7198, Revision 1 (NRC, 2017a) for static bend testing of
26 aggressively hydride-reoriented Zircaloy-4 HBU SNF rods supports the staff's conclusion that
27 the use of best-estimate cladding mechanical properties that do not account for the presence of
28 the fuel pellet continues to be adequate for assessing the structural performance of HBU SNF
29 rods during a hypothetical 9-m (30-ft) drop accident, per the requirement in 10 CFR 71.73(c)(1).
30 The same conclusion applies to the lower loads experienced during a 0.3-m (1-ft) drop, per the
31 requirement in 10 CFR 71.71(c)(7), and postulated drop and cask tip-over accident scenarios
32 during dry storage operations, per the requirement in 10 CFR 72.122(b). Further, the staff finds
33 that the orientation of the hydrides is not a critical consideration when evaluating the adequacy of
34 cladding-only mechanical properties. Therefore, the use of mechanical properties for cladding in
35 either the as-irradiated or hydride-reoriented condition is considered acceptable for the
36 evaluation of drop accident scenarios. If an applicant is unable to demonstrate satisfactory
37 performance of the HBU SNF rod by assuming cladding-only mechanical properties, the staff has
38 proposed an alternative approach for using the results from static bend testing to account for the
39 increased flexural rigidity imparted by the fuel pellet.

40 After considering the aggressive hydride reorientation treatment used for the Zircaloy-4 HBU
41 SNF rods, the staff concludes that the same response is expected for all modern commercial
42 cladding alloy types that may experience hydride reorientation (i.e., Zircaloy-2, ZIRLO and M5).
43 The staff has also reviewed proprietary and non-proprietary data on end-of-life rod internal
44 pressures for fuel rods with boron-based integral fuel burnable absorbers (see Section 1.5.3)
45 and considers these rods to be reasonably bound by the maximum rod internal pressure used in
46 the radial hydride treatment of the Zircaloy-4 HBU SNF rods. The staff's expectation is that
47 additional static bend testing and fatigue testing of HBU SNF composite rods with other

1 claddings will provide confirmation of this conclusion. The U.S. Department of Energy is
2 currently planning to conduct these tests, which the NRC will evaluate when available (Hanson
3 et al., 2016).

4 In addition, the results in NUREG/CR-7198, Revision 1 (NRC, 2017a), on the fatigue testing of
5 aggressively hydride-reoriented Zircaloy-4 HBU SNF rods have provided an adequate technical
6 basis for establishing a reasonable lower-bound fatigue curve and endurance limit for tensile
7 axial-bending loads experienced during transport. Therefore, the staff finds that applicants can
8 use a cumulative damage approach and the curve mentioned above in support of their structural
9 evaluation to assess vibration normally incident to transport of Zircaloy-4 HBU SNF, per the
10 requirement in 10 CFR 71.71(c)(5). Fatigue test data for other cladding alloy types would be
11 needed to develop their respective lower-bound fatigue curves and endurance limits. The U.S.
12 Department of Energy is currently planning to conduct additional fatigue strength testing of HBU
13 SNF composite rods with other claddings, which will provide the necessary data to develop
14 those curves and define the respective endurance limits (Hanson et al., 2016).

15 This report also presents example licensing and certification approaches for HBU SNF to
16 address age-related uncertainties associated with conclusions based on accelerated separate-
17 effects testing. One of these approaches, the use of a surveillance and monitoring program for
18 confirmation of design basis HBU SNF configuration, is consistent with the guidance in NUREG-
19 1927, Revision 1, "Standard Review Plan for Renewal of Specific Licenses and Certificates of
20 Compliance for Dry Storage of Spent Nuclear Fuel," issued June 2016 (NRC, 2016b).
21 Alternatively, the staff has proposed an example approach based on demonstrating compliance
22 with the pertinent regulatory requirements even if hypothetical reconfiguration of the design
23 basis fuel were to occur. This example approach considers lessons learned from an NRC-
24 sponsored generic consequence assessment for transportation packages, as discussed in
25 NUREG/CR-7203, "A Quantitative Impact Assessment of Hypothetical Spent Fuel
26 Reconfiguration in Spent Fuel Storage Casks and Transportation Packages," issued
27 September 2015 (NRC, 2015).

6 REFERENCES

- 1
- 2 Ahn, T., R. Sun, T. Wilt, S. Kamas and S. Whaley. 2012. "Source Term Analysis in Handling
3 Canister-Based Spent Nuclear Fuel: Preliminary Dose Estimate," U.S. Nuclear Regulatory
4 Commission, Washington DC. ADAMS Accession No. ML112640440.
- 5 Aomi, M., T. Baba, T. Miyashita, K. Kaminura, T. Yasuda, Y. Shinohara, and T. Takeda. 2008.
6 "Evaluation of Hydride Reorientation and Mechanical Properties for High-Burnup Fuel-Cladding
7 Tubes in Interim Dry Storage," *J. ASTM Intl.*, JA101262.
- 8 American National Standards Institute (ANSI) N14.5-2014, "American National Standard for
9 Radioactive Materials - Leakage Tests on Packages for Shipment."
- 10 Bai, J., J. Gilbon, C. Prioul, and D. Francois. "Hydride Embrittlement in Zircaloy-4 Plate, Part I,
11 Influence of Microstructure on the Hydride Embrittlement in Zircaloy-4 at 20°C and 350°C" and
12 Part II, "Interaction Between the Tensile Stress and the Hydride Morphology." *Metallurgical and
13 Materials Transactions A*. Vol. 25A, Issue 6. pp. 1,185–1,197. June 1994.
- 14 Benke, R., H. Jung, A. Ghosh, Y.-M. Pan and J. Tait. 2012. "Potential Releases inside a Spent
15 Nuclear Fuel Dry Storage Cask due to Impacts: Relevant Information and Data Needs,"
16 CNWRA-2012-001, Center for Nuclear Waste Regulatory Analyses (CNWRA), San Antonio,
17 Texas. ADAMS Accession No. ML12226A177.
- 18 Biggs, J. M., "Introduction to Structural Dynamics." 1964, McGraw-Hill.
- 19 Billone, M.C, T.A. Burtseva, and Y. Yan. 2012. *Ductile-to-Brittle Transition Temperature for
20 High-Burnup Zircaloy-4 and ZIRLO™ Cladding Alloys Exposed to Simulated Drying-Storage
21 Conditions*, ADAMS Accession No. ML12181A238.
- 22 Billone, M.C., T.A. Burtseva, Z. Han and Y.Y. Liu. 2013. *Embrittlement and DBTT of High-
23 Burnup PWR Fuel Cladding Alloys*, DOE Used Fuel Disposition Campaign Report FCRD-UFD-
24 2013-000401, ANL Report ANL-13/16.
- 25 Billone, M.C., T.A., Burtseva, Z. Han, and Y.Y. Liu, 2014. *Effects of Multiple Drying Cycles on
26 High-Burnup PWR Cladding Alloys*, DOE Used Fuel Disposition Report FCRD-UFD-2014-
27 000052, ANL Report ANL-12/11.
- 28 Billone, M.C., T.A. Burtseva, and M.A Martin-Rengel. 2015. *Effects of Lower Drying-Storage
29 Temperatures on the DBTT of High-Burnup PWR Cladding Alloys*, DOE Used Fuel Disposition
30 Report FCRD-UFD-2015-000008, ANL Report ANL-15/21.
- 31 Bouffioux, P., A. Ambard, A. Miquet, C. Cappelaere, Q. Auxzoux, M. Bono, O., Rabouille, S.,
32 Alegre, V., Chabretou, and C.P Scott. 2013. "Hydride Reorientation in M5® Cladding and its
33 Impact on Mechanical Properties," Proc. LWR Fuel Performance Meeting (TopFuel2013),
34 Charlotte, NC, Sept. 15-19, 2013, paper 1155.
- 35 Bratton, R.N., M.A. Jessee and W.A. Wieselquist. 2015. Rod Internal Pressure Quantification
36 and Distribution Analysis Using FRAPCON, DOE Report FCRD-UFD-2015-000636, ORNL
37 Report ORNL/TM-2015/557, Sept. 30, 2015.

- 1 Cazalis, B., C. Bernaudat, P. Yvon, J. Desquines, C. Poussard, and X. Averty. 2005. "The
2 PROMETRA program: a reliable material database for highly irradiated Zircaloy-4, ZIRLO™ and
3 M5™ fuel claddings," Proc. 18th Int. Conf. on Structural Mechanics in Reactor Technology, 18th
4 ed., Aug. 2005, Paper SMiRT18-C02-1.
- 5 Chung, H.M. 2004. "Understanding Hydride- and Hydrogen-Related Processes in High-Burnup
6 Cladding in Spent-Fuel-Storage and Accident Situations," Proc. 2004 Intl. Meeting on LWR Fuel
7 Performance, Orlando, FL, Sept. 19-22, 2004, Paper 1064.
- 8 Colas, K., A. Motta, M.R. Daymond, and J. Almer. 2014. "Mechanisms of Hydride Reorientation
9 in Zircaloy-4 Studied in Situ," Proc. ASTM 17th Intl. Symp. on Zirconium in the Nuclear Industry,
10 STP 1543, 1107-1137.
- 11 Einziger, R.E., H. Tsai, M.C. Billone, B.A. Hilton, "Examination of Spent PWR Fuel Rods after
12 15 Years in Dry Storage," NUREG/CR-6831, Argonne National Laboratory, Argonne, IL., 2003,
13 ADAMS Accession No. ML032731021.
- 14 Einziger, R. and C. Beyer. 2007. "Characteristics and Behavior of High-Burnup Fuel that Affect
15 the Source Terms for Cask Accidents," *Nuclear Technology*, 59: 134-146.
- 16 Fourgeaud, S., J. Desquines, M. Petit, C. Getrey and G. Sert. 2009. "Mechanical
17 characteristics of fuel-rod cladding in transport conditions," *Packaging, Transport, Storage &
18 Security of Radioactive Material*, 20: 69-76.
- 19 Gaylord, Jr., E. H., C. H. Gaylord, 1979. "Structural Engineering Handbook," McGraw-Hill, 2nd
20 Edition.
- 21 Geelhood, K.J., W.J. Luscher and C.E. Beyer. 2008. PNNL Stress/Strain Correlation for
22 Zircaloy, PNNL-17700, July 2008.
- 23 Geelhood, K.J., W.J. Luscher and P.A. Raynaud. 2013. Material Properties Correlations:
24 Comparison Between FRAPCON-3.5, FRAPTRAN-1.5, and MATPRO, NUREG/CR-7024,
25 Revision 1, Oct. 2013, available as ML14296A063.
- 26 Gruss, K. A, C.L. Brown and M.W. Hodges. 2004. "USNRC Acceptance Criteria and Cladding
27 Considerations for the Dry Storage and Transportation of SNF" Proc. PATRAM 2004 meeting,
28 Berlin, Germany, Sept 20-24, 2004.
- 29 Hanson, B., H. Alsaed, C. Stockman, D. Enos, R. Meyer, and K. Sorenson. 2012. "Used Fuel
30 Disposition Campaign: Gap Analysis to Support Extended Storage of Used Nuclear Fuel
31 Revision 0." Richland, Washington: Pacific Northwest National Laboratory.
- 32 Hanson, B. D., S. C. Marschman, Billone, M. C., Scaglione, J., Sorenson, K. B., Saltzstein, S. J.
33 2016. "High Burnup Spent Fuel Data Project. Sister Rod Test Plan Overview." Pacific
34 Northwest National Laboratory. FCRD-UFD-2016-000063 PNNL-25374.
- 35 Hirose, T., M. Ozawa and A. Yamauchi. 2015. "Fuel Rod Mechanical Behavior under Dynamic
36 Load Condition on High Burnup Spent Fuel of BWR and PWR." *International Conference on
37 Management of Spent Fuel from Nuclear Power Reactors: An Integrated Approach to the Back-
38 End of the Fuel Cycle*, Vienna, Austria, June 15-19.

1 International Atomic Energy Agency (IAEA). 2011. "Impact of High Burnup Uranium Oxide and
2 Mixed Uranium-Plutonium Oxide Water Reactor Fuel on Spent Fuel Management," IAEA
3 Nuclear Energy Series NF-T-3.8.

4 Ito, K., K. Kamimura and Y. Tsukada. 2004. "Evaluation of Irradiation Effect on Fuel, Cladding
5 Creep properties" Proc. 2004 International Meeting on LWR Fuel performance, Orland, FL, Sept
6 19-22, 2004.

7 Kammenzind, B.F., D.G. Franklin, H.R. Peters, and W.J. Duffin, "Hydrogen Pickup and
8 Redistribution in Alpha-Annealed Zircaloy-4," *Zirconium in the Nuclear Industry: 11th Intl. Symp.*,
9 ASTM STP 1295, E.R. Bradley and G.P. Sabol, Eds., ASTM, pp. 338–370, 1996.

10 Kearns, J.J. 1967. "Terminal Solubility and Partitioning of Hydrogen in the Alpha Phase of
11 Zirconium, Zircaloy-2 and Zircaloy-2," *J. Nucl. Mater.* 22:292–303.

12 Machiels, A. 2013. *End-of-Life Rod Internal Pressures in Spent Pressurized Water Reactor*
13 *Fuel*, EPRI Report 3002001949, 2013.

14 McMinn, A., E.C. Darby and J.S. Schofield. 2000. "The Terminal Solid Solubility of Hydrogen in
15 Zirconium Alloys, *Zirconium in the Nuclear Industry: 12th Intl. Symp.*, ASTM STP 1354, G.P.
16 Sabol and G.D. Moan, Eds., ASTM, pp. 173–195, 2000.

17 NRC. 2000a. "Standard Review Plan for Spent Fuel Storage Facilities" NUREG-1567,
18 Washington D.C. ADAMS Accession No. ML003686776.

19 NRC. 2000b. "Standard Review Plan for Transportation Packages for Spent Nuclear Fuel,"
20 NUREG-1617, Washington D.C. ADAMS Accession No. ML003696262.NRC. 2000c.
21 "Reexamination of Spent Fuel Shipment Risk Estimates," NUREG/CR-6672, SAND2000-0234,
22 Washington D.C. ADAMS Accession No. ML003698324.

23 NRC. 2001. "Dry Cask Storage Characterization Project—Phase 1; CASTOR V/21 Cask
24 Opening and Examination." NUREG/CR-6745, Washington D.C. ADAMS Accession No.
25 ML013020363.

26 NRC. 2003a. "Cladding Considerations for the Transportation and Storage of Spent Fuel,"
27 Interim Staff Guidance 11, Revision 3, Washington, DC. ADAMS Accession No. ML033230335.

28 NRC. 2003b. "Examination of Spent PWR Fuel Rods after 15 Years in Dry Storage."
29 NUREG/CR-6831, Washington D.C. ADAMS Accession No. ML032731021.

30 NRC. 2003c. "Moderator Exclusion under Hypothetical Accident Conditions and
31 Demonstrating Subcriticality of Spent Fuel under the Requirements of 10 CFR 71.55(e)," Interim
32 Staff Guidance 19, Washington, DC. ADAMS Accession No. ML031250639.

33 NRC. 2006. "Potential Rod Splitting Due to Exposure to an Oxidizing Atmosphere During
34 Short-term Cask Loading Operations in LWR or Other Uranium Oxide Based Fuel," Interim Staff
35 Guidance 22, Washington, DC. ADAMS Accession No. ML061170217.

36 NRC. 2007a. "A Pilot Probabilistic Risk Assessment of a Dry Cask Storage System at a
37 Nuclear Power Plant," NUREG-1864, Washington D.C. ADAMS Accession No. ML071340012.

1 NRC. 2007b. "Classifying the Condition of Spent Nuclear Fuel for Interim Storage and
2 Transportation Based on Function," Interim Staff Guidance 2, Revision 1, Washington, D.C.
3 ADAMS Accession No. ML071420268.NRC. 2010. "Standard Review Plan for Spent Fuel Dry
4 Storage Systems at a General License Facility, Revision 1." NUREG-1536, Revision 1,
5 Washington D.C. ADAMS Accession No. ML101040620.

6 NRC. 2011. "FRAPCON-3.4: A Computer Code for the Calculation of Steady-State Thermal-
7 Mechanical Behavior of Oxide Fuel Rods for High Burnup," NUREG/CR-7022, Vol. 1,
8 Washington D.C. ADAMS Accession No. ML11101A005.

9 NRC. 2012. "Burnup Credit in the Criticality Safety Analyses of PWR Spent Fuel in
10 Transportation and Storage Casks," Interim Staff Guidance 8, Revision 3, Washington, D.C.
11 ADAMS Accession No. ML122261A433.

12 NRC. 2014. "Spent Fuel Transportation Risk Assessment – Final Report." NUREG-2125,
13 Washington D.C. ADAMS Accession No. ML14031A323.

14 NRC. 2015. "A Quantitative Impact Assessment of Hypothetical Spent Fuel Reconfiguration in
15 Spent Fuel Storage Casks and Transportation Packages." NUREG/CR-7203, Washington D.C.
16 ADAMS Accession No. ML15266A413.

17 NRC. 2016a. "Fuel Retrievability in Spent Fuel Storage Applications," Interim Staff Guidance 2,
18 Revision 2, Washington, D.C. ADAMS Accession No. ML16117A080.

19 NRC. 2016b. "Standard Review Plan for Renewal of Specific Licenses and Certificates of
20 Compliance for Dry Storage of Spent Nuclear Fuel," NUREG-1927, Revision 1, Washington,
21 DC. ADAMS Accession No. ML16179A148.

22 NRC. 2017a. "Mechanical Fatigue Testing of High-Burnup Fuel for Transportation
23 ApplicationApplications." NUREG/CR-7198, Revision 1, Washington DC. ADAMS Accession
24 No. ML17292B057.

25 NRC. 2017b. "Standard Review Plan for Spent Fuel Dry Storage Systems and Facilities. Draft
26 for Comment." NUREG-2215, Washington DC. ADAMS Accession No. ML17310A693.

27 NRC. 2017c. "Managing Aging Processes in Storage (MAPS) Report." NUREG-2214,
28 Washington DC. ADAMS Accession No. ML17289A237.

29 NRC. 2018. "Standard Review Plan for Approval of Transportation Packages" NUREG -2216,
30 Washington DC. ADAMS Accession No. MLXXXXXXXX.

31 Pan, G., A.M. Garde, and A.R. Atwood. 2013. "Performance and Property Evaluation of High-
32 Burn-up Optimized ZIRLO™ Cladding," Proc. 17th ASTM Sym. on Zirconium in the Nuclear
33 Industry, Feb. 3-7, 2013, Hyderabad, India.

34 Patterson, C. and F. Garzarolli. 2015. "Dry Storage Handbook: Fuel Performance in Dry
35 Storage", A.N.T. International: Mölnlycke, Sweden.

36 Peehs, M. 1998. "Assessment of Dry Storage Performance of Spent LWR Fuel Assemblies
37 with Increasing Burnup" Proc 1st RCM meeting, Washington, DC., April 20-24, 1998.

- 1 Pickard, A. 2015. Fatigue Crack Propagation in Biaxial Stress Fields," *J Strain Analysis for*
2 *Engineering Design*. 50(1): 25–39.
- 3 Richmond, D. J. and K. J. Geelhood, FRAPCON Analysis of Cladding Performance during Dry
4 Storage Operations; PNNL. 2017 Water Reactor Fuel Performance Meeting, Korea.
- 5 Roark, R. and W. Young, "Formulas for Stress and Strain," McGraw-Hill, 5th Edition, 1975.
- 6 Sanders, T., Seager, K., Rashid, Y., Barrett, P., Malinauskas, A., Einziger, R., Jordan, H.,
7 Duffey, T., Sutherland, S., Reardon, P., 1992, "A Method for Determining the Spent Fuel
8 Contribution to Transport Cask Containment Requirements," SAND90-2406, Sandia National
9 Laboratories, Albuquerque, New Mexico.
- 10 Spino, J., M. Coquerelle and D. Baron. 1996. "Microstructure and Fracture Toughness
11 Characterization of Irradiated PWR Fuels in the Burnup Range of 40-67 GWd/MTU."
12 *Proceedings of the Technical Committee Meeting IAEA on Advances in Fuel Technology*.
- 13 Spino, J., J. Cobos-Sabate and F. Rousseau. 2003. "Room-temperature Microindentation
14 Behavior of LWR-fuels, Part 1: fuel microhardness." *J. Nucl. Mater.* 322:204–216.
- 15 Tang, D., A. Rigato, and R.E. Einziger. 2015. "Flaw Effects and Flaw Reorientation on Spent
16 Fuel Rod Performance, a Simulation with Finite Element Analysis" Proceedings of the ASME
17 2015 Pressure Vessels and Piping Conference, July 19–23, 2015, Boston, MA, USA.
- 18 Wang, J.-A., H. Wang, H. Jiang, Y. Yan, B. B. Bevard, J. M. Scaglione. 2016. "FY 2016 Status
19 Report: Documentation of All CIRFT Data including Hydride Reorientation Tests." Oak Ridge
20 National Laboratory, ORNL/SR-2016/424, September 14, 2016.
- 21 Winter, G. and A. Nelson. 1979. "Design of Concrete Structures," McGraw-Hill, 9th Edition,
22 1979.
- 23 Wisner, S. and R. Adamson. "Combined Effects of Radiation Damage and Hydrides on the
24 Ductility of Zircaloy-2." *Nuclear Engineering and Design*. Vol. 185. pp. 33–49. 1998.

GLOSSARY

Accident condition of storage	The extreme level of an event or condition, which has a specified resistance, limit of response, and requirement for a given level of continuing capability, which exceeds off-normal events or conditions. Accident conditions include both design-basis accidents and conditions caused by natural and manmade phenomena.
Aging Management Program	See Title 10 of the <i>Code of Federal Regulations</i> (10 CFR) 72.3, "Definitions".
Amendment of a license or certificate of compliance (CoC)	An application for amendment of a license or a CoC must be submitted whenever a holder of a specific license or CoC desires to change the license or CoC (including a change to the technical specifications that accompany the license or CoC conditions). The application must fully describe the desired change(s) and the reason(s) for such change(s), and following as far as applicable the form prescribed for original applications. See 10 CFR 72.56, "Application for Amendment of License," and 10 CFR 72.244, "Application for Amendment of a Certificate of Compliance".
Assembly defect	Any change in the physical as-built condition of the spent fuel assembly except for normal in-reactor changes such as elongation from irradiation growth or assembly bow. Examples of assembly defects include: (1) missing rods; (2) broken or missing grids or grid straps (spacers); and (3) missing or broken grid springs.
Breached spent nuclear fuel rod	A spent nuclear fuel (SNF) rod with cladding defects that permit the release of gases or solid fuel particulates from the interior of the fuel rod. SNF rod breaches include pinhole leaks, hairline cracks, and gross ruptures.
Burnup	The measure of thermal power produced in a specific amount of nuclear fuel through fission, usually expressed in gigawatt-day per metric ton uranium (GWd/MTU). For the purpose of assessing the allowable contents, the maximum burnup of the fuel is generally specified in terms of the average burnup of the entire fuel assembly (i.e., assembly average). For the purpose of assessing fuel cladding integrity in the materials and structural review, the rod with the highest burnup within the fuel assembly is generally specified in terms of peak rod average burnup.
Can for damaged fuel	A metal enclosure that is sized to confine damaged SNF contents. A can for damaged fuel must satisfy fuel-specific and dry storage system/package-related functions for undamaged SNF, as required by the applicable regulations.

Canister (in a dry storage system)	A metal cylinder that is sealed at both ends and may be used to perform the function of confinement. Typically, a separate overpack performs the radiological shielding and physical protection function.
Certificate of compliance (CoC) (for a dry storage system)	The certificate issued by the U.S. Nuclear Regulatory Commission (NRC) that approves the design of a spent fuel storage cask in accordance with the provisions of 10 CFR Part 72, "Licensing Requirements for the Independent Storage of Spent Nuclear Fuel, High-Level Radioactive Waste, and Reactor-Related Greater Than Class C Waste," Subpart L, "Approval of Spent Fuel Storage Casks." See 10 CFR 72.3.
Certificate of Compliance (CoC) (for a transportation package)	The certificate issued by the NRC that approves the design of a package for the transportation of radioactive material in accordance with the provisions of 10 CFR Part 71, "Packaging and Transportation of Radioactive Material," Subpart D, "Application for Package Approval." See 10 CFR 71.4, "Definitions."
Certificate holder (for a dry storage system)	A person who has been issued a CoC by the NRC for a spent fuel storage cask design under 10 CFR Part 72. See 10 CFR 72.3.
Certificate holder (for a transportation package)	A person who has been issued a CoC or other package approval by the NRC under 10 CFR Part 71. See 10 CFR 71.4.
Certificate of compliance user (CoC user)	The general licensee that has loaded a dry storage system, or purchased a dry storage system (DSS) and plans to load it, in accordance with a CoC issued under 10 CFR Part 72.
Confinement (in a dry storage system for spent nuclear fuel)	The ability to limit or prevent the release of radioactive substances into the environment.
Confinement systems	Those systems, including ventilation, that act as barriers between areas containing radioactive substances and the environment. See 10 CFR 72.3.
Containment system	The assembly of components of the packaging intended to retain the radioactive material during transport. See 10 CFR 71.4.
Controlled area	See 10 CFR 72.3 and 10 CFR 20.1003, "Definitions.". The definition in 10 CFR 20.1003 is broader in scope and allows for, or includes, establishment of access controls to areas within the site for any reason (for radiation protection).
Criticality	The condition wherein a system or medium is capable of sustaining a nuclear chain reaction.
Damaged spent nuclear fuel	Any spent fuel rod or spent fuel assembly that cannot meet the pertinent fuel-specific or system-related regulations for the

	transportation package (10 CFR Part 71) or dry storage system (10 CFR Part 72).
Degradation	Any change in the properties of a material that adversely affects the performance of that material; adverse alteration. See NUREG-1536, Revision 1, "Standard Review Plan for Spent Fuel Dry Storage Systems at a General License Facility.," issued July 2010.
Design bases (storage)	Information that identifies the specific function(s) to be performed by structures, systems, and components (SSCs) (both important-to-safety and not important-to-safety) of a facility or of a spent fuel storage cask and the specific values or ranges of values chosen for controlling parameters as reference bounds for design. These values may be (1) restraints, derived from generally accepted "state-of-the-art" practices for achieving functional goals, or (2) requirements, derived from analysis (based on calculation, experiments, or both) of the effects of a postulated event under which SSCs must meet their functional goals. See 10 CFR 72.3.
Dry storage	The storage of SNF in a DSS, which typically involves drying the DSS cavity and backfilling with an inert gas.
Dry storage system (DSS)	A system that typically uses a cask or canister in an overpack as a component in which to store SNF in a dry environment. A DSS provides confinement, radiological shielding, sub-criticality control, structural support, and passive cooling of its SNF during normal, off-normal, and accident conditions. A DSS design may be approved under a CoC, as listed in 10 CFR 72.214, "List of Approved Spent Fuel Storage Casks," or licensed under a specific license for an independent spent fuel storage installation.
g-load	The acceleration experienced by an object with mass under its own self weight.
General license (storage)	Authorizes the storage of spent fuel in an ISFSI at a power reactor site to persons (see definition of person in 10 CFR 72.3) authorized to possess or operate nuclear power reactors under 10 CFR Part 50 ("Domestic Licensing of Production and Utilization Facilities") or 10 CFR Part 52 ("Licenses, Certifications, and Approvals for Nuclear Power Plants"). The general license is limited to (1) that spent fuel which the general licensee is authorized to possess at the site under the specific 10 CFR Part 50 or 10 CFR Part 52 license for the site, and (2) storage of spent fuel in casks approved under the provisions of 10 CFR Part 72, Subpart L and listed in 10 CFR 72.214. See 10 CFR 72.210 ("General License Issued") and 72.212(a)(1)-(2).
Gross breach	A breach in the spent fuel cladding that is larger than either a pinhole leak or a hairline crack and allows the release of particulate matter from the spent fuel rod.

Hairline crack	A minor SNF cladding defect that will not permit significant release of particulate matter from the spent fuel rod and therefore presents a minimal as low-as-is-reasonably-achievable concern during fuel handling operations.
High burnup (HBU) spent nuclear fuel	SNF with assembly average burnup (see “Burnup”) generally exceeding 45 GWd/MTU.
Hoop stress	The tensile stress in cladding wall in the circumferential orientation of the fuel rod.
Important to safety (storage)	See SSCs important to safety.
Independent spent fuel storage installation (ISFSI)	A complex designed and constructed for the interim storage of spent nuclear fuel, solid reactor-related greater-than-Class-C (GTCC) waste, and other radioactive materials associated with spent fuel and reactor-related GTCC waste storage. See 10 CFR 72.3.
Intact spent nuclear fuel	A subset of undamaged SNF. Any fuel rod or fuel assembly that can meet the pertinent fuel-specific or system-related regulations for the transportation package (10 CFR Part 71) or dry storage system (10 CFR Part 72). Intact SNF rods may not contain pinholes, hairline cracks, or gross ruptures. Intact SNF assemblies may have assembly defects if able to meet the pertinent fuel-specific or system-related regulations.
Intended function (storage)	A design-basis function defined as either (1) important to safety or (2) the failure of which could impact a safety function.
Interim staff guidance (ISG)	Supplemental information that clarifies important aspects of regulatory requirements. An ISG provides review guidance to NRC staff in a timely manner until standard review plans are revised accordingly.
k_{eff} “k-effective”	Effective neutron multiplication factor including all biases and uncertainties at a 95-percent confidence level for indicating the level of subcriticality relative to the critical state. At the critical state, $k_{eff} = 1.0$. This has also been used to represent effective thermal conductivity.
Low-burnup (LBU) spent nuclear fuel	Spent nuclear fuel with an assembly average burnup (see “Burnup”) generally less than 45 GWd/MTU.
M5® (M5)	AREVA-trademarked fuel cladding alloy, which contains zirconium and niobium
Non-fuel hardware	Hardware that is not an integral part of a fuel assembly. This is the term used to identify what the regulation refers to as “other radioactive materials associated with fuel assemblies” (see SNF definition in 10 CFR 72.3). While not integral to the assembly, it includes those items that are designed to operate and are positioned or operated within the

	envelope of the fuel assembly during reactor operation and are stored within the assembly envelope in the storage container. Typical examples of non-fuel hardware include: burnable poison rod assemblies (BPRAs), control element assemblies, thimble plug assemblies, and boiling-water reactor (BWR) fuel channels. Examples of items that do not meet this definition include boron sources, BWR in-core instruments, and BWR control blades.
Non-mechanistic event (dry storage)	An event, such as cask tip-over, which should be evaluated for acceptable system capability, although a cause for such an event is not identified in the analyses of off-normal and accident events and conditions.
Normal events or conditions of storage	Conditions that are intended operations, planned events, and environmental conditions that are known or reasonably expected to occur with high frequency during storage operations. "Normal" refers to the maximum level of an event or condition that is expected to routinely occur (similar to Design Event I as defined in American National Standards Institute/American Nuclear Society (ANSI/ANS) 57.9, "Design Criteria for an Independent Spent Fuel Storage Installation (Dry Storage Type)"). The DSS or ISFSI SSCs are expected to remain fully functional and to experience no temporary or permanent degradation of that functionality from normal operations, events, and conditions. Specific normal conditions to be addressed are evaluated for the DSS or ISFSI and are documented in a safety analysis report for that system or facility.
Normal means (dry storage)	The ability to move a fuel assembly with a crane and grapple used to move undamaged assemblies at the point of cask loading. The addition of special tooling or modifications to the assembly to make the assembly suitable for lifting by crane and grapple does not preclude the assembly from being considered movable by normal means.
Off-normal events or conditions of storage	An event or condition that, although not occurring regularly, can be expected to occur with moderate frequency and for which there is a corresponding maximum specified resistance, limit of response, or requirement for a given level of continuing capability. "Off-normal" events and conditions are similar to a "Design Event II" in ANSI/ANS 57.9. A DSS or ISFSI SSC is expected to experience off normal events and conditions without permanent degradation of capability to perform its full function (although operations may be suspended or curtailed during off-normal conditions) over the full storage term (the license period for a specific license facility or the storage period equivalent to the certificate term for a DSS). Off-normal events or conditions are referred to as anticipated occurrences in 10 CFR 72.104, "Criteria for Radioactive Materials in Effluents and Direct Radiation from an ISFSI or MRS."
Package (transportation)	The packaging together with its radioactive contents as presented for transport. See 10 CFR 71.4.

Packaging (transportation)	The assembly of components necessary to ensure compliance with the packaging requirements of 10 CFR Part 71. It may consist of one or more receptacles, absorbent materials, spacing structures, thermal insulation, radiation shielding, and devices for cooling or absorbing mechanical shocks. The vehicle, tie-down system, and auxiliary equipment may be designated as part of the packaging. See 10 CFR 71.4.
Pinhole leak	A minor cladding defect that will not permit significant release of particulate matter from the spent fuel rod and therefore present a minimal as low-as-is-reasonably-achievable concern during fuel handling operations.
Renewal of a license or CoC (dry storage)	A request to the NRC to extend the expiration date of a license or CoC. Renewal requests must meet the requirements specified in 10 CFR 72.42, "Duration of License; Renewal," for a license or 10 CFR 72.242, "Recordkeeping and Reports," for a CoC. A certificate holder may apply for renewal of an ISFSI license or a spent fuel storage cask CoC for a term not to exceed 40 years.
Ready retrieval (dry storage)	The ability to safely remove the spent fuel from storage for further processing or disposal.
Recovery (dry storage)	The capability of returning the stored radioactive materials from an accident to a safe condition without endangering public health and safety or causing significant or unnecessary exposure to workers. Any potential release of radioactive materials during recovery operations must not result in doses or radiation exposures that exceed the limits in 10 CFR Part 20, "Standards for Protection against Radiation." Doses during recovery operations are included in the dose estimates for accidents, the total of which must not exceed the limits in 10 CFR 72.106, "Controlled Area of an ISFSI or MRS."
Retrievability (dry storage)	See definition of ready retrieval above. Storage systems must be designed to allow ready retrieval of SNF, high-level radioactive waste, and reactor-related GTCC waste for further processing or disposal. See 10 CFR 72.122(l).
Safety analysis report (SAR) (dry storage)	The report submitted to the NRC staff by an applicant for a CoC for a DSS design, or for a specific license for an ISFSI, to present information on the design and operations of the system or facility. This document provides the justification and analyses to demonstrate that the design meets regulatory requirements and acceptance criteria (10 CFR 72.24, "Contents of Application: Technical Information," and 10 CFR 72.230(a)). The SAR is submitted for approval of the ISFSI or DSS design. The final SAR is as defined in 10 CFR 72.48(a)(5).
Safety function (dry storage)	The functions that DSS and DSF SSCs important to safety (see 10 CFR 72.3) are designed to maintain/perform, including the following:

	<ul style="list-style-type: none"> • protection against environmental conditions • content temperature control • radiation shielding • confinement • sub-criticality control, and • retrievability.
Specific license (dry storage)	A license issued by the NRC to authorize the receipt, handling, storage, and transfer of spent fuel, high-level radioactive waste, or reactor-related GTCC waste at an ISFSI or MRS facility. The NRC issues the license to a named person (see definition of person in 10 CFR 72.3) after the NRC has reviewed an application filed under regulations in 10 CFR Part 72, Subpart B, "License Application, Form, and Contents" (see 10 CFR 72.6 License Required; Types of Licenses.)
Spent nuclear fuel (SNF) or spent fuel	<p>Nuclear fuel that has been withdrawn from a nuclear reactor after irradiation, has undergone at least a 1-year decay process since being used as a source of energy in a power reactor, and has not been chemically separated into its constituent elements by reprocessing. Spent fuel includes the special nuclear material, byproduct material, source material, and other radioactive materials associated with fuel assemblies. See 10 CFR 71.4 and 10 CFR 72.3.</p> <p>For purposes of this report, spent nuclear fuel refers to high burnup SNF unless otherwise noted.</p>
Structures, systems, and components (SSCs) important to safety (storage)	<p>See 10 CFR 72.3. Those features of the ISFSI and spent fuel storage cask whose functions are at least one of the following:</p> <ul style="list-style-type: none"> • to maintain the conditions required to safely store spent fuel, high-level radioactive waste, or reactor-related GTCC waste • to prevent damage to the spent fuel, the high-level radioactive waste, or reactor-related GTCC waste container during handling and storage • to provide reasonable assurance that spent fuel, high-level radioactive waste, or reactor-related GTCC waste can be received, handled, packaged, stored, and retrieved without undue risk to the health and safety of the public.
Undamaged spent nuclear fuel	Any fuel rod or fuel assembly that can meet the pertinent fuel-specific or system-related regulations for the transportation package (10 CFR Part 71) or dry storage system (10 CFR Part 72). Undamaged (non-intact) SNF rods may contain pinholes or hairline cracks, but may not contain gross ruptures. Undamaged SNF assemblies may have assembly defects if they are still able to meet the pertinent fuel-specific or system-related regulations.

Zircaloy	An alloy of zirconium, tin, and other metals, used chiefly as cladding for nuclear reactor fuel.
ZIRLO™ (ZIRLO)	Westinghouse-trademarked fuel cladding alloy, which contains zirconium, tin and niobium

BIBLIOGRAPHIC DATA SHEET

(See instructions on the reverse)

NUREG-2224

2. TITLE AND SUBTITLE

Dry Storage and Transportation of High Burnup Spent Fuel

Draft for Comment

3. DATE REPORT PUBLISHED

MONTH

July

YEAR

2018

4. FIN OR GRANT NUMBER

5. AUTHOR(S)

T. Ahn, H. Akhavannik, G. Bjorkman, F.C. Chang, W. Reed, A. Rigato,
D. Tang, R.D. Torres, B.H. White, V. Wilson

6. TYPE OF REPORT

Technical

7. PERIOD COVERED (Inclusive Dates)

8. PERFORMING ORGANIZATION - NAME AND ADDRESS (If NRC, provide Division, Office or Region, U. S. Nuclear Regulatory Commission, and mailing address; if contractor, provide name and mailing address.)

Division of Spent Fuel Management
Office of Nuclear Material Safety and Safeguards
U.S. Nuclear Regulatory Commission
Washington, DC 20555-0001

9. SPONSORING ORGANIZATION - NAME AND ADDRESS (If NRC, type "Same as above", if contractor, provide NRC Division, Office or Region, U. S. Nuclear Regulatory Commission, and mailing address.)

Same as above

10. SUPPLEMENTARY NOTES

.

11. ABSTRACT (200 words or less)

The potential for changes in the cladding performance of high burnup (HBU) spent nuclear fuel (SNF) to compromise the analyzed fuel configuration in dry storage systems and transportation packages has been historically addressed through safety review guidance. The guidance defines adequate fuel conditions, including peak cladding temperatures during short-term loading operations to prevent or mitigate degradation of the cladding. The purpose of this report is to expand the technical basis in support of that guidance, as it pertains to the mechanism of hydride reorientation in HBU SNF cladding.

This report also provides an engineering assessment of the results of NRC-sponsored research on the mechanical performance of HBU SNF following hydride reorientation and, per the conclusions of that assessment, provides example approaches for licensing and certification of HBU SNF for dry storage (under 10 CFR Part 72) and transportation (under 10 CFR Part 71).

12. KEY WORDS/DESCRIPTORS (List words or phrases that will assist researchers in locating the report.)

High Burnup Spent Fuel
Dry Storage Systems
Transportation Packages
Hydride Reorientation

13. AVAILABILITY STATEMENT

unlimited

14. SECURITY CLASSIFICATION

(This Page)

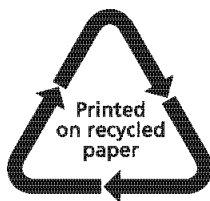
unclassified

(This Report)

unclassified

15. NUMBER OF PAGES

16. PRICE



Federal Recycling Program



**UNITED STATES
NUCLEAR REGULATORY COMMISSION**
WASHINGTON, DC 20555-0001

OFFICIAL BUSINESS



**NUREG-2224
Draft**

Dry Storage and Transportation of High Burnup Spent Fuel

July 2018